UNCOVERING THE ROLE OF PROTEIN KINASE TAOK2 AS AN ENDOPLASMIC RETICULUM-MICROTUBULE TETHER

Kimya Nourbakhsh

A dissertation

submitted in partial fulfillment of the

requirements for the degree of

Doctor of Philosophy

University of Washington

2021

Reading Committee: Smita Yadav, Chair

Shao-En Ong

Linda Wordeman

Program Authorized to Offer Degree: Pharmacology

University of Washington

ABSTRACT

Uncovering the Role of Protein Kinase TAOK2 as an Endoplasmic Reticulum-Microtubule Tether

Kimya Nourbakhsh

Chair of Supervisory Committee: Smita Yadav

Department of Pharmacology

Kinase signaling drives a multitude of components of neuronal development such as establishment of polarity, dendritic growth and arborization, dendritic spine formation, and synaptogenesis. Thousand And One amino acid Kinases (TAOKs) are a subfamily of sterile-20 (STE20) kinases possessing an N-terminal kinase domain and diverging C-terminal extended regulatory domains. As evolutionarily conserved kinases, TAO kinases have been shown to play important roles in neuronal development in rodents and invertebrates. Recent studies have linked de novo variants of human TAOK1/2 to neurodevelopmental diseases, thus making it imperative to understand their role in neuronal development. Despite its disease association, the molecular functions of TAO kinases remain unknown. Here, I focus on understanding the molecular and cellular function of the largest member of the TAO family, TAOK2 kinase. We find that TAOK2 is an endoplasmic reticulum (ER) resident multi-pass membrane-spanning kinase that localizes to distinct junctures of the ER through six transmembrane helices and an

amphipathic helix. Additionally, we found that TAOK2 associates to microtubules directly and with high affinity through its cytoplasmic facing C-terminal tail. Furthermore, TAOK2 acts as a functional ER-microtubule tether, knockout of which leads to increased ER motility, increased microtubule growth but decreased ER tip attachment-complex movement. We determine that TAOK2 interacts with microtubule plus-end binding (EB) proteins through a distinctive SxIP motif. Finally, we determine that TAOK2 microtubule binding is regulated by its catalytic activity, loss of which leads to perturbations of ER and microtubule motility. This work identifies TAOK2 as an ER-microtubule tether and reveals a kinase-regulated mechanism for control of ER dynamics critical for cell growth and division. To further understand the context of TAOK2 signaling and determine TAOK2 interactors between the ER and microtubules, I propose the use of proximity labeling utilizing BioID2 and mass spectrometry. I lay out the blueprint for these experiments and the preliminary data from pilot experiments. Finally, I provide implications of these findings on how TAOK2 functions as an ER-microtubule tether might contribute to neurodevelopment.

ACKNOWLEDGEMENTS

I would like to whole-heartedly thank Dr. Smita Yadav, my doctoral advisor, for the opportunity to pursue my graduate career in her laboratory. Smita, thank you for your support, kindness, and guidance. I greatly appreciate all of the confidence and trust you have had in me over the years. It is truly an honor to be the first graduate student to graduate from the Yadav Lab. Thank you to my thesis committee members Dr. Shao-En Ong, Dr. Linda Wordeman, Dr. Nephi Stella, and Dr. Jane Sullivan for your feedback, support, and thoughtful suggestions. An extra thank you to my dissertation reeding committee, Dr. Smita Yadav, Dr. Linda Wordeman, and Dr. Shao-En Ong for reading over my thesis and giving constructive feedback. Thank you to the Ong Laboratory, namely Dr. Shao-En Ong, Dr. Ho-Tak Lau, and Tanmay Sapre for the tremendous help with the BioID2 experiments. I want to express my gratitude for Dr. John D. Scott, chair of the Department of Pharmacology for his support in my endeavors throughout my time in the department. Additionally, a great deal of thanks to the Scott Laboratory for their help with equipment and reagents. Thank you to Juan Jesus Vicente of the Wordeman lab for the help figuring our good constructs and cell lines to visualize microtubules.

Thank you to all of the members of the Yadav lab, it has been a distinct pleasure to work with all of you. I will miss the wit, jokes, and long conversations while we are waiting for our gels to run. An enormous thank you to Amy, without whom this work would not have been possible. I have been so lucky to call you both a coworker and friend, thank you for the support and advice over the years. Thank you to Reilly, Sujin, Bailey and Josie for the great conversations, coffee runs, and advice during times of stress.

Thank you to Matt and Neal for your advice over the years. I am so happy to have had the chance to meet all of you lovely people over the past 4 years.

Thank you to my family for your unwavering support through this entire process. Thank you to Maman Pari and Baba Tousi (my grandparents), Nader, Gelare, and Dario (my brother, sister-in-law, and nephew), and Maryam, Hesam and Kian (my aunt, uncle, and cousin). I would like to thank my partner, Geoffrey, who has kept me sane throughout graduate school, never let me back down from a challenge, and gave me comfort and a place to regroup when experiments failed. Finally, I would like to thank my parents, Ladan and Hamid, who have taught me resilience, fueled my drive to ask questions, and supported me endlessly. You have made me who I am today, and I could not do any of this without you.

TABLE OF CONTENTS

PREFACE

Portions of the text and data from this dissertation are reprinted (adapted) from the following works under fair use and/or with permission under the terms of the CC-BY License:

1. Nourbakhsh, K., and Yadav, S. (2021). Kinase Signaling in Dendritic Development and Disease. Front Cell Neurosci 15, 624648.
2. Nourbakhsh, K.,* Ferreccio, A.A.,* Bernard M.J., and Yadav, S. (2021). TAOK2 is an ER-Localized Kinase that Catalyzes the Dynamic Tethering of ER to Microtubules. (In Press) Developmental Cell.

CHAPTER 1: INTRODUCTION TO KINASES IN NEURONAL DEVELOPMENT

1.1 - Introduction

Dendrites are specialized neuronal processes that receive and integrate synaptic or sensory input. While dendrites are extremely heterogeneous morphologically, dendrites associated with specific neuron types generally exhibit stereotyped morphology (Jan and Jan, 2001). Dendritic phenotypes are sculpted by intrinsic genetic programs, external cues, and patterns of neuronal activity during development (Cline, 2001; Jan and Jan, 2010). These factors together confer dendrites their type specific morphology, and ensure fidelity in forming synaptic connections. Owing to the critical role dendrites play in establishing neuronal connectivity, their dysfunction is strongly associated with several neurological disorders (Forrest et al., 2018). Over the last four decades, multiple molecular signaling pathways that mediate structural and functional development of dendrites have been identified. Protein kinases play a pivotal role in almost all aspects of dendritic development and function, while their dysregulation contributes extensively to disease states.

Kinases catalyze the transfer of a phosphate group from ATP molecule to hydroxyl group containing amino acids primarily serine, threonine, and tyrosine on substrate proteins, in a process termed as phosphorylation (Cohen, 2002; Fabbro et al., 2015). Several characteristics make kinase signaling uniquely powerful and versatile: (1) Phosphorylation occurs in a highly specific yet reversible fashion. (2) Phosphorylation can affect substrates in distinct ways: such as induce a gain or loss of substrate activity, change substrate localization or interactome. (3) Kinases often act in cascades and are capable of remarkable signal integration and amplification that can be tuned to achieve a variety of responses (Cobb, 1999) (4) Kinases are highly druggable making them

promising therapeutic targets (Cohen, 2002). Of the ~518 human kinases, several protein kinases are genetically linked to neurological disorders. These include neurodevelopmental disorders such as autism spectrum disorder as well as neurodegenerative diseases such as Parkinson's disease, yet little is known about how dysfunction in kinase signaling leads to pathological states (Baltussen et al., 2017; Krahn et al., 2020; Manning et al., 2002). Phosphorylation mediated by kinases is countered by phosphatases, a large family of enzymes that catalytically remove phosphate groups from their substrates (Barford et al., 1998; Peng and Maller, 2010). Phosphatases are divided into subfamilies of serine/threonine and tyrosine phosphatases, and dysfunction of these enzymes is associated with several diseases (Tonks, 2006). Activity of phosphatases is tightly regulated by diverse mechanisms that include binding with inhibitory proteins, direct oxidation, and kinase mediated phosphorylation (Hertog, 2003). Thus, the true phosphorylation status of a protein in time and space is determined by the opposing action of protein kinases and phosphatases.

Herein, we describe how kinase signaling exquisitely orchestrates each step of dendrite development, beginning at neurogenesis to its maturation into synaptic networks. Evidence for critical and causative role of kinase dysfunction in neurodevelopmental and degenerative disorders is presented. Finally, we detail the emergent technologies that will be instrumental in delineating kinase function in dendritic development and how kinase dysfunction leads to pathologies associated with neurological disorders.

1.2 - Kinase Pathways That Regulate Dendrite Structure, Function and Plasticity

Before the inception of neurogenesis, the developing brain is comprised of polarized neuroepithelial cells that line the neural tube (Martin-Belmonte and Mostov, 2008;

Taverna et al., 2014). Apical-basal polarity is established early in the developing brain and is achieved through spatial patterning of junctional complexes and polarized protein trafficking. These are regulated by kinase signaling through the conserved Par complex. The Par complex is comprised of scaffolding proteins Par3 and Par6, and the kinase atypical protein kinase C (aPKC) that together establish the apical-basal polarity (McCaffrey and Macara, 2012). The Rho GTPase Cdc42 targets and activates the Par complex at the apical membrane, which is separated from the basolateral membrane domain by adherens junctions. In the mammalian neocortex, intrinsic neuroepithelial polarity set up by the Par complex asymmetrically orients the mitotic spindle, that remarkably, during cell cycle can give rise to asymmetric division (Lancaster and Knoblich, 2012; Rodríguez-Fraticelli et al., 2011). Radial glial cells arising from the asymmetrical division of polarized neuroepithelial cells can further differentiate into neural progenitor cells (NPCs) or neurons through asymmetrical division (Götz and Huttner, 2005). The arising NPCs further self-renew or undergo a terminal differentiation into neurons (Florio and Huttner, 2014). Radial glial cells retain the epithelial polarity set up by the Par complexes. Knockout of one of the isoforms of aPKC, aPKC-λ, in neuroepithelial cells and radial glial cells results in the loss of apical processes that cause disordered layering of the cortex, highlighting the role of aPKC in apical-basal polarity (Imai et al., 2006). Apically located Par complex promotes self-renewing of progenitors at the expense of neurogenic differentiation in the developing cerebral cortex (Costa et al., 2007; Sottocornola et al., 2010). While the Par complex proteins set up intrinsic polarity, extrinsic cues greatly affect neuronal polarity, migration, and layer formation in brain development. Secreted factors such as reelin, semaphorins, and neurotrophic factors

play important roles in instructing neuronal polarity and migration during early development and are controlled by distinct kinase pathways. We direct readers to in depth reviews detailing how these extrinsic cues and growth factors regulate early brain development (Huang and Reichardt, 2001; Jossin, 2020; Yazdani and Terman, 2006). Here we will focus primarily on the kinase signaling pathways important for dendritic growth, structure, and functional maturation.

1.3 - Dendritic Arborization: Kinases That Regulate Dendritic Growth, Branching, and Tiling

Most newly generated mammalian neurons migrate from the site of neurogenesis to their final destination where they are integrated into neural networks. It is during this migration process that they acquire axon-dendrite polarity (Polleux and Snider, 2010). Some neurons, such as retinal ganglion cells, acquire the polarity of the progenitors from which they arise. Others, such as cortical pyramidal neurons, consolidate multiple extended neurites into one leading and one lagging neurite that gives rise to axo-dendritic polarity (Barnes and Polleux, 2009; Polleux and Snider, 2010). On reaching their final destination, neurons extend their dendrites through growth, dendrites scale in size with organismal development, and mature in an exquisitely controlled fashion. Control of dendritic development in response to neuronal activity and neurotrophic factors is mediated by kinases, which play an instrumental role in regulating dendritic size and maturation to form synaptic contacts (Figures 1.1 A–D).

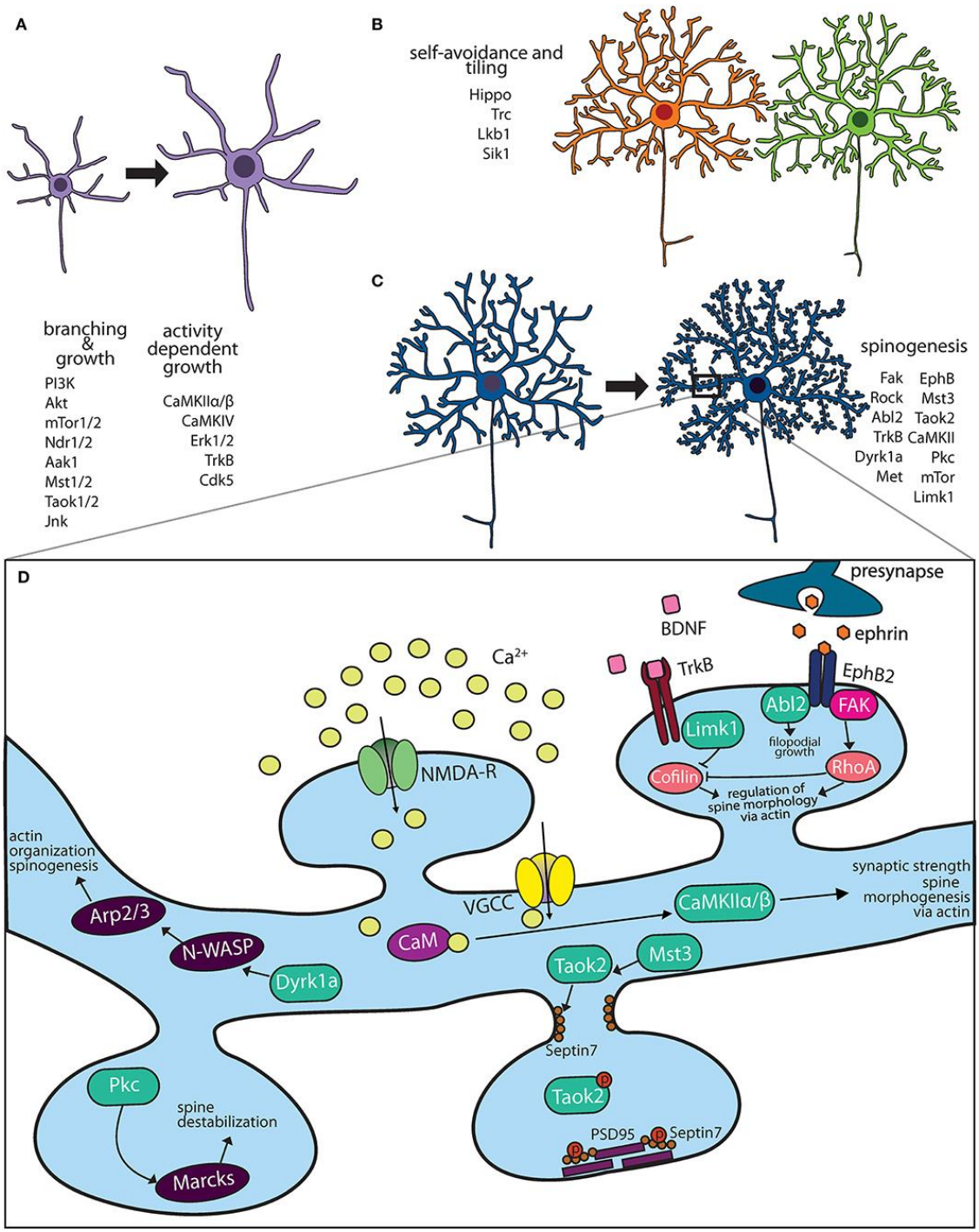

Figure 1.1 - Kinase pathways mediate dendritic morphogenesis and maturation.

(A) Immature dendritic neurites undergo expansive growth and branching during early development. The PI3K-Akt-mTor kinase and Hippo pathway are critical for growth.

Activity dependent growth is primarily mediated by Ca+2 influx and downstream signaling by CaMK family members.

(B) During arborization, dendrites of the same neuron avoid overlap through a principle known as self-avoidance, while neighboring neurons of the same type grow in well-defined territories. Kinases that mediate self-avoidance and dendritic tiling have been identified through screens in Drosophila peripheral sensory da neurons.

(C) Most excitatory neurons on maturation form actin rich protrusions called dendritic spines that serve as sites of synapse formation. Several kinases that regulate the synaptic cytoskeleton are important regulators of spine formation in hippocampal and cortical neurons.

(D) Calcium influx through N-methyl D-aspartate (NMDA) receptors and voltage gated calcium channels (VGCC) activate CaMK kinases, which mediate spine morphogenesis and plasticity. Mutations in several kinases important for dendritic spine formation are associated with neuropsychiatric diseases.

Kinases as Biochemical Switches for Activity Dependent Dendritic Development

Neuronal activity during brain development profoundly impacts dendritic growth and retraction (Cline, 2001). Experiments where neuronal activity is manipulated such as in sensory deprivation (Wiesel and Hubel, 1963), pharmacological block of activity in Xenopus tadpoles (Rajan and Cline, 1998), or enhanced environmental enrichment in rodents (Volkmar and Greenough, 1972), induces dramatic alteration in both dendritic development and its structural complexity. Calcium influx in response to neuronal activity leads to kinase activation, providing the biochemical signal that mediates activity dependent dendritic growth dynamics (Ghosh and Greenberg, 1995). Calcium enters through glutamate receptor NMDA or voltage gated calcium channels (VGCC) and is sequestered by the calcium binding protein, calmodulin. In the Ca^{+2} bound state, calmodulin binds calcium/calmodulin-dependent protein kinases (CaMK), which then undergo autophosphorylation mediated activation. Several CaMKs have been implicated in dendritic development, and these act either via local effects or though transcriptional changes (Redmond and Ghosh, 2005). CaMKII has been extensively studied, most famously in relation to dendrite development and synaptic long-term potentiation. Two isoforms of CaMKII are expressed in the brain, CaMKIIα and CaMKIIβ, which each mediate distinct roles in dendrite development in hippocampal neurons, primarily on account of their differential ability to associate with actin (Shen et al., 1998). CaMKIIα expression in tectal neurons in tadpoles was found to stabilize dendritic arbors, as premature expression of CaMKIIα causes dendrites to slow their growth rate to that of more mature neurons. Conversely, blocking endogenous CaMKII maintains neurons in their rapid growth phase, such that dendritic arbors grow larger than normal (Wu et al., 1999; Zou and Cline, 1999). CaMKIIβ, on the other hand promotes actin polymerization,

thereby increasing filopodial extension and growth of fine dendrites in rat hippocampal neurons (Fink et al., 2003). Another member of the CaM kinase family, CaMKIV, is also crucial for activity dependent dendritic growth. Blocking CaMKIV signaling reduces calcium-induced dendritic growth, while expression of an activated form of CaMKIV in rat cortical neurons mimics the dendrite growth induced by calcium influx (Redmond et al., 2002). CaMKIV is enriched in the nucleus and its effect on dendrite growth is primarily mediated through transcriptional changes. Interfering with activity of transcriptional targets of CaMKIV blocks the ability of active CaMKIV to induce dendrite growth (Redmond and Ghosh, 2005). Importantly, activity induced changes in dendritic growth mediated by CaMKs are developmentally regulated. While the peak expression of CaMKIIβ and CaMKIV coincides with the period of maximal dendritic growth of cortical neurons in rodents, highest expression of CamKIIα occurs later during dendritic maturation when the arbor is elaborated (Cline, 2001; Redmond and Ghosh, 2005; Wong and Ghosh, 2002). Another kinase pathway activated in response of neuronal activity is Ras-MAPK signaling (Konur and Ghosh, 2005). In rat hippocampal pyramidal neurons, persistent dual phosphorylation of ERK1/2 (MAPKs) in response to calcium influx and Ras signaling is important for local cytoskeletal effects and transcriptional changes that lead to dendritic remodeling (Wu et al., 2001). One key protein important for dendritic growth is MAP2 (microtubule associated protein 2), which is phosphorylated by MAPK kinases in response to neuronal activity (Vaillant et al., 2002). In rat cortical neurons, both CaM kinases and Ras/MAPK signaling can regulate gene transcription in response to neuronal activity. This is mediated by phosphorylation of transcription factors, cAMP response element binding protein (CREB), calcium-responsive transactivator (CREST),

LMO4 and NeuroD2 (Aizawa et al., 2004; Kashani et al., 2006; Redmond and Ghosh, 2005; Redmond et al., 2002). Both CREB and CREST bind the transcriptional coactivator, CREB binding protein (CBP) on phosphorylation, although the mechanisms by which transcription regulates dendritic growth are not well-understood (Aizawa et al., 2004). Many cytoplasmic and secreted proteins whose expression increases after activity have been identified. Some of these have shown clear and essential function in modulating dendrite and spine morphology such as candidate plasticity gene-15 (cpg15) (Nedivi et al., 1998), Arc (Peebles et al., 2010), Homer (Sala et al., 2001), and brain-derived neurotrophic factor (BDNF) (Lom and Cohen-Cory, 1999) Other than kinases belonging to the CaM kinase and MAP kinase families, cyclin dependent kinase 5 (CDK5) kinase is translocated to the nucleus in an activity dependent manner in hippocampal neurons where it regulates the transcription of BDNF by phosphorylating the transcriptional repressor MeCP2 (Cheung et al., 2007). It is likely that a quantitative and comprehensive analysis of activity induced kinases might reveal yet unidentified pathways that regulate activity dependent dendritic development.

Kinase Signaling Mediate Dendritic Growth in Response to Neurotrophic Factors

Neurotrophins are secreted growth-promoting proteins that are essential for dendritic development both in peripheral and central nervous system (CNS). The four neutotrophins, nerve growth factor (NGF), brain derived growth factor (BDNF) and neurotrophins 3 and 4 (NT-3, NT-4) signal by binding and activating their receptors, which are members of the tropomyosin receptor kinases (Trk) and the structurally unrelated p75 neurotrophin receptor (Huang and Reichardt, 2001). Trk proteins are receptor tyrosine kinases that dimerize and transactivate on binding their respective neurotrophin ligand. In the mouse CNS, neurotrophins regulate the dendritic growth of pyramidal neurons in

the developing neocortex (McAllister et al., 1995). Each of the four neurotrophins rapidly increases the length and complexity of dendrites of cortical pyramidal neurons when applied exogenously (McAllister et al., 1995). Experiments involving Trk “receptor bodies,” which are fusion proteins of the ligand-binding domains of each Trk receptor and the Fc domain of human IgG, clearly demonstrate that removing endogenous neurotrophins has dramatic consequences for the dendritic growth of pyramidal neurons in developing cortex (McAllister et al., 1997; Shelton et al., 1995). Consistent with the results derived from the addition of exogenous factors, endogenous BDNF is required for the growth and maintenance of dendritic arbors of layer 4 neurons whereas endogenous NT-3 is required for the growth and maintenance of dendritic arbors of layer 6 neurons. The distribution of receptors and secreted neurotrophin is exquisitely regulated. Not only do neurons in each cortical layer respond to subsets of neurotrophins, but also within a single cortical layer, each neurotrophin elicits a unique pattern of dendritic changes. Further, there are distinct changes in apical vs. basal dendrites evident at the individual neuron level (Horch and Katz, 2002). This precise level of neuronal and dendritic specificity suggests that neurotrophins do not simply enhance neuronal growth but, rather, act instructively to modulate particular patterns of dendritic arborization (McAllister, 2000). Another level of kinase regulation is added by Cdk5, which phosphorylates TrkB at the intracellular juxtamembrane region. In hippocampal cultures, reducing Cdk5 activity or expression of a TrkB mutant lacking the Cdk5 phosphorylation site abolishes BDNF triggered dendritic growth (Cheung et al., 2007). Thus, kinases act as both a signal detector (neurotrophin factors or calcium influx) and a biochemical switch

(phosphorylation state) that turn on in response to stimuli and play critical roles in dendritic growth and remodeling (Figure 1.1A).

Kinase Signaling That Controls Dendritic Growth, Tiling and Self-Avoidance

The phosphoinositide-3 kinase (PI3K)–Akt–mammalian target of rapamycin (mTOR) signaling pathway promotes dendritic growth and branching through upregulation of protein and lipid synthesis. The lipid kinase PI3K signals through AKT and is inhibited by phosphatase, Phosphatase and Tensin homolog deleted on chromosome Ten (PTEN). In neurons, mTOR senses and integrates nutrient and growth factor availability through extracellular signals such as BDNF, insulin, insulin-like growth factor 1 (IGF1), vascular endothelial growth factor (VEGF), ciliary neurotrophic factor (CNTF) and glutamate, to mediate neuronal proliferation, dendritic growth and synaptic function (Lipton and Sahin, 2014). Constitutively active Ras, PI3K, and Akt that activate the mTOR kinase induce growth and elaboration of dendrites in cultured hippocampal neurons. In these neurons, this effect can be potently blocked by mTOR inhibitor rapamycin or activation of PTEN that counteracts the action of lipid kinase PI3K (Jaworski et al., 2005). Loss of upstream regulators of mTOR either TSC1/2 or lipid phosphatase PTEN, result in structural neuronal defects. PTEN null mutant mice exhibit dendritic hypertrophy and macrocephaly (Kwon et al., 2003; Lugo et al., 2014). Loss of TSC1/2 increased size of both neuronal somata and dendritic arbors (Tavazoie et al., 2005). Conversely, dendritic complexity is reduced by inhibition of PI3K, knockdown of mTOR, or its effector p70 ribosomal S6 kinase that upregulates protein synthesis. MTOR is composed of two complexes mTORC1 and mTORC2. These share the mTOR kinase but comprise other distinct proteins such as Raptor and Rictor, respectively, that make the two complexes functionally distinct (Hoeffer and Klann, 2010). Both mTORC1 and mTORC2 are integral

to the proper formation of dendrites and their arbor. Knockdown of their essential components Raptor and Rictor in rat hippocampal and cortical neurons inhibits dendritic growth (Urbanska et al., 2012)

The conserved Hippo kinase signaling pathway plays an important role in dendritic growth, tiling and function (Jan and Jan, 2010). Hippo is a conserved serine/threonine kinase of the Ste family, that is important for dendritic growth in Drosophila peripheral sensory neurons (Emoto et al., 2006). Hippo kinase mediates dendritic arbor growth and maintenance through the action of downstream kinase Wts. The mammalian homolog of hippo are MST1/2 kinases, which phosphorylates and activates kinases involved in cytoskeletal modulation including Ndr1/2 (nuclear Dbf2-related) kinases and Lats1/2 (large tumor suppressor 1/2) kinases (Emoto, 2011). In Drosophila and C. elegans sensory neurons, Ndr kinase is required for dendrite branching where it likely promotes neurite outgrowth and branching through Rho family GTPase (Emoto, 2011). Mammalian Ndr1/2 kinases analogous to the roles of their fly homolog Trc, limit dendrite branching and length in hippocampal primary cultures and in vivo (Ultanir et al., 2012). The ability of Ndr kinases to limit dendritic branching is mediated by its direct substrate Aak1 kinase which is a downstream substrate implicated in regulation of intracellular trafficking (Ultanir et al., 2012). In hippocampal neuron cultures, Ndr2 kinase was shown to regulate dendritic growth through phosphorylation of integrins, its subsequent translocation to the neurite tips where it facilitate neurite extension (Rehberg et al., 2014). The Tao family of Ste kinases are regulators of Hippo kinase signaling (Huang et al., 2014; Poon et al., 2011). The mammalian Tao kinase, Taok2, is a serine-threonine kinase that specifically regulates the development of basal, but not apical, dendrites in cortical

pyramidal neurons (Anda et al., 2012). The secreted guidance molecule Semaphorin3a activates its receptor Neuropilin, which in turn binds Taok2 and regulates Jnk kinase signaling development of basal dendrites (Anda et al., 2012). Taok2 associates with microtubules (Mitsopoulos et al., 2003), as well as mediates septin phosphorylation (Yadav et al., 2017). Mechanistically, how interaction of Taok2 with various cytoskeletal elements contributes to its role in dendritic development is not well-understood.

Elaboration of the dendritic arbor through growth and branching is fine-tuned by mechanisms of self-avoidance and tiling, which prevent redundancy and increase efficient use of receptive field (Figure 1.1 B). Dendrites avoid overlapping with other dendrites of the same neuron in a process known as self-avoidance, well-studied in Drosophila ((Grueber et al., 2003; Jan and Jan, 2010). Dendrite self-avoidance is important in order to prevent self-crossing of dendrites, clumping of dendrites as well as to maximize the receptive field. In Purkinje cells, the liver kinase B1 (Lkb1) is developmentally expressed in the dendrites. Depletion of Lkb1 in these neurons results in increased dendritic crossing (Kuwako and Okano, 2018). Exogenous expression of salt inducible kinase 1 (Sik1), a downstream target of Lkb1 kinase is able to rescue self-crossing defects through regulation of the guidance cue receptor Robo2 (Kuwako and Okano, 2018), these data suggest that the Lkb1-Sik1 kinase pathways is required for dendritic self-avoidance in cerebellar Purkinje neurons. Dendritic tiling ensures that dendrites of different neurons of the same type avoid each other (Grueber and Sagasti, 2010; Jan and Jan, 2010). Dendritic tiling has been best studied in the Drosophila peripheral sensory da neurons and in retinal ganglion cells. In flies, loss of either the serine/threonine kinase, Tricornered (Trc), or Furry (Fry), a protein required

for Trc kinase activity, leads to sensory neurons that produce excessive numbers of dendritic branches, which fail to tile normally (Emoto et al., 2004)

1.4 - Regulation of Dendritic Spine and Synapse Development by Kinases

Dendritic spines are actin-rich protrusions on the dendritic membrane of most excitatory neurons. Early in development, thin actin filopodia extend from dendritic branches, which then mature into stable mushroom shaped spines likely on contact with the axonal membrane (Matus, 2000; Yuste and Bonhoeffer, 2004). However, spines retain remarkable structural plasticity even after development, and on exposure to the right stimuli can extensively retract, morph or become larger (Hering and Sheng, 2001). Spines are enriched in F-actin that contributes greatly to their structure and plasticity (Hotulainen and Hoogenraad, 2010). Repetitive firing of synapses, such as that which occurs during high-frequency synaptic stimulation of hippocampal neurons (long term potentiation), leads to an increase in F-actin which causes the spine to enlarge (Okamoto et al., 2004). Conversely, in long-term depression, decrease in F-actin/G-actin ratio causes dendritic spine shrinkage (Zhou et al., 2004). In addition to actin, other cytoskeletal elements such as septin and microtubules regulate dendritic spine structure. In cortical and hippocampal neurons, septin proteins mark the site of dendritic filopodia extension, and are important for dendritic spine stability (Ewers et al., 2014; Xie et al., 2007; Yadav et al., 2017). Interestingly, transient entry of microtubules into dendritic spines of hippocampal neurons regulates actin dynamics and spine morphology (Jaworski et al., 2009). It is therefore, not surprising, that several kinases (Figure1.1C) and GTPases that regulate actin, septin and microtubule dynamics are implicated in spine formation and its plasticity (Hotulainen and Hoogenraad, 2010; Lin and Koleske, 2010).

Several kinases modulate spinogenesis through regulation of the actin cytoskeleton (Figure 1.1 D). In addition to their role in dendrite development (described above) the calcium/calmodulin-dependent protein kinase II (CaMKII) is important for dendritic spine formation. In hippocampal neurons, the two main neuronal CaMKII isoforms have distinct roles, while CaMKIIα regulates synaptic strength, the CaMKIIβ isoform controls dendritic spine morphology and synapse number via its ability to bundle actin filaments ((Fink et al., 2003; Okamoto et al., 2007)). Knock-in mice expressing kinase dead CaMKIIα, show impaired learning and memory as well as a loss of long-term potentiation (Yamagata et al., 2009). Neuronal activity or NMDA receptor activation regulates spine morphogenesis by mediating Ca^{2+} influx into postsynaptic neurons, which modulate the activity of many actin binding proteins, including CaMKIIβ (Lisman et al., 2002). The dual specificity kinase Dyrk1a, negatively regulates filopodia and spine formation through phosphorylation of N-WASP, an actin filament assembly protein (Park, 2009). In cultured hippocampal neurons, N-WASP activates the actin branching protein Arp2/3, which is required for spine formation (Wegner et al., 2008). LIM-kinase1 (LIMK1) inhibits the activity of actin depolymerizing protein cofilin by phosphorylation (Yang et al., 1998) and hence affects dendritic spine morphology and synaptic function (Meng et al., 2002) LIM-Kinase1 (Limk1) functions as an actin destabilizer. Hippocampal neurons in Limk1 knockout mice exhibit aberrant spines and enhanced LTP (Meng et al., 2002). Another actin destabilizing kinase is PKC, several isoforms of which are enriched at the synapse. PKC phosphorylates myristoylated, alanine-rich C-kinase substrate (MARCKS) inhibiting its ability to cross link the actin cytoskeleton to membrane thereby destabilizing dendritic spines in hippocampal neurons (Calabrese and Halpain, 2005).

Receptor tyrosine kinases, notably Trk kinase and Eph/ephrin family members are important for dendritic spine formation. TrkB acts as a receptor for the neurotrophic factor BDNF and is crucial for neuronal plasticity such as structural remodeling associated with LTP (Huang et al., 2013). In rat hippocampal slices, BDNF stimulates activity of serine/threonine kinase p21 activated kinase (Pak), which inactivates cofilin through phosphorylation causing increase in spine size and stability. TrkB also activates Ras GTPase inducing spine enlargement and stability (Yasuda et al., 2006). Eph receptors expressed on dendrites are activated by ephrins on opposing membranes such as axonal/glial. Signaling through these receptors regulate dendritic spine and synapse formation or activity induced LTP in hippocampal cultured neurons (Klein, 2009). Activation of Eph receptors leads to tyrosine phosphorylation of target molecules, such as proteoglycan syndecan-2, which clusters them at the postsynapse promoting spine maturation (Ethell et al., 2001). Activation of EphB on binding EphrinB leads to the receptor interaction with NMDA receptors and subsequent synaptic targeting of NMDA receptors (Dalva et al., 2000; Nolt et al., 2011). Further, Eph receptors also mediate structural changes in dendritic spines. Optogenetic local activation of expressed OptoEphb2 in dendrites led to rapid actin polymerization causing filopodial growth. While inhibition of Rac1 and Cdc42 did not abolish OptoEphB2-induced actin polymerization, Abelson tyrosine-protein kinase 2 (Abl2/Arg) were found to be downstream effector of filopodia growth in dendrites (Locke et al., 2018)). Hippocampal neurons derived from EphB1/B2/B3 receptor triple knockout mice are unable to form mature dendritic spines (Henkemeyer et al., 2003), consistent with the essential role of Eph tyrosine kinases in spinogenesis. Another pathway that contributes to EphB2-mediated dendritic spine

stabilization is FAK kinase that activates RhoA-ROCK-LIMK-1 pathway to suppress cofilin activity and remodel dendritic spines (Koleske, 2013; Shi et al., 2009).

In addition to actin, the septin cytoskeleton plays essential roles in dendritic spine morphogenesis (Figure 1.1 D). Septin7 localizes to the base of dendritic spines at the spine neck and is required for spine formation (Tada et al., 2007; Xie et al., 2007) and spine stability (Ewers et al., 2014) in both hippocampal and cortical neurons. The serine/threonine kinase TAOK2 directly phosphorylates Septin7 at an evolutionarily conserved residue. In cultured hippocampal neurons, phosphorylation at its C-terminal tail promotes septin7 translocation from the base of the dendritic spine to spine head, where it associates and stabilizes the synaptic scaffold protein PSD95 (Yadav et al., 2017). TAOK2 depletion or expression of phospho-dead Septin7 leads to exuberant filopodial extension and inhibits spine maturation (Yadav et al., 2017).

1.5 - Aberrant Kinase Signaling Contributes to Dendritic Dysfunction in Neurological Disorders

Structural and functional dendritic defects are strongly associated with several neurodevelopmental and psychiatric disorders including autism spectrum disorder, schizophrenia, and Down syndrome (Kulkarni and Firestein, 2012; Raymond et al., 1995). Homeostatic balance between dendritic stability and instability is perturbed during neurodegenerative diseases or injury insults such as stroke. Most neurodegenerative diseases lead to dystrophy of dendrites and synapses, with some evidence suggesting that synaptic dysfunction precedes axonal degeneration (Gan et al., 2018). The evidence implicating kinase pathways in neurological disorders, and the potential mechanisms through which mutations in these kinase pathways contribute to disease are outlined below (Table 1).

Kinase	Role in dendrite morphogenesis	Model system	Cell type/brain region	Manipulation	Phenotype	Disease association	References
ERK1/2	Activity dependent growth through gene regulation, dendritic remodeling, phosphorylation of MAP2	Rat; Transgenic mouse	Hippocampal neurons; Sympathetic neurons	Pharmacological inhibition	Loss of filopodial stability in dendritic spine formation; loss of dendritic formation	16p11.2 CNV	Wu et al., 2001; Vaillant et al., 2002; Blizinsky et al., 2016
GSK3b	Neurite growth, specification of axons	Mouse, human tau transgenic mice; postmortem brain	Cortex, spinal cord	Pharmacological inhibition	Attenuated tau hyperphosphorylation	AD	Ferrer et al., 2002; Tackenberg et al., 2013; Griebel et al., 2019
FYN	Upstream of CDK5, regulation of cytoskeletal dynamics	Mouse	Hippocampal neurons	Pharmacological inhibition	Rescues synaptic depletion	AD	Rong et al., 2001; Ittner et al., 2010; Kaufman et al., 2015
DYRK1A	Regulates filopodia and spine formation through phosphorylation of N-WASP, Phosphorylates tubulin	Mouse; transgenic mouse	Dissociated mouse cortical and pyramidal neurons	Overexpression; pharmacological inhibition	Overexpression reduces dendritic arbor and spine density. Thinner spines. Inhibition leads to reduced tau hyperphosphorylation and aggregates.	AD, DS, ASD	Courcet et al., 2012; Martinez de Lagran et al., 2012; Park et al., 2012; Ori-McKenney et al., 2016; van Bon et al., 2016; Dang et al., 2018; Melchior et al., 2019
CaMKIIa	Stabilizes dendritic arbor, regulates synaptic strength	Mouse, *Xenopus*	Hippocampal neurons, optic tectal neurons	Catalytic domain mutation (E183V)	Increased dendritic arborization and decreased dendritic spine density.	ASD	Shen et al., 1998; Wu and Cline, 1998; Küry et al., 2017; Stephenson et al., 2017; Akita et al., 2018
CaMKIIb	Promotes actin polymerization increases filopodial extension, regulation of spine number and morphology through actin bundling	Rat	Hippocampus; hippocampal neurons	RNAi KD	Reduced number of mature dendritic spines	ASD	Shen et al., 1998; Fink et al., 2003; Okamoto et al., 2007; Küry et al., 2017; Akita et al., 2018
PI3K	Growth and elaboration of dendrites through PI3k-Akt-mTOR axis, polarity	Rat	Hippocampal neurons	Pharmacological Inhibition	Reduced dendritic number and crossings	ASD, AD	Jaworski et al., 2005; Jansen et al., 2015; Winden et al., 2018
AKT	Growth and elaboration of dendrites through mTOR	Rat	Hippocampus	Constitutive activation	Increased arborization and increased spine size.	ASD	Jaworski et al., 2005; Jansen et al., 2015
mTOR	Growth and elaboration of dendrites	Mouse	Hippocampal neurons; Olfactory bulb neurons	RNA interference; Conditional knockout	Simplification of dendritic arbor	Cortex structural defects; ASD	Zhou et al., 2009; Urbanska et al., 2012; Mirzaa et al., 2016; Sato, 2016; Skalecka et al., 2016
PAK1/2	Regulation of spine size through inactivation of cofilin	Mouse; rat	Hippocampus	Knockout	Decreased number of immature dendritic spines	ASD, ID	Asrar et al., 2009; Harms et al., 2018; Horn et al., 2019; Kernohan et al., 2019
MET	Dendritic complexity, spine morphogenesis	Mouse, transgenic mouse	Hippocampal neurons	Overexpression; RNAi KD	Overexpression Increases dendritic spine density, dendritic intersections. RNAi reduces dendritic spine density and branches.	ASD	Campbell et al., 2007; Thanseem et al., 2010; Qiu et al., 2014
TAOK2	Basal dendrite development in cortical neurons, dendritic spine formation through septin 7	Mouse, rat	Cortical neurons; hippocampal neurons	RNAi KD, knockout	Reduced basal dendrite number and complexity; reduction in mature dendritic spines.	ASD, AD, 16p11.2 CNV	de Anda et al., 2012; Tavares et al., 2013; Yadav et al., 2017
CDKL5	Dendritic complexity	Mouse	Cortical neurons	Knockout	Reduction in spine density, spine stability and PSD95 puncta	CDKL5 Syndrome, ID	Weaving et al., 2004; Bahi-Buisson et al., 2012; Fuchs et al., 2014; Sala et al., 2016; Baltussen et al., 2018; Tang et al., 2019
LRRK2	Maintenance of dendritic length and branching	Mouse, *Drosophila*	Cortical neurons, slices, sensory neurons	Mutation G2019S	Mislocalized tau in dendrites leading to dendritic degeneration. Phosphorylated α-synuclein accumulation	PD	MacLeod et al., 2006; Lin et al., 2010; Di Maio et al., 2018
PINK1	Dendritic growth and arborization	Mouse	Primary cortical and midbrain dopaminergic neuron	Overexpression; knockout	Increased dendritic length on overexpression. Knockout causes dendritic length reduction.	PD	Valente et al., 2004; Dagda et al., 2014
ULK4	Pseudokinase, promotes microtubule acetylation; dendritic arborization	Mouse	Cortical neurons	Knockdown	Impaired neuritogenesis.	SZ	Lang et al., 2014, 2016; Liu et al., 2016

Table 1. Kinase signaling pathways implicated in neurological diseases and their role in dendrite development.

Autism Spectrum Disorder

Autism spectrum disorder (ASD) is a neurodevelopmental disorder with a strong genetic basis, and is defined by deficits in social communication, language development as well as repeated behaviors (Geschwind and Levitt, 2007). Several kinases have been genetically associated with autism spectrum disorders. DYRK1A has one of strongest genetic association with ASD (Iossifov et al., 2014; Rubeis et al., 2014). The encoded protein DYRK1a is a dual-specificity tyrosine phosphorylation-regulated serine/threonine kinase. Several ASD associated variants of DYRK1A affect its kinase function causing either loss or gain of kinase activity. Mouse hippocampal neurons transfected with these variants show defects in neuronal development including in dendritic outgrowth and dendritic spine density (Dang et al., 2017). Further overexpression of these pathogenic variants in developing mice embryos perturb neuronal migration in vivo (Dang et al., 2017). DYRK1A mutations lead to syndromic form of autism and intellectual disability with many shared features. DYRK1A is affected in 21q22 microdeletion in human, and is associated with growth retardation, primary microcephaly, facial dysmorphism, seizures, ataxic gait, absent speech and intellectual disability (Bon et al., 2016; Courcet et al., 2012; Ji et al., 2015; Møller et al., 2008).

Aberrant signaling through the PI3K/AKT/mTOR pathway is associated with ASD (Winden et al., 2018). A range of structural brain abnormalities are associated with mutations in the mTOR pathway. Activating mutations in PI3K/AKT/mTOR pathway result in megalencephalies and hemimegaloencephalies associated with ASD (Jansen et al., 2015). Mutations in PTEN are linked to macrocephaly and ASD (Butler et al., 2005). Pten knockout mice exhibit enlarged dendritic arbors and neuronal soma and exhibit autism-like behavior (Lugo et al., 2014). Mutations in genes involved in the mTOR signaling

pathway have been identified in some cases of syndromic ASD (Mirzaa et al., 2016). While mutations that inhibit mTOR are associated with microcephaly, hyperactive mTOR signaling is associated with monogenic ASD. Inhibition of mTOR signaling is a potential pharmacotherapy for ASD (Sato, 2016).

TAOK2 is an autism susceptibility gene encoding a serine/threonine kinase. De novo mutations in TAOK2 have been found in ASD patients (Richter et al., 2018). TAOK2 is one of the two kinases within the 16p11.2 gene locus, a region prone to copy number variations (CNV) associated with ASD and schizophrenia (Kumar et al., 2007; McCarthy et al., 2009; Weiss et al., 2008). ASD patients with 16p11.2 CNV exhibit a strong correlation between TAOK2 expression and head circumference (Luo et al., 2012). Further, Taok2 knockout mice exhibit increased total brain volume compared to wildtype (Richter et al., 2018), suggesting that perturbation in TAOK2 gene dosage might contribute to reciprocal brain size difference associated with the 16p11.2 CNV. However, mechanisms and extent to which TAOK2 might affect brain size have yet to be elucidated. TAOK2 kinase regulates the microtubule cytoskeleton (Mitsopoulos et al., 2003; Moore et al., 2000), septin cytoskeleton (Yadav et al., 2017) and RhoA signaling (Richter et al., 2018). It is likely that many of these signaling pathways converge to mediate structural changes in the brain. In cultured hippocampal neurons, depletion or expression of kinase dead TAOK2 results in a loss of mature mushroom-shaped spines (Richter et al., 2018; Ultanir et al., 2014; Yadav et al., 2017), increased shaft synapses (Yadav et al., 2017). Further in cortical neurons, TAOK2 is required for proper basal dendrite development (Anda et al., 2012). Interestingly, de novo mutations in another member of the TAO

family, TAOK1, are associated with neurodevelopmental delay (Dulovic-Mahlow et al., 2019).

Additional kinases associated with ASD are MET, CaMKII and the PAK kinases. MET is associated with ASD and encodes a receptor tyrosine kinase MET (Campbell et al., 2007; Thanseem et al., 2010). Loss or gain of function of Met leads to opposing changes in dendritic complexity, spine morphogenesis, and timing of glutamatergic synapse maturation in CA1 hippocampal neurons (Qiu et al., 2014). De novo mutations in CAMK2A and CAMK2B are associated with autism, intellectual disability and neurodevelopmental disorders (Akita et al., 2018; Chiocchetti et al., 2018; Küry et al., 2017). De novo mutation in the CaMKIIα catalytic domain (E183V) was identified in a ASD proband (Stephenson et al., 2017). In cultured hippocampal neurons, the E183V mutation reduces CaMKIIα targeting to dendritic spines, increases dendritic arborization and decreases dendritic spine density. Mice with a knock-in CaMKIIα-E183V mutation display aberrant behavioral phenotypes, including hyperactivity, social interaction deficits, and increased repetitive behavior (Stephenson et al., 2017). Characterization of 19 rare de novo CAMK2A or CAMK2B variants identified in individuals with intellectual disability revealed that mutations that decreased or increased CAMKII autophosphorylation at Thr286/Thr287 also affected neuronal migration (Küry et al., 2017). PAK1 and PAK2 kinases are associated with autism and neurodevelopmental delay (Harms et al., 2018; Horn et al., 2019; Kernohan et al., 2019). PAK1 mutations in patients with intellectual disability are located within or proximal to the autoinhibitory switch domain, suggesting a gain of function mechanism of disease (Harms et al., 2018). The Pak1/2 serine/threonine protein kinases regulate cell motility, cell cycle progression, apoptosis, or proliferation

through downstream GTPases Cdc42 and Rac1. PAK2 is encoded in the 3q29 genomic region, deletion of which can result in numerous neurodevelopmental defects including ASD (Quintero-Rivera et al., 2010). Haploinsufficiency of PAK2 in mice results in decreased spine density and synapse number in the hippocampus (Wang et al., 2018b). In addition to PAK1/2, mutations in PAK3 gene are associated with X-linked intellectual disability (Allen et al., 1998)

CDKL5 Syndrome

CDKL5 Syndrome is a rare X-linked genetic disorder that results in severe neurodevelopmental impairment, infantile seizures and intellectual disability (Weaving et al., 2004). Mutations in CDKL5 gene encoding a serine/threonine kinase is causative of the syndrome. The severity of the disease seems to depend on the site of mutation, where those in the kinase domain are more pathogenic (Bahi-Buisson et al., 2012). CDKL5 knockout mouse exhibit dendritic hypotrophy in granule cells of the hippocampus (Fuchs et al., 2014). Enhanced NMDAR signaling and circuit hyperexcitability were shown to underlie autistic-like features in mouse models of CDKL5 Syndrome (Tang et al., 2019). Recently, direct target substrates of CDKL5 in the brain were identified, which included microtubule regulators Microtubule Associated Protein 1S (MAP1S), Microtubule End Binding Protein 2 (EB2) and Rho GTPase activator ARHGEF2 (Baltussen et al., 2018). Importantly, hypophosphorylation of these targets were confirmed in vivo as well as in induced pluripotent stem cell (iPSC) derived neurons differentiated from CDKL5 patients, suggesting that these are physiologically relevant kinase and substrates. Further, this important study also identified the consensus sequence of CDKL5 phosphorylation as RPXpS motif (Baltussen et al., 2018), which will be useful for identification of other downstream substrates.

Schizophrenia

ULK4 is a rare susceptibility gene for schizophrenia (Lang et al., 2013; Tassano et al., 2018), a devastating neuropsychiatric disease with high heritability but few monogenetic associations. The ULK (UNC51-like) kinase family member ULK4 is classified as a pseudokinase, as it is catalytically inactive. While ULK can bind ATP molecules it does not have phosphotransfer activity (Khamrui et al., 2020). The expression of ULK4 is neuron-specific and developmentally regulated, and its depletion in mice leads to defects in neural proliferation, migration as well as reduced dendritic arborization of cortical neurons (Lang et al., 2016). Knockdown of Ulk4 disrupts the composition of microtubules by reducing tubulin acetylation. Targeted disruption of the Ulk4 in the cortex decreases the neural stem cell pool at birth, which significantly reduced cerebral cortex size in postnatal mice (Liu et al., 2016). The implications of these changes in pathogenesis of schizophrenia are unknown.

16p11.2 CNV Syndrome

Copy number variation (CNV) in the 16p11.2 genomic locus are strongly associated with neurodevelopmental disorders including ASD, schizophrenia, and structural brain changes (Kumar et al., 2007; McCarthy et al., 2009; Owen et al., 2017; Qureshi et al., 2014; Weiss et al., 2008). This genomic locus spans 29 annotated genes, two of which encode kinases: TAOK2 and MAPK3. Transcriptomic analysis of 16p11.2 CNV patients suggests there is a strong correlation between TAOK2 gene expression and head circumference (Luo et al., 2012). Further, TAOK2 knockout mice exhibit increased total brain volume compared to wildtype (Richter et al., 2018). Dissociated primary cortical neurons from 16p11.2 microduplication mice model show increased dendritic elaboration, which was rescued with ERK1 inhibitors (Blizinsky et al., 2016), suggesting increase in

MAPK3 dosage might contribute to changes in brain structure and function. Paradoxically, ERK1 inhibition in 16p11.2 deletion also seems to rescue cortical defects in mice models. It is important to note that mouse models of 16p11.2 CNVs do not faithfully recapitulate the human condition in terms of structural brain changes (Deshpande et al., 2017; Portmann et al., 2014), and human relevant models of this CNV are needed to understand the mechanisms of many defects associated with these CNVs. Interestingly, TAOK2 and MAPK3, are the only two genes in this locus that have been independently associated with autism (Pinto et al., 2014; Richter et al., 2018).

Down Syndrome

Down Syndrome (DS) is a severe neurodevelopmental disorder caused by presence of an extra copy (or parts) of chromosome 21 (Dierssen, 2012). Postmortem analysis of neuronal morphology in DS patients showed increased complexity of dendritic arbors in early postnatal period followed by much reduced dendritic length and arborization in older children (Becker et al., 1986). Among the DS Critical genes, increased dosage of DYRK1A has been identified to play a crucial role in the disease pathology. Dyrk1a overexpression in mouse neocortex inhibits neural stem cell proliferation and leads to premature neuronal differentiation (Yabut et al., 2010). Overexpression of Dyrk1A leads to reduced dendritic arbor complexity and synaptogenesis in layer II/III pyramidal cells, indicating this kinase is a major contributor to the dendritic phenotypes in DS (Lagran et al., 2012). Both the mammalian Dyrk1a and its Drosophila ortholog minibrain regulate dendritic morphogenesis through direct phosphorylation of β-tubulin which inhibits microtubule polymerization (Ori-McKenney et al., 2016).

Alzheimer's Disease

Alzheimer's disease (AD) is a progressive neurodegenerative disease that affects wide areas of the cerebral cortex and hippocampus. Human neuropathology data from AD patients suggests that dendritic abnormalities in AD are widespread and often are present in the early stages of disease. Dendritic abnormalities associated with AD include dystrophic dendrites, reduction in dendrite complexity, and loss of dendritic spines (Cochran et al., 2013). Hallmark features of AD include accumulation of extracellular insoluble forms of amyloid-β (Aβ) and intracellular aggregation of hyperphosphorylated microtubule associated protein tau in neurofibrillary tangles (Congdon and Sigurdsson, 2018; Giacobini and Gold, 2013). Aβ refers to peptides that are 38–43 amino acids in length, derived by the proteolytic cleavage of amyloid precursor protein (APP). Aβ is released into the extracellular matrix in oligomeric form where it is normally cleared by macrophages and microglia. Defects in efficient clearing of Aβ and certain oligomeric Aβ conformations lead to formation of fibrils that ultimately form amyloid plaques (Ittner and Ittner, 2018). Plaques induce neurotoxicity through numerous pathways, including through recruitment of the microtubule binding proteins tau (Masters et al., 2015). Experiments in hippocampal neurons show that Aβ oligomers accumulate at synapses, inducing clustering and dysfunction of metabotropic glutamate receptors (Renner et al., 2010). Exposure to Aβ oligomers disrupts polarized trafficking causing mis-sorting of axonal proteins including tau into somatodendritic compartment. Defects in axonal trafficking of tau promotes axonal degeneration and corresponding decrease in synaptic inputs (Zempel et al., 2010). Further, missorted tau in dendrites induces tubulin polyglutamylation which recruits the microtubule severing protein spastin, ultimately leading to dendritic dystrophy (Zempel et al., 2013). Of note, disease modifying

treatments targeting Aβ, have so far failed in clinical trials. Recent evidence suggests that amyloid deposition is not strongly correlated with cognition in multivariate analyses. Hyperphosphorylated tau, as well as synaptic and neuronal loss are, however, associated with memory deficits (Giacobini and Gold, 2013). AD is associated with high amount of hyperphosphorylated tau. Tau contains 77 potential serine/threonine and 4 tyrosine phosphorylation sites clustered in the proline-rich region and the tail domain adjacent to the microtubule targeting domains (Noble et al., 2013) Tau hyperphosphorylation decreases its binding to microtubules. As tau becomes progressively hyperphosphorylated, deficits in molecular chaperones and degradation contribute to tau oligomerization and paired helical filament formation, ultimately forming neurofibrillary tangles (Iqbal et al., 2016; Ittner and Ittner, 2018). Emergent evidence suggests that AD is a synaptopathy (Li et al., 2018). Synaptic dysfunction due to pathogenic Aβ oligomers and tau pathology is one of the earliest signs of disease, preceding synaptic loss and neurodegeneration (DeVos et al., 2018; Hoover et al., 2010; Selkoe, 2002). In addition to its axonal role, tau plays a dendritic function important for postsynaptic targeting of Fyn kinase, a modulator of NMDA receptor activity. Tau KO mice exhibit disrupted postsynaptic targeting of Fyn, which reverses the excitotoxicity caused by NMDA receptor dysfunction due to Aβ toxicity (Ittner et al., 2010). In addition to Fyn kinase, dysfunction in several kinase pathways have been implicated in AD. Overactivation of Gsk3β (Lauretti et al., 2020) and Dyrk1a (Coutadeur et al., 2015) has been independently shown to increase tau phosphorylation as well as Aβ production. Overactivated TAOK2 kinase was found in the neurofibrillary tangles in AD postmortem brain (Tavares et al., 2013), and its inhibition reduces tau phosphorylation in cellular models (Giacomini et al., 2018). Another

important kinase pathway that has emerged in AD is the Cdk5. Deregulation of Cdk5 by overexpression of its activator p25 triggers progressive neurodegeneration and neurofibrillary tangle formation in mice (Cruz and Tsai, 2004). In addition to its effect on microtubule stability and synaptic function, hyperphosphorylated tau promotes Aβ toxicity mediated neuropathology (Ittner et al., 2010; Mairet-Coello et al., 2013), hence targeting tau hyperphosphorylation might prove to be a viable therapeutic strategy for AD. Several small molecule inhibitors targeting kinases that phosphorylate tau are currently in clinical trial for AD (Table 2) (Krahn et al., 2020; Tell and Hilgeroth, 2013).

Kinase	Disease	Agent	Mechanism of action	Therapeutic goal	Clinical trial ID
GSK3β	AD	Tideglusib	Non-ATP competitive inhibitor of GSK3β	Reduction of tau phosphorylation	NCT00948259 NCT01350362 NCT02586935 (USA)
DYRK1A	AD DS	SM07883	ATP competitive inhibitor of DYRK1A	Inhibition of tau hyperphosphorylation, aggregation, and NFT formation	ACTRN12619000327189 (Australia)
		Epigallocatechin-3-gallate (EGCG)	Non-ATP competitive inhibitor of DYRK1A	Amelioration of DS cognitive symptoms through DYRK1A inhibition	NCT01394796 (USA)
FYN	AD	Saracatinib	ATP-competitive inhibitor of Src family of tyrosine kinases	Reduced Fyn activation by Aβ	NCT02167256 (USA)
ABL	AD	Nilotinib	ATP competitive inhibitor of ABL	Stabilization of levels of phosphorylated tau, total tau and Aβ	NCT02947893 (USA)
p38 MAPK	AD DLB	Neflamapiod	ATP-competitive inhibitor of p38 MAPK	Decrease neuroinflammatory markers, reduced decline in cognitive function	NCT03402659 NCT03435861 NCT04001517 (USA)
LRRK2	PD	DNL151	Inhibition of LRRK2 kinase	Decrease neuroinflammatory markers	NCT04056689 (USA)

Table 2. Kinase inhibitors in clinical trials for the treatment of neurological disorders.

Parkinson's Disease

Parkinson's disease (PD) is pathologically defined by the neurodegeneration of dopaminergic neurons of the substantia nigra and is characterized by the presence of cytoplasmic inclusions composed of α-synuclein protein aggregates called Lewy bodies (Poewe et al., 2017). Some of the strongest disease associated genes in Parkinson's disease encode for kinases; LRRK2 and PINK1. Mutations in leucine-rich repeat kinase 2 (LRRK2) underlie an autosomal-dominant, inherited form of PD. The PD-associated LRRK2 mutations display disinhibited kinase activity and induce a progressive reduction in dendrite length and branching in primary cortical cultures and in vivo mouse models (MacLeod et al., 2006). Increased LRRK2 kinase activity was observed in idiopathic PD, and in neurons exposed to mitochondrial toxins, suggesting that LRRK2 kinase activity might have a broader role in PD pathogenesis (Maio et al., 2018). Small-molecule LRRK2 kinase inhibitors have shown promise in preclinical models of PD, and has brought LRRK2 to the forefront of disease modifying efforts in PD (Tolosa et al., 2020). Homozygous loss of function mutations in PTEN-induced kinase 1 (PINK1) are associated with early onset PD (Valente et al., 2004). PINK1 encodes a serine/threonine kinase that acts as a sensor for mitochondrial health. In healthy mitochondria, PINK1 is targeted to mitochondria where it is rapidly degraded. In unhealthy membrane potential ($\Delta\Psi m$)-deficient mitochondria, however, PINK1 accumulates and recruits an E3-ubiquitin ligase Parkin, which in turn initiates mitophagy (Okatsu et al., 2012). Loss of function PD associated PINK1 mutations perturb normal neuronal mitophagy, and accumulated damaged mitochondria in neurons lead to disease pathology. In mouse primary cortical and midbrain dopaminergic neurons, PINK1 kinase activity was found to promote dendritic arborization and its depletion resulted in shortened dendritic length (Dagda et

al., 2014). While mechanisms through which PINK1 might regulate dendritic length are not well elucidated, there is some indication that control of mitochondrial motility and trafficking within dendrites by PINK1 could contribute to its dendritic role (DasBanerjee et al., 2017).

1.6 - Technologies to Dissect Kinase Signaling in Dendritic Structure and Function

Kinase signaling occurs in a spatiotemporally precise fashion, however, traditional biochemical tools do not provide information on when and where kinase activation occurs during neuronal development. A major challenge in understanding kinase function is the identification of direct substrates of the kinase of interest (KOI).

Kinase Sensors and Optokinases

A key method for studying temporal and spatial kinetics of kinase signaling is the use of kinase sensors (Figure 1.2A). Fundamentally, kinase sensors are comprised of two parts, a sensing unit, which is sensitive to a phosphorylation event on substrate and a reporting unit to indicate the phosphorylation state (Oldach and Zhang, 2014). Fluorescent kinase sensors work in three ways (Turk, 2005) FRET kinase sensors rely on Förster resonance energy transfer (FRET) between a fluorophore donor attached to a peptide designed to harbor the kinase specific phosphorylation site, and an acceptor fluorophore bound phospho-peptide binding motif (Sato et al., 2002). The phosphopeptide sensing motif interacts with the phosphorylated peptide, bringing donor and acceptor fluorophores together achieving resonant fluorescence that can be visualized through microscopy. Environmentally sensitive kinase sensors utilize a phosphorylation sequence peptide conjugated to a fluorophore that shifts wavelengths or intensity when in close proximity to phosphate (Sharma et al., 2008; Yeh et al., 2002). Chelation sensitive sensors use

fluorophores sensitive to Mg^{2+} concentrations found in the ATP binding site of the kinase, paired with a phosphopeptide (Shults and Imperiali, 2003). Activation of ERK, PKA, and CaMKIIα in single dendritic spines during LTP has been studied using FRET based kinase sensors ((Tang and Yasuda, 2017). Optogenetic regulation of kinases enables fast, reversible, and non-invasive manipulation of protein kinase activities providing exquisite control on regulation by bypassing upstream factors like growth factors, protein kinase inhibitors or chemical crosslinker that induce changes in kinase activity (Leopold et al., 2018). Design of opto-kinases is based on the plant photoreceptor domain light, oxygen, or voltage (LOV) or photoswitchable caging using Dronpa fluorophore. The light, oxygen, or voltage (LOV) domains are the sites for initial photochemistry in blue light photoreceptors in plant flavoprotein kinases, which have inspired creation of light activated kinases (Crosson and Moffat, 2002). LOV domains can be used to drive light mediated homodimerization of engineered tyrosine kinase domain thereby leading to their activation. The dimeric protein, pdDronpa, dissociates in cyan light and reassembles in violet light (Zhou et al., 2017). Switchable kinases have been designed by attaching two pdDronpa domains in the kinase domain thereby caging the kinase. When Dronpa dimers dissociate in cyan light it allows the kinase domains to come together to get activated, which can be rapidly shut down with violet light. Dronpa based photo-switchable (ps) psRaf1, psMEK1, psMEK2, and psCDK5 kinases were recently designed to uncover a direct and rapid inhibitory feedback loop from ERK to MEK1. Dronpa-kinases were also shown to work in vivo where they could acutely regulate synaptic vesicle transport (Zhou et al., 2017). Challenges such as low dynamic range, low signal to noise ratio, applicability to in vivo studies and control of expression level are some of the difficulties in design of

useful kinase sensors (Oldach and Zhang, 2014). Iterative sensor optimization combined with improvements in imaging capabilities will further expand the scope of kinase sensors in understanding dendritic development and function.

Kinase Substrate Identification

Cascades of protein phosphorylation downstream of kinase activation make precise identification of direct substrates difficult. A breakthrough in this field was the development of a technique that enables covalent capture of analog-sensitive kinase substrates (Figure 1.2B). This technique involves genetic engineering of the KOI to allow for utilization of bulkier ATPγS analogs. Thiophosphorylated proteins that represent direct substrates of KOI are covalently captured by thiol-reactive iodoacetyl agarose beads, and identified by mass spectrometry (Blethrow et al., 2008). As this method also yields the site of phosphorylation on the identified substrate, validation of substrate identity can be easily performed by point mutation of these sites in downstream biochemical assays. This method has been used for identification of direct targets of several kinases that play key role in dendrite morphogenesis including Cdkl5 (Baltussen et al., 2018), Taok2 (Yadav et al., 2017), and Hippo kinase members (Ultanir et al., 2012, 2014). Biological function of KOI and validated substrates can then be inferred through independent methods such as purified in vitro kinase assays and rescue of biological phenotypes with phosphomimetic substrates. An innovative application of this method was the finding that certain kinases such as PINK1, can utilize artificial ATP analogs (kinetin triphosphate), more efficiently than ATP, enhancing kinase activity of wild type as well as rescuing effects of low activity PD associated PINK1 mutant (Hertz et al., 2013). A limitation of this technique is that since phosphorylation reaction is performed in vitro in a cell or tissue lysate, the physiological context of kinase and substrate localization is lost. This can lead to false

positive substrates, and therefore further validation of candidate substrates identified through this technique is essential.

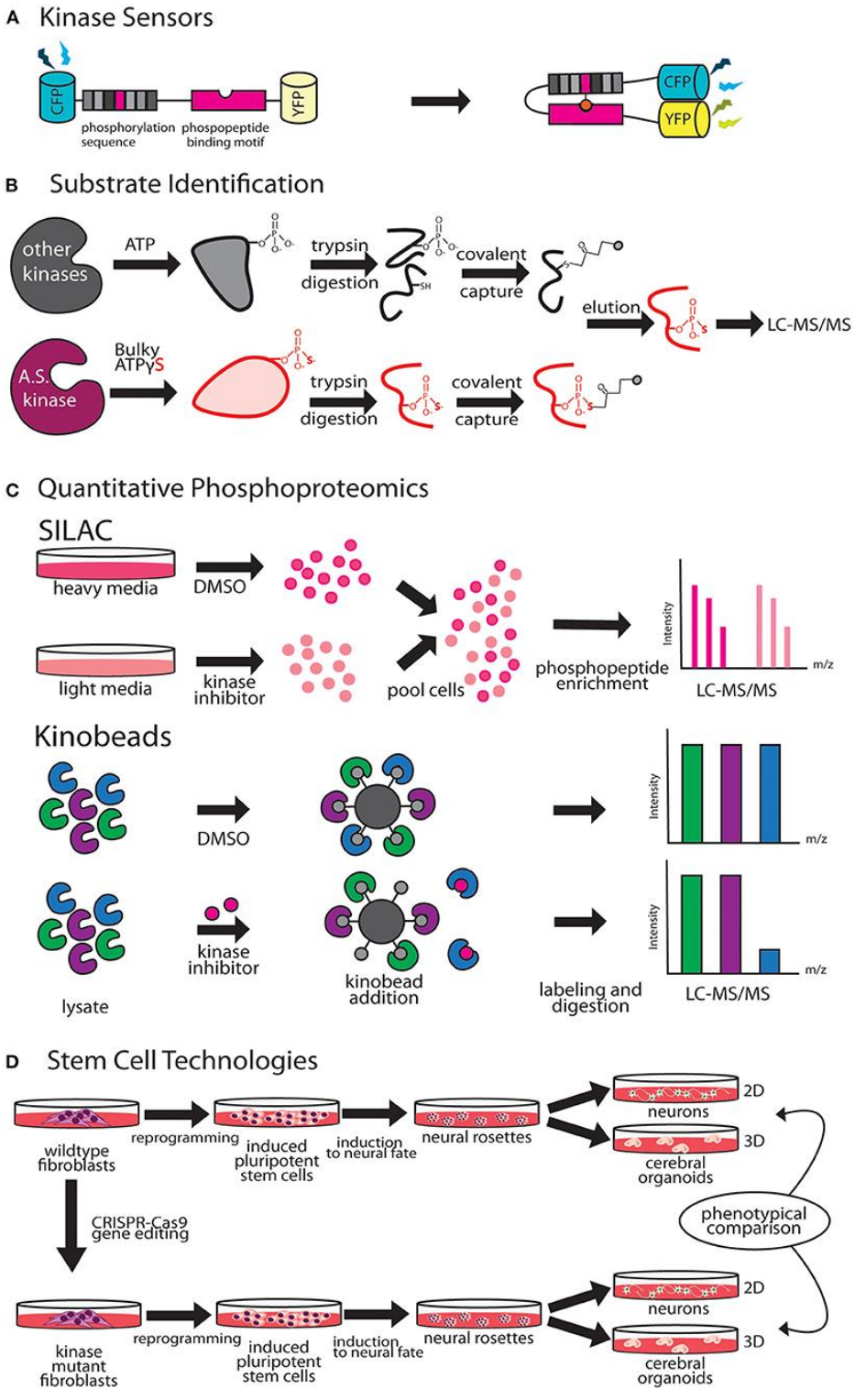

Figure 2. Emergent technologies to investigate kinase pathways

(A) FRET-based kinase sensors are comprised of kinase specific phosphopeptide sequence and a phosphopeptide binding motif.

(B) Analog-sensitive kinases are an important tool for direct substrate identification through covalent capture of phosphopeptides and mass spectrometry.

(C) Stable isotope labeling of amino acids in culture (SILAC), is a versatile metabolic labeling proteomic technique that can be applied to study the effect of kinase inhibitors on neuronal growth by quantifying changes in proteome. Kino-beads can be employed for profiling the neuronal kinome in healthy and disease states.

(D) Human iPSCs have been used to model neurological diseases associated with kinase genes.

SILAC

Stable isotope labeling by amino acids in cell culture (SILAC) is a metabolic labeling technique that can be used to incorporate amino acids carrying specific heavy and light isotopes of C and N, allowing for simultaneous identification and quantitation of complex protein mixtures (Ong et al., 2002). SILAC can be employed in neuronal cultures or in vivo animal models to detect changes in the proteomic landscape upon different genetic or pharmacological perturbations (Krüger et al., 2008; Spellman et al., 2008). Therefore, SILAC can be a powerful method to study kinase pathways during dendrite development or disease (Figure 1.2C). SILAC was utilized to identify novel interactors of Tao kinases on phosphorylation by upstream kinase Mst3, to reveal unique interaction with cytoskeletal motor protein MyosinVa (Ultanir et al., 2014). Fragile X Syndrome is caused by transcriptional silencing of Fmr1, which encodes a protein that regulates mRNA translation in neuronal dendrites. SILAC labeling revealed profound up- or down-regulation of proteins related to synaptic structure and morphogenesis, dendritic mRNA transport, and synaptic transmission in Fmr1 knockout mouse cortical synapses compared to wild type (Liao et al., 2008). Improvements in SILAC technologies include use of “spike in” SILAC that can be utilized to compare more than three distinct comparisons (Geiger et al., 2010). However, optimization of proper spike-in-standard can be time consuming and variable based on the sample type (Wang et al., 2018a).

Quantitative Phosphoproteomics

Quantitative phosphoproteomics has emerged as a powerful tool to perform unbiased and quantitative measurement of changes in signaling pathways in normal and diseased states (Hosp and Mann, 2017) Chemical labeling methods like tandem mass tag (TMT) or iTRAQ allow for multiplexing and are powerful when used with human tissue samples

as labeling is performed in vitro after obtaining the tissue lysate ((Glibert et al., 2015; Navarrete-Perea et al., 2018). Dendritic differentiation and maturation occur in distinct stages, and proteomic techniques can be applied to systematically delineate kinase pathways that mediate each of these processes. The developmental proteomic profile of cultured rat hippocampal neurons at different stages was recently mapped. Here, a combination of stable isotope labeling, and high-resolution liquid chromatography-tandem mass spectrometry (LC-MS/MS) was utilized to detect extensive remodeling of the neuronal proteome, where one third of 4,500 proteins quantified were found to undergo 2-fold change in expression during neuronal differentiation (Frese et al., 2017). Phosphoproteomic techniques are especially powerful in identification of signaling aberrations in disease states. Haploinsufficiency of the gene SHANK3 causes Phelan-McDermid syndrome (PMDS) that is associated with a high risk of autism (Mitz et al., 2018). Unbiased, quantitative proteomics revealed profound changes in the phosphoproteome of Shank3-deficient neurons, including downregulation of Akt-mTORC1 signaling due to increased steady-state levels of upstream kinase, Cdc2-like kinase 2 (Clk2) (Bidinosti et al., 2016). Pharmacological and genetic activation of Akt or inhibition of Clk2 relieved synaptic and behavioral deficits in PMDS patient-derived neurons and mouse models, thereby highlighting the value of using unbiased proteomic approaches in discovery of novel drug targets. Another powerful example is the use of phosphoproteomics screening analysis of Parkinson disease associated kinase LRRK2, in combination with different pharmacological inhibitors that uncovered Rab GTPases as key LRRK2 substrates, and pointed toward a new disease mechanism in PD (Steger et al., 2016)

Kinome Profiling

Immobilized broad-spectrum kinase inhibitors can be used in affinity pulldown to probe full-length kinases from whole neuronal or brain tissue proteomes (Bantscheff et al., 2007). This chemical proteomics method uses as multiplexed kinase inhibitor beads or kinobead-profiling enabling simultaneous profiling of over 200 kinases in a single experiment. Combining kinobead pulldown with SILAC or isobaric chemical labeling can increase analytical throughput dramatically, as well as allow comparison of proteomes from normal and disease states (Golkowski et al., 2017). In addition, kinobeads can be used to map drug-induced changes in the phosphorylation state of the kinome, enabling analysis of signaling downstream of target kinases (Golkowski et al., 2020). A limitation of kinobeads is that their applicability in providing spatial and temporal information on the kinome has not been proven. Most applications of kinobeads to date have focused on whole cell or tissue samples to query the kinome. ATP probes can be used in a similar fashion for profiling the entire kinome, kinases and other ATP utilizing proteins such as ATPases. This complementary chemical proteomic method trademarked as KiNativ, utilizes highly reactive biotinylated acyl phosphate derivatives of ATP as an affinity tag to profile the cellular kinome (Patricelli et al., 2007). In addition, the KiNativ platform can be used to determine the proteomic response to specific kinase inhibitors, which allows characterization of inhibitor interactions with endogenous kinases in native conditions (Patricelli et al., 2011). Application of these advanced kinome profiling techniques to better understand and delineate kinase signaling in dendritic development and disease states would likely reveal novel mechanistic insight (Figure 1.2C).

Modeling Dendritic Dysfunction Using iPSC Derived Neurons

Human induced pluripotent stem cell (hiPSC) derived neurons can be a powerful tool to model dendritic development and for studying how kinase signaling contributes to development and dendritic dysfunction. Stem cells can be reprogrammed from affected patient fibroblasts or from health controls, and differentiated into different neuronal and non-neuronal cell types to model neurological diseases in vitro (Dolmetsch and Geschwind, 2011; Paşca et al., 2014). There are three primary applications of this technology in studying dendrite development. First, iPSCs from healthy individuals can be gene edited using CRISPR-Cas9 to introduce truncations and single nucleotide polymorphisms (SNPs) to model the effect of kinase disease variants (Vermilyea et al., 2020) Secondly, iPSCs derived from patients with known neurological disorder can be differentiated to study neuronal development (Figure 1.2D). Forebrain cortical neurons differentiated from iPSCs derived from fibroblasts of 16p11.2 deletion and duplication carriers, exhibit opposing changes in dendritic arbor size (Deshpande et al., 2017), suggesting that reciprocal changes in neuronal size could contribute to brain size defects associated with 16p11.2 CNVs. Neurons derived from iPS cells are an excellent human cellular model for investigating neuronal development in an isogenic background. For example, female iPSCs harboring CDKL5-mutations were shown to maintain X-chromosome inactivation, with clones expressing either mutant CDKL5 allele or the wild-type allele ((Amenduni et al., 2011). Neurons differentiated from patient iPSCs with CDKL5 mutations develop increased number of dendritic protrusions (Ricciardi et al., 2012). Another study utilized iPSC derived neurons from patients with distinct mutations to show that loss of CDKL5 led to a decrease in phosphorylation of CDKL5 substrate EB2. A microtubule regulator, EB2 phosphorylation status was shown to be critical for

microtubule dynamics within dendrites (Baltussen et al., 2018). Finally, human iPSC derived 2D neuronal and 3D organoid models can be used in high throughput screens, for identification of novel modulators of dendrite development. A recent high-throughput screening of human iPSC-derived neurons focused on neurite growth employed a collection of 4,421 bioactive compounds, and identified 108 hit compounds, including 37 approved drugs, that regulate neurite growth (Sherman and Bang, 2018). Human iPSC derived neurons can be used as a preclinical model for drug toxicity tests relevant to human physiology, an issue that has hampered progress in generation of new therapeutics (Inoue et al., 2014). Continued innovation in the field of stem cell technologies have greatly improved reproducibility and reliability of iPS derived neurons. The prolonged developmental timeline of human neuronal development compared to rodents (Dolmetsch and Geschwind, 2011), however, necessitates further improvement that enable longer in vitro 2D and 3D culturing capacities, and allow for co-culturing of various brain cell types to recapitulate in vivo dendritic development, maturation and synaptic pruning (Kelava and Lancaster, 2016)

1.7 - Summary

Kinase signaling pathways act in a concerted fashion to mediate almost all aspects of dendritic development. These complex signaling pathways are elegantly intertwined, with key kinase signaling elements recurring throughout neuronal development. The human genome encodes a total of 518 kinases (Manning et al., 2002). While genetic models and genome-wide association study (GWAS) analyses have identified several kinase-encoding genes implicated in neurological disease (Krahn et al., 2020), there remains much to discover about kinase function in dendrite development and how their dysregulation contributes to neuronal disease. Unbiased mapping of kinase signaling that instruct distinct stages of dendritic growth may reveal novel pathways that can be further genetically dissected. Comparative phosphoproteomic analyses of normal and disease states will serve as a powerful tool for future identification of novel therapeutic kinase targets. Advances in neurobiological and proteomic techniques will greatly facilitate the exploration of kinase pathways that impact dendrite structure and dysfunction in disease states.

CHAPTER 2: INTRODUCTION TO THE TAO FAMILY KINASES IN NEURODEVELOPMENT AND DISEASE

2.1 - Introduction TAO family of kinases

TAO Kinases: Discovery, Structure, and Signaling

The TAO (Thousand And One) subfamily kinases are members of the sterile-20 (STE20) family of kinases. While in invertebrates such as D. melanogaster and C. elegans there is only one TAO kinase ortholog dtao encoded by tao and KIN-18 encoded kin-18 respectively (Berman et al., 2001; Liu et al., 2010), the mammalian members of this kinase family are encoded by genes TAOK1, TAOK2, and TAOK3 and express proteins of the same name (Chen et al., 1999; Hutchison et al., 1998; Tassi et al., 1999). The first member of this group of kinases, TAOK1, was originally discovered in rats during a cDNA screen for homologs of S. cerevisiae protein kinase sterile 20 protein (STE20) in S. pombe and mammals (Hutchison et al., 1998). This kinase was aptly named for its Thousand and One amino acids. Subsequently, TAOK2 was identified by the same group through similar screening methods (Chen et al., 1999). Concurrently, TAOK2 was discovered as prostate-derived STE20-like kinase (PSK1) in a degenerate polymerase chain reaction against kinase domains in prostatic carcinoma tissue samples (Moore et al., 2000). Further, TAOK3 (also known as JNK/SAPK inhibitory kinase (JIK)) was discovered in a human embryonic fibroblast expression library (Tassi et al., 1999) (Figure 2.1A).

Each of the members of the TAO family of kinases, exhibit an N-terminal kinase domain followed by a serine rich region and coiled coils (Fang et al., 2020). There is a striking sequence homology between the kinase domains of TAOK1 and TAOK2 (Chen et al., 1999), and between the kinase domains of TAOK1 and TAOK3 (Yustein et al., 2003). Notably, these kinases are ubiquitously expressed, but highly enriched in the brain and testis (Yustein et al., 2003). In the next chapters, I focus on understanding the molecular

and cellular function of the largest member of the TAO family, TAOK2 kinase, and its contribution to cellular processes.

TAOKs are upstream regulators of numerous pathways. In response to radiation or carbachol based activation of $G\alpha_0$, TAOKs are highly activated and participate in the activation of the p38/mitogen-activated protein kinase (MAPK) pathway through phosphoactivation of MAPK kinases MKK3/6 (Chen et al., 1999; Hutchison et al., 1998; Raman et al., 2007). Further, TAOK1/2 are implicated in the c-Jun N-terminal kinase (JNK)/stress-activated protein kinase (SAPK) signaling cascade through phosphorylation of MKK4/7 as a response to apoptotic triggers (Chen et al., 1999; Hutchison et al., 1998; Moore et al., 2000; Zihni et al., 2006, 2007) (Figure 2.1B).

Moreover, TAO kinases are implicated in the Hippo pathway, a kinase cascade well studied in Drosophila. Hippo signaling has several key players, mammalian STE20-like 1/2 (MST1/2) an ortholog of drosophila Hippo, Salvador-1 (SAV1), large tumor suppressor 1/2 (LATS1/2) an ortholog of drosophila Warts, and transcriptional activators Yes-associated protein (YAP) and transcriptional coactivator with PDZ binding motif (TAZ)(Jan and Jan, 2010). When activated, MST1/2 and SAV1 form a complex, MST1/2 activates LATS1/2 which then phosphorylates YAP/TAZ ensuring their translocation from the nucleus to the cytoplasm and subsequent degradation, resulting in decreased transcription of cell proliferative and anti-apoptotic genes. (Reviewed by (Ma et al., 2018)). Interestingly, this pathway is activated by dtao which phosphorylates a regulatory site on the activation loop of Hippo (Boggiano et al., 2011). This phosphorylation event is evolutionarily conserved as TAOK3 phosphorylated MST1/2 (Boggiano et al., 2011; Poon et al., 2011). Furthermore, TAOK1/3 can bypass MST1/2 and phosphorylate LATS1/2

directly to inhibit YAP/TAZ (Plouffe et al., 2016). These studies show a highly interesting and dynamic role in TAO subfamily kinases in cellular signaling.

(A)

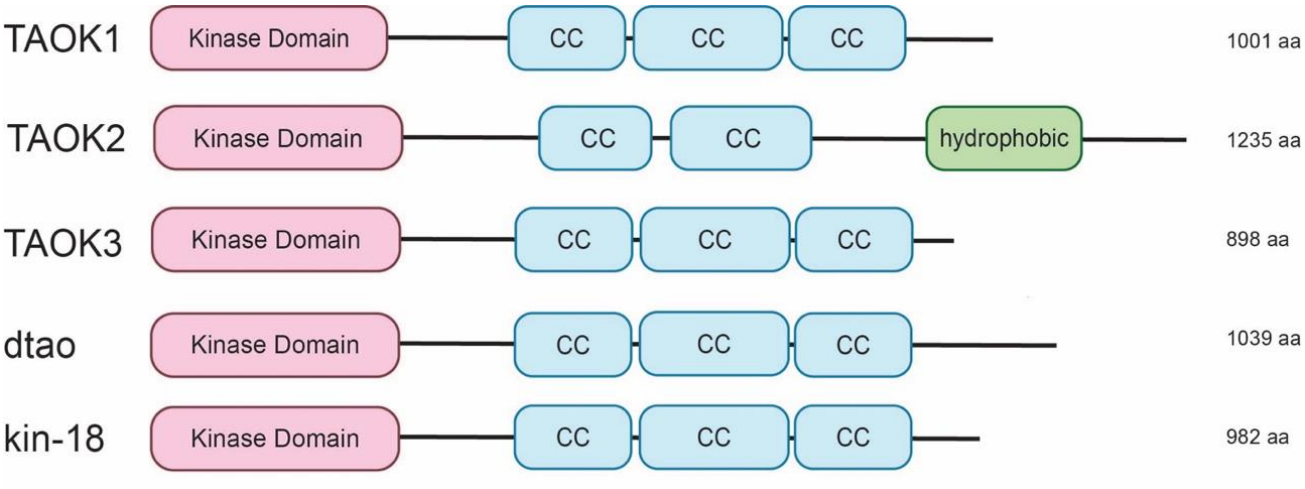
TAOK1
Kinase Domain
CC
CC
CC
1001 aa
TAOK2
Kinase Domain
CC
CC
hydrophobic
1235 aa
TAOK3
Kinase Domain
CC
CC
CC
898 aa
dtao
Kinase Domain
CC
CC
CC
1039 aa
kin-18
Kinase Domain
CC
CC
CC
982 aa

(B)

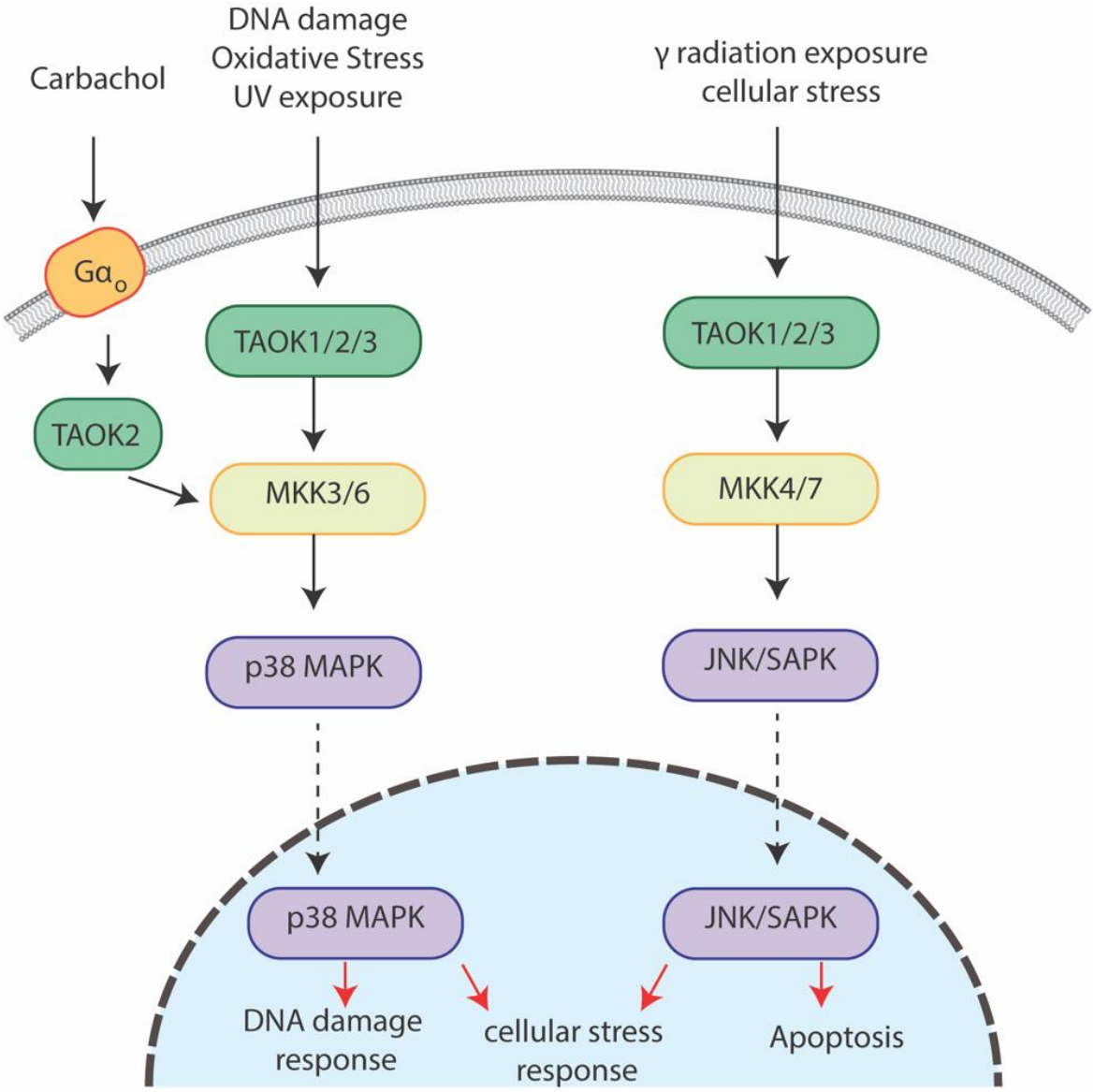
Carbachol
DNA damage
Oxidative Stress
UV exposure
γ radiation exposure
cellular stress
Gαo
TAOK1/2/3
TAOK1/2/3
TAOK2
MKK3/6
MKK4/7
p38 MAPK
JNK/SAPK
p38 MAPK
JNK/SAPK
DNA damage response
cellular stress response
Apoptosis

Figure 2.1 TAO kinases have highly conserved features and are activated in response to numerous factors.

(A) Depicts human TAOK1, TAOK2, TAOK3, Drosophila tao (dtao), and C. elegans isoform kin-18 with N-terminal kinase domain and coiled coil regions. Protein length labeled on right side.

(B) Depicts TAOK1/2/3 activation and resultant downstream pathway activation in response to cellular stress, oxidation, DNA damage, radiation and carbachol.

2.2 - TAO kinase subfamily in neurodevelopment

TAO kinases are essential for regulation of actin and microtubule cytoskeleton

The TAO subfamily kinases are highly involved in the regulation of the actin and microtubule cytoskeleton. TAOK1 plays an indirect role in microtubule destabilization through the phosphoactivation of microtubule affinity-regulating kinase (MARK) resulting in increased phosphorylation of tau and other microtubule associated proteins (MAPs) (Timm et al., 2003, 2006, 2008). Further, TAOK1 has been shown to interact with sprout-related protein with EVH-1 domain1 (Spred1) and testis-specific protein kinase (TESK1) (Johne et al., 2008). TESK1 is a protein kinase phosphorylates cofilin resulting in stabilized actin and binds to TAOK1 to inhibit microtubule stabilization (Johne et al., 2008). Spred1 can inhibit TESK1 kinase function but does not change TESK1-mediated TAOK1 inhibition resulting in stabilized microtubules but highly dynamic actin when in complex (Johne et al., 2008)

TAOK2, when microinjected into cells results in a loss of actin organization from long parallel bundles to disorganized shorted fragments in the cell periphery or a marked decrease in actin stress fibers (Moore et al., 2000). This loss of organization is a consequence of TAOK2 kinase activity as the kinase-dead mutant does not share this effect on actin cytoskeleton (Moore et al., 2000) Interestingly, it was found that TAOK2 colocalizes with microtubules leading to nocodazole resistant, stabilized microtubules which were consequently highly acetylated (Mitsopoulos et al., 2003). Further, it was found that, TAOK2 kinase activity was not required for microtubule localization and that it was conferred by the c-terminal 295 amino acids (Mitsopoulos et al., 2003). Additionally, it was shown that TAOK2 can phosphorylate both α and β tubulin (Mitsopoulos et al.,

2003). It is worth noting, the research into the interaction of TAOK2 and microtubules is a remarkable and important study but does not show direct binding.

In drosophila, dtao localizes to microtubules similarly to TAOK2 but behaves similarly to TAOK1 in destabilizing microtubules through its kinase activity (Liu et al., 2010). A striking phenotype was shown when dtao was depleted or kinase dead dtao was expressed, rather than microtubules undergoing catastrophe when entering the actin-rich lamellipodia the microtubules continued growing resulting in elongated microtubule-rich projections (Liu et al., 2010). This interaction suggests that dtao is one of the linking nodes between the actin and microtubule cytoskeleton.

TAO kinases influence Axonal Growth

The axon is a specialized outgrowth of the neuron important for delivery of afferent signals toward the next neuron on which a synapse is made, reviewed by (Gibson and Ma, 2011). Axons are specified early in neuronal development and are the longest and most narrow neurite (Bradke and Dotti, 1999; Witte and Bradke, 2008). These long processes are rich in stabilized microtubules and led by the actin-rich axonal growth cone in response to axonal guidance cues (Bradke and Dotti, 1999; Witte and Bradke, 2008). Though it is not well understood whether and how TAOKs contribute to axonal growth and elongation, some data suggests that this family of kinases could be involved. TAOK1 mediated phosphorylation of PAR1 resulting in increased phosphorylation of tau, an axonal specific stabilizing microtubule associated protein (Timm et al., 2003); TAOK1 and TAOK2 can directly phosphorylate tau (Tavares et al., 2013). TAOK2 is enriched in the axonal growth cone during neuronal development and is activated by axonal guidance molecules semaphorin3a and neuropilin (de Anda et al., 2012). Fascinatingly, depletion of TAOK2 results impairments in the formation of axon in vitro while overexpression results in a

higher fraction of multi-axonal neurons (de Anda et al., 2012). In both mice transfected in utero with TAOK2 shRNA as well as knockout mice decreased corpus callosum density was reported indicating decreased callosal axons across the midline between the cortical hemispheres (de Anda et al., 2012; Richter et al., 2018). Defects in dtao can result in impaired axonal guidance in the mushroom body of the fly brain (King et al., 2011). Moreover, it has been suggested that dtao interacts with par-1 to control microtubule dynamics during axonal development through tau. These data together suggest that TAO family kinases are important signaling molecules necessary for proper axonal development.

TAO kinases influence dendritic growth and spine formation

As cytoskeletal regulatory kinases that are highly expressed in the brain, it is no surprise that the TAO family of kinases play a role in dendrite formation and spinogenesis. Through knockdown studies, it was determined that TAOK2 is implicated in the arborization of basal dendrites through activation of the JNK signaling pathway (de Anda et al., 2012). Further studies, through a chemical-genetics screen, have shown that TAOK1 and 2 are both substrates of mammalian STE20 3 MST3, a serine/threonine kinase of the hippo family (Ultanir et al., 2014). Phosphorylation by MST3 at T468 allows for proper formation of dendritic spines and association of TAOK1/2 to association with actin motor protein, Myosin Va, for recruitment to the dendrites (Ultanir et al., 2014). Subsequently, it was found that loss of TAOK2 catalytic activity leads to a loss of mature, mushroom-shaped dendritic spines but instead the formation of filopodial protrusions, leading to the formation of shaft-synapses (Yadav et al., 2017). Further probing using chemical genetics and mass spectrometry showed that TAOK2 phosphorylates Septin7 to translocate it to the dendritic spine where it stabilizes the post-synaptic density protein PSD-95 (Yadav et al., 2017).

Interestingly, alternatively spliced variant of TAOK2, TAOK2β is activated by arcadlin to activate p38 MAPK which in return phosphorylates TAOK2β c-terminus allowing for the endocytosis of N-cadherin-arcadlin complex at the hippocampal neuron synapse (Yasuda et al., 2007). The drosophila ortholog of the TAO kinases, dtao is expressed throughout dendritic arborization (da) neurons, however, the phospho-activated form specifically localizes in dendrites (Hu et al., 2021). In direct opposition with the TAOK2 knockout mouse (Richter et al., 2018), the tao knockout fly shows increased dendritic complexity (Hu et al., 2020) (Figure 2.2).

TAO kinases are implicated in neurological disease

Given the vast role of TAO kinases in neuronal development and neuronal cytoskeleton, it is unsurprising that these kinases are implicated in neuronal diseases. De novo variants of both TAOK1 and TAOK2 have been found in patients with neurodevelopmental disorders (NDD) (Dulovic-Mahlow et al., 2019; Richter et al., 2018; Woerden et al., 2021). Initially, an extremely rare microdeletion on the genomic locus encoding TAO1, 17q11.2 was found in a microcephalic patient with NDD (Xie et al., 2016) and subsequently, two tandem deletions were found in other patients with NDD (Cooper et al., 2011). Further, through analysis of exome sequencing data from patients with NDDs such as delayed speech and language development, intellectual deficiency autism spectrum disorder (ASD), motor development delay, and macrocephaly, were analyzed to find distinct mutations in the gene, two of which may act with dominant-negative effect (Dulovic-Mahlow et al., 2019; Woerden et al., 2021). TAOK2 is encoded in 16p11.2, a genetic locus that is susceptible to copy number variations such as microdeletion and microduplications which are connected to ASD and schizophrenia respectively (Weiss et al., 2008; McCarthy et al 2009). Through genome-wide association studies in ASD

patients, 24 TAOK2 variants were found including one loss of function mutant, encoded as A135P, in the α isoform and a gain of function mutant encoded as P1022* in the β isoform (Richter et al., 2018). Further, this study produced used a Taok2 knockout and haploinsufficient mouse that exhibited dose-dependent increases in brain size and decreased social behavior (Richter et al., 2018). Fascinatingly, in previous studies, Taok2 knockout mice have displayed quick recovery from alcoholic sedative effects, increased alcohol consumption, and reduced place preference suggesting that TAOK2 may play a role in addiction (Kapfhamer et al., 2013). Similarly, mutations in dtao result in decreased sensitivity and diminished behavioral responses to cocaine and nicotine (King et al., 2011). Considering that TAOK1/2 phosphorylate tau (Travers et al., 2013), it is predictable that these kinases are implicated in Alzheimer's Disorder (AD) where tau is aberrantly hyperphosphorylated to form neurofibrillary tangles (Giacomini et al., 2018). Catalytically activated TAOK1/2 colocalize with phosphorylated tau in post-mortem brain slices of AD patients (Giacomini et al., 2018). Finally, TAOK3 is also implicated in neuronal disease as a unique substrate of Leucine-rich repeat kinase 2 (LRRK2), a kinase that is often mutated to be highly active in Parkinson's Disease (Zach et al., 2010). The TAOK family of kinases are highly interesting to study due to their involvement in diverse functions from cytoskeletal reorganization to neuronal development and their implications for disease.

Kinase signaling drives numerous components of neuronal development such as establishment of polarity, dendritic growth and arborization, dendritic spine formation, and synaptogenesis. Thousand And One amino acid Kinases (TAOKs) are a subfamily of sterile-20 (STE20) kinases possessing an N-terminal kinase domain and diverging C-

terminal extended regulatory domains. As an evolutionary conserved kinase TAO kinases have been shown to play important role in neuronal development in rodents and invertebrates. Recent studies have linked de novo variants of human TAOK1/2 to neurodevelopmental diseases, thus making it imperative to understand their role in neuronal development. Despite its disease association, the molecular functions of TAO kinases remain unknown. **Here, I focus on understanding the molecular and cellular function of the largest member of the TAO family, TAOK2 kinase, and its contribution to cellular processes.** I find that TAOK2 is an endoplasmic reticulum (ER) resident multi-pass membrane-spanning kinase that localizes to distinct junctures of the ER through six transmembrane helices and an amphipathic helix. Additionally, I found that TAOK2 associates to microtubules directly and with high affinity through its cytoplasmic facing C-terminal tail. Furthermore, TAOK2 acts as a functional ER-microtubule tether, knockout of which leads to increased ER motility, increased microtubule growth, but decreased ER tip attachment-complex movement. We determine that TAOK2 interacts with microtubule plus end binding EB proteins through a distinctive SxIP motif. Finally, I determine that TAOK2 microtubule binding is regulated by its catalytic activity, loss of which leads to perturbations of ER and microtubule motility. This work identifies TAOK2 as an ER-microtubule tether and reveals a kinase-regulated mechanism for control of ER dynamics critical for cell growth and division. To further understand the context of TAOK2, I propose the use of proximity labeling utilizing BioID2 and mass spectrometry. I lay out the blueprint for these experiments and the preliminary data from pilot experiments. Finally, I provide implications of these findings on how TAOK2 function as an ER-microtubule tether might contribute to neurodevelopment.

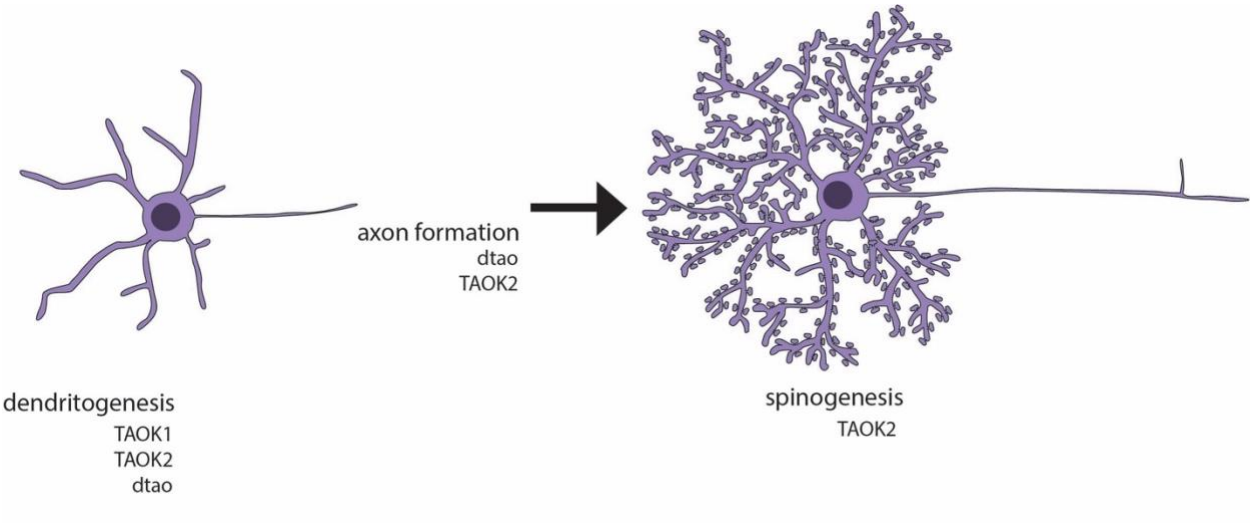

Figure 2.2 – TAO kinases in neuronal development

Schematic depicting TAO kinases and their involvement in dendrite formation, axon formation and dendritic spine formation.

2.3 Project Aims

Important for several aspects of neurodevelopment, TAOK2 is expressed in both neural progenitor cells and in neurons during early brain development. TAOK2 knockout mice exhibit defects in dendritic arborization and dendritic spine maturation. Recently, targeted sequencing has uncovered several TAOK2 mutations in ASD patients. Despite the growing evidence for the role of TAOK2 in neuronal development, the mechanisms through which aberrations in TAOK2 signaling lead to neurodevelopmental deficits remain unknown. TAOK2 is a large multidomain kinase comprised of 1235 amino acids, and has been highly characterized on the basis of catalytic activity and kinase domain (Chen et al., 1999). However, the functions of the remaining 900 amino acids of TAOK2 remains largely uncertain and ambiguous. In the last two chapters, I have described the importance of kinase signaling in neuronal development and the known functions of TAO kinases. Understanding the molecular basis of TAOK2 function and regulation of such will allow for greater understanding of how TAOK2 can influence dynamic processes such as neuronal development. I have dedicated my graduate studies to uncovering the function of this so-called regulatory domain using a cell biological and biochemical approach.

The central hypothesis of this thesis is that TAOK2 is membrane-associated, microtubule-binding kinase whose function is sensitive to catalytic activity.

Aim 1: Ascertain how structural domains in TAOK2 contribute to its physiological function

TAOK2 has an N-terminal kinase domain, associates with microtubules, and is predicted to have 6 putative transmembrane domains. How these different domains facilitate its function during neuronal development is unclear.

Aim 1.1: Determine if TAOK2 is the localization and nature of binding conferred by six putative transmembrane helices.

Aim 1.2: Characterize TAOK2 c-terminal microtubule-binding domain to determine the minimal region necessary for binding.

Aim 2: Elucidate the role of TAOK2 mediated ER-microtubule tethering in ER movement and dynamic restructuring.

ER-microtubule tethering is important for ER growth and movement especially in the processes wherein the ER and cytoskeleton are largely restructured such as mitosis. In aim 1, I found that TAOK2 is a multi-pass ER-resident protein that binds directly to microtubules, likely acting as an ER-microtubule tether. Here, I will further delve into the minimal elements necessary for tethering and how ER-microtubule tethering contributes to ER and microtubule dynamics and cell division.

Aim 2.1: Determine the minimal tethering elements of TAOK2 necessary for ER-microtubule tethering.

Aim 2.2: Ascertain the role of TAOK2 KO on ER and microtubule dynamics during interphase and mitosis

Aim 3: Establish how TAOK2 contributes to tip-attachment complex (TAC) movement of the ER.

TAOK2 knockout lowers the number of ER TAC movements but increases overall ER motility. In this aim, I will focus on how TAOK2 contributes to ER TAC movement.

Aim 3.1: Uncover if and how TAOK2 interacts with canonical TAC proteins end binding protein 1 (EB1) and stromal interaction molecule 1 (STIM1).

Aim 3.2: Elucidate the role of TAOK2 SxIP motif on EB1 binding and microtubule-binding.

Aim 4: Classify the role of TAOK2 catalytic activity on ER-microtubule tethering.

TAOK2 acts as an ER-microtubule tether, but what is the key to the regulation of this tethering function? This aim will allow us to further understand if and how TAOK2 catalytic activity contributes to tethering.

Aim 4.1: Characterize the role of TAOK2 kinase activity on ER motility and microtubule plus-end growth

Aim 4.2: Determine how expression of catalytically dead TAOK2 influences cell division.

Aim 5: Identify proteins that specifically interact with TAOK2 in neurons using BioID2

Given that TAOK2 is an ER-microtubule tether important for various cellular processes, understanding the pathways and proteins with which it interacts will give an insight to the contribution of TAOK2 neuronal development.

Aim 5.1: Utilize BioID2 to create a list of potential TAOK2 interactors in both HEK293T cells and neurons.

Aim 5.2: Validate and interpret hits to determine pathways and processes in which TAOK2 is implicated.

These experiments will allow us to understand the molecular basis of TAOK2 function in neuronal development.

CHAPTER 3: TAOK2 IS AN ER-LOCALIZED KINASE THAT CATALYZES THE DYNAMIC TETHERING OF ER TO MICROTUBULES

3.1 - Summary

The endoplasmic reticulum (ER) depends on extensive association with the microtubule cytoskeleton for its structure, function, and mitotic inheritance. The identity of molecular tethers that mediate ER-microtubule coupling, and mechanisms through which dynamic tethering is regulated are poorly understood. Here, we identify, Thousand And One amino acid Kinase 2 (TAOK2) as a pleiotropic protein kinase that mediates tethering of ER to microtubules. We show that TAOK2 is a unique multi-pass membrane spanning serine/threonine kinase localized in distinct ER domains via six transmembrane helices and an adjacent amphipathic region. Using in vitro and cellular assays, we find that TAOK2 directly binds microtubules with high affinity. We define the minimal TAOK2 determinants that induce ER-microtubule tethering and delineate the mechanism for its autoregulation. While ER membrane dynamics are increased in TAOK2 knockout cells, the movement of ER along growing microtubule plus-ends is disrupted in absence of TAOK2. Distinct microtubule binding region and an SxIP motif, confer TAOK2 with the ability to associate with microtubule lattice as well as microtubule plus ends through interaction with EB proteins. We show that ER-microtubule tethering is tightly regulated by catalytic activity of TAOK2 in both interphase and mitotic cells, perturbation of which leads to profound defects in ER morphology, its association with microtubules and cell division. Our study identifies TAOK2 as an ER-microtubule tether and reveals a kinase regulated mechanism for control of ER dynamics critical for cell growth and division.

3.2 - Introduction

The endoplasmic reticulum is an expansive and complex membranous cellular organelle. Composed of a continuous interconnected web of membrane sheets and tubules, the ER has distinct domains; namely the nuclear envelope, the rough ER sheets and smooth peripheral ER tubules (Voeltz et al., 2002). In addition, the ER makes specialized membrane contact sites with other organelles and the plasma membrane (Scorrano et al., 2019; Wu et al., 2018). Each of these domains are thought to be structurally discrete regions of the ER serving specialized physiological functions. This vast network of ER membranes relies on the microtubule cytoskeleton not only for structurally supporting its intricate shape and functional domains, but also for its motility and remodeling in response to stimuli. In animal cells, ER tubules align along microtubules (Terasaki et al., 1986). Disruption of microtubules by depolymerization agent nocodazole collapses the reticulated ER network into primarily ER sheets around the nucleus (Terasaki and Reese, 1994). In addition to its structural dependence, movement of ER membrane tubules occurs on microtubule tracks. The ER membranes utilize the microtubule cytoskeleton as tracks for movement[13-15]. Three distinct mechanisms of ER motility have been defined; (1) 'sliding' movements are kinesin-based rapid movement, (2) 'tip-attachment complex' (TAC) movements occur when the ER attaches to the MT plus ends and tracks along the growing MT (Friedman et al., 2010; Waterman-Storer and Salmon, 1997), and (3) ER 'hitchhiking' where ER tubules comigrate with an associated organelle such as endosome, peroxisome or lipid droplets (Guo et al., 2018). Stabilization of microtubules by the drug taxol prevents new microtubule growth, and also inhibits ER tubule extension (Terasaki and Reese, 1994).

Motor mediated ER ‘sliding’ movement occurs on stable acetylated microtubules (Friedman et al., 2010). Motor independent ER tubule extension along growing microtubule plus-ends is also dependent on microtubules and is carried out by the tip attachment complex (TAC) composed of ER protein STIM1 and microtubule plus-end protein EB1 (Waterman-Storer and Salmon, 1998). Additionally, membrane contact sites between ER and organelles appear to be supported by microtubules. For example, ER-mitochondria contact sites are preferentially aligned with acetylated microtubules (Friedman et al., 2010). Endosome maturation occurs at junctions where ER-endosome contact sites and microtubules converge (Wu and Voeltz, 2021). Store-operated calcium entry occurs through the Stim1-Orai channels at ER-plasma membrane contact sites (Grigoriev et al., 2008). Stim1 interaction with microtubules plays a facilitative role in organizing Stim1 for optimal Ca2+ sensing through its interaction with Orai channels (Smyth et al., 2007). In geometrically complex cells such as neurons, the ER is dependent on microtubules for its distribution throughout the fine processes such as dendrites, dendritic spines and axons. Presence of fine caliber ER tubules in axons is critical for neuronal polarity and is dependent on ER membrane interactions with microtubules (Farías et al., 2019). On the other hand, unlike elongated ER in axons and dendrites, which is closely associated with microtubules, ER organization at dendritic branch points and dendritic spines is structurally complex and exhibits decreased microtubule association (Cui-Wang et al., 2012). Bidirectional regulation of ER-microtubule tethering, therefore, not only influences ER morphology but can also dictate cell shape and function. Identity of molecular tethers that mediate ER-microtubule coupling, and mechanisms through which tethering is physiologically regulated are not well understood. Studying

ER-microtubule association and its feedback control is challenging, owing to the considerably expansive morphology of the ER, one that exhibits extreme overlap with the microtubule cytoskeleton. The nanoscale organization of sites at which ER is coupled with microtubules and its molecular composition is unclear. Constantly in flux, ER membranes undergo a range of dynamic and structural changes including membrane extension, retraction, three-way junction formation and tubule fusion (Pendin et al., 2011). Cell division brings about extensive ER remodeling, causing the ER membranes to coalesce around the spindle poles, but remain largely absent from the mitotic microtubule spindle at metaphase (Jongsma et al., 2015; Smyth et al., 2015). Before insight into ER-microtubule dynamics and its physiological regulation can be gained, the mechanisms through which molecular tethers drive ER-microtubule association must be understood. Here, we investigate ER-microtubule association in interphase and mitotic human cells and identify TAOK2 as an ER localized multifunctional protein kinase that serves as a molecular tether linking ER to microtubules. An ER-microtubule tether should in principle be ER localized and be capable of direct and strong binding to microtubules. The tether would likely be under physiological regulation such that ER-microtubule binding can not only be ectopically induced, but also importantly turned off. Loss of molecular tether should disrupt ER association with microtubules. Our study demonstrates that the kinase TAOK2 meets all the above criteria of a bona fide ER-microtubule tethering molecule.

Thousand And One amino acid (TAO) kinases are ubiquitously expressed serine/threonine protein kinases belonging to the Ste20 kinase family (Chen et al., 1999; Manning et al., 2002). While there is only one Tao kinase encoding gene in invertebrates, three distinct TAOK genes are expressed in human (Chen et al., 2003; Manning et al.,

2002). The encoded kinases TAOK1, TAOK2 and TAOK3 share a highly conserved N-terminal kinase domain, followed by distinct C-terminal domains (Chen et al., 2003; Manning et al., 2002). TAO kinases were originally identified as stress sensitive kinases that activate the p38 kinase cascades through activation of MEK kinases (Chen et al., 1999). Among the TAO family of protein kinases, TAOK2 coordinates several aspects of neuronal development and function (Nourbakhsh and Yadav, 2021). TAOK2 is highly expressed during neuronal development and is important for basal dendrite formation as well as for axon elongation in cortical neurons (de Anda et al., 2012). TAOK2 is enriched in dendritic spines and is essential for their formation and stability (de Anda et al., 2012; Ultanir et al., 2014; Yadav et al., 2017). TAOK2 knockout mice exhibit cognitive and social-behavioral deficits and show structural changes in brain size (Richter et al., 2018). Recently, mutations is TAOK2 have been associated with autism spectrum disorder, with several mutations present outside the kinase domain of the protein (Richter et al., 2018). Despite its clear relevance to human development and its disease association, little is known about the molecular and cellular functions of TAOK2 kinase.

In our study, we demonstrate that TAOK2 is a pleiotropic protein, with distinct catalytic kinase and ER-microtubule tethering functions, mediated through defined and dissociable domains. TAOK2 is enriched at junctions where the ER membrane makes contacts with the microtubule cytoskeleton. We show that TAOK2 is embedded in the ER membrane through transmembrane helices, and an amphipathic region that limits its localization to discrete subdomains of the ER. The cytoplasm facing ER-anchored C-terminal tail of TAOK2 directly binds microtubules with high specificity and is essential for tethering of the ER membranes to microtubules. The ER and microtubule binding domains together

are sufficient for inducing ectopic tethering of ER to microtubules. TAOK2 knockout cells display significantly reduced overlap of ER membrane with microtubules and increased ER membrane movement in absence of tethering to the microtubule cytoskeleton. Additionally, we found that Stim1-EB1 mediated extension of

ER tubules on growing microtubule plus tips is significantly decreased in TAOK2 knockout cells. We show that TAOK2 can associate with EB1 through the conserved SxIP motif in its C-terminal tail. Further, we show that the tethering function of TAOK2 is negatively regulated by its kinase activity. During mitosis, we find that TAOK2 is highly activated, and inhibition of its catalytic function prevents ER disengagement from the mitotic spindle causing profound mitotic defects. This study identifies TAOK2 as an ER protein kinase and elucidates a hitherto unknown autoregulated mechanism for ER-microtubule tethering important for ER dynamics and mitotic segregation.

3.3 - Results

TAOK2 is a multi-transmembrane protein kinase that resides on the endoplasmic reticulum

To investigate the unique role that non-kinase domains of TAO family members might impart on their biological function, we performed bioinformatic analysis of secondary protein structure of TAO kinases. We found that TAOK2a (hereafter TAOK2) harbors unique hydrophobic regions in its C-terminal domain not present is its alternatively spliced isoform TAOK2b or paralogous genes TAOK1 and TAOK3. Sequence analysis of TAOK2 through the transmembrane helix prediction software TMHMM2.0 (Krogh et al., 2001) indicates that TAOK2 is a multipass membrane protein containing six distinct hydrophobic regions (Figures 3.1A and 3.1B). Additional predicted region of hydrophobicity following

the predicted transmembrane domains was analyzed using AMPHIPASEEK (Combet et al., 2000) and HeliQuest (Gautier et al., 2008). This analysis revealed an amphipathic helical (AH) region with a sharply defined hydrophobic face (hydrophobicity <H>=0.75, hydrophobic moment <mM>=0.4) and a polar face rich in positively charged residues (net charge z=4) (Figure 3.1A inset). To further gain insight into the structural domains of TAOK2, we used the artificial intelligence driven protein structure prediction software AlphaFold2.0 (Jumper et al., 2021). The prediction revealed a coiled coil bundle that folded over length of the kinase domain and transmembrane region, six transmembrane helices followed by another helical region that was predicted to be amphipathic by AMPHISEEK. The C terminal tail was predicted to be likely intrinsically disordered region (Figure 3.S1A).

To determine the cellular localization of the membrane spanning TAOK2 kinase, we generated a rabbit polyclonal antibody against the unique C-terminal tail (residues 1220-1235) of TAOK2a (Figure 3.1B). Antibody staining in HEK293T and HeLa cells revealed that endogenous TAOK2 colocalized extensively with the expressed ER marker EGFP-Sec22b (Figures 3.S1B). We noted that TAOK2 exhibited a striking localization on subdomains of the ER membrane in distinct punctate pattern. Therefore, we generated a GFP-tagged TAOK2 construct and performed super resolution microscopy (super resolution by optical reassignment using SoRa disk) to visualize the ER localization of TAOK2 at higher resolution (Figure 3.1C and D). GFP-TAOK2 localized on the ER membrane and was present in discrete membrane subdomains in both HeLa cells as well as HEK293T cells. Manders' overlap coefficient was used to quantify the overlap of the GFP-TAOK2 and endogenous TAOK2 with the ER marker EGFP-Sec22b (Figure 3.1D).

To test biochemically whether TAOK2 is an ER membrane protein, we fractionated HEK293T cell homogenates into ER membrane fraction using differential centrifugation (Hoyer et al., 2018). TAOK2 was enriched in the ER membrane fraction along with other known ER membrane proteins such as STIM1 (Grigoriev et al., 2008) and Rtn3a (Hu et al., 2008). 97.6% of the total TAOK2 in the post-nuclear homogenate was enriched in the ER fraction, as compared to 6.17% of tubulin (Figure 3.1E). On differential centrifugation, TAOK2 partitioned in the membrane fraction but not the cytoplasmic fraction, and treatment with detergent led to its release in the supernatant (Figure 3.1F). To identify the mechanism through which TAOK2 achieves its ER localization, we generated four GFP-tagged deletion constructs (Figure 3.1G) which were transiently expressed in HEK293T cells with the ER membrane marker ER-mRFP (Snapp et al., 2006). Truncated construct lacking the transmembrane and amphipathic helices (1-622) was entirely cytosolic, while the six transmembrane helices alone (amino acids 941-1066) were sufficient to target the kinase to the ER (Figure 3.1H). This construct containing just the TAOK2 transmembrane domains localized uniformly throughout the ER (Figure 3.1H) and was not restricted to ER subdomains like the full length GFP-TAOK2 or the endogenous TAOK2 (Figure 3.1C, 3.S1B). We found that the predicted amphipathic helical region together with the transmembrane domains (amino acids 941-1162) is required for localization of TAOK2 to discrete ER subdomains (Figure 3.1H) and captures the localization patterns of the endogenous TAOK2 protein. TAOK2 did not show significant overlap with other organelles that we tested such as mitochondria, Rab5 positive endosomes and lysosomes (Figure 3.S1C). Therefore, using super resolution microcopy and biochemical assays, we show that TAOK2 is an ER resident protein kinase. Further, our data show

that TAOK2 associates with the ER through its six transmembrane helices, while the amphipathic region confers its localization to distinct punctate subdomains within the ER.

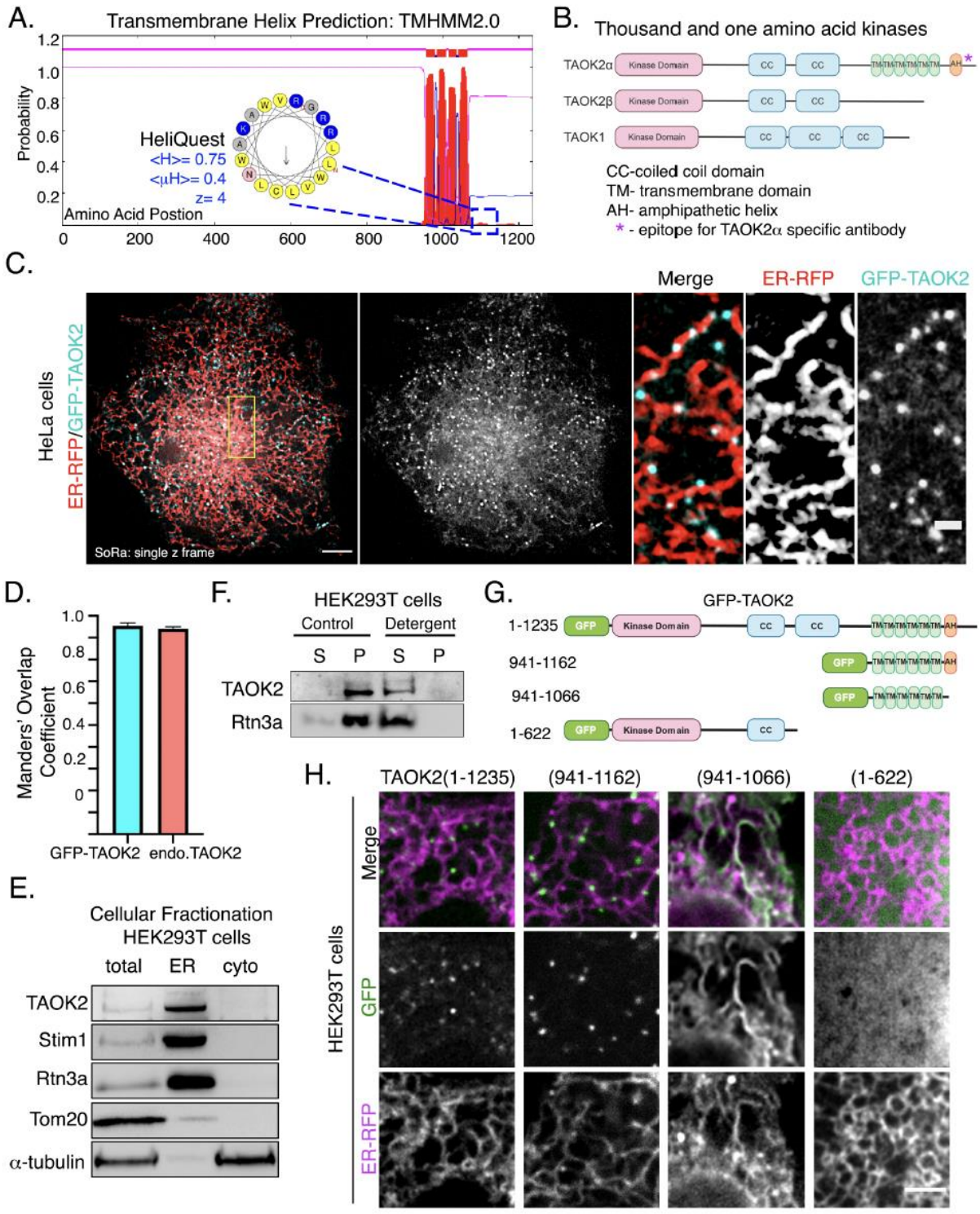

Figure 3.1. TAOK2 is an ER protein kinase that localizes to the ER membrane through four transmembrane domains and an amphipathic helix

(A) Transmembrane Hidden Markov Model (TMHMM v2.0) prediction plot shows the posterior probabilities (y axis) of inside/outside(magenta) / TM helix (red) along the length of TAOK2 sequence (x axis). Hydrophobic region following the sixth predicted TMD was analyzed through AMPHIPASEEK which predicted residues 1146-1162 to be amphipathic. Charged (blue) and hydrophobic (yellow) residues are indicated in the inset. HeliQuest was used to calculate hydrophobicity <H>, hydrophobic moment <μH> and net charge z.

(B) Schematic representation of TAOK2 isoforms α, β and TAOK1. The coiled coils (CC), six transmembrane domains (TM) and amphipathic helix (AH) predicted in TAOK2 are depicted. The unique C-terminal tail region of TAOK2 marked by the asterisk indicates the epitope used to generate the TAOK2α specific antibody.

(C) Super resolution (SoRa: super resolution by optical reassignment) images of HeLa cells expressing GFP-TAOK2 (cyan) and ER marker ER-mRFP (red). Scale bar is 5μm Yellow inset region is magnified and shown on the right. Grayscale images of TAOK2 and ER-RFP are shown separately. Scale bar is 1μm.

(D) Manders' overlap coefficient for colocalization of expressed GFP-TAOK2 and ER-mRFP, and endogenous TAOK2 and EGFP-Sec22b are plotted. Values indicate mean, error bars depict S.E.M. and n=10 for each condition.

(E) Western blot of cell homogenate fractionated into ER membrane and cytosol probed with antibodies against TAOK2, known ER membrane proteins Stim1 and Rtn3, mitochondrial protein Tom20 and tubulin.

(F) Western blot of cell homogenate fractionated into membrane pellet (P) and cytosolic supernatant (S) components, in the absence (control) or presence of detergent, probed with antibodies against TAOK2 and ER protein Rtn3a.

(G) Schematic shows the GFP-tagged TAOK2 deletion constructs used in Fig.1H

(H) Confocal images of HEK293T cells transiently transfected with distinct GFP-tagged TAOK2 deletion constructs as shown in 1G. (green) and ER-mRFP (magenta). Scale bar is 3µm.

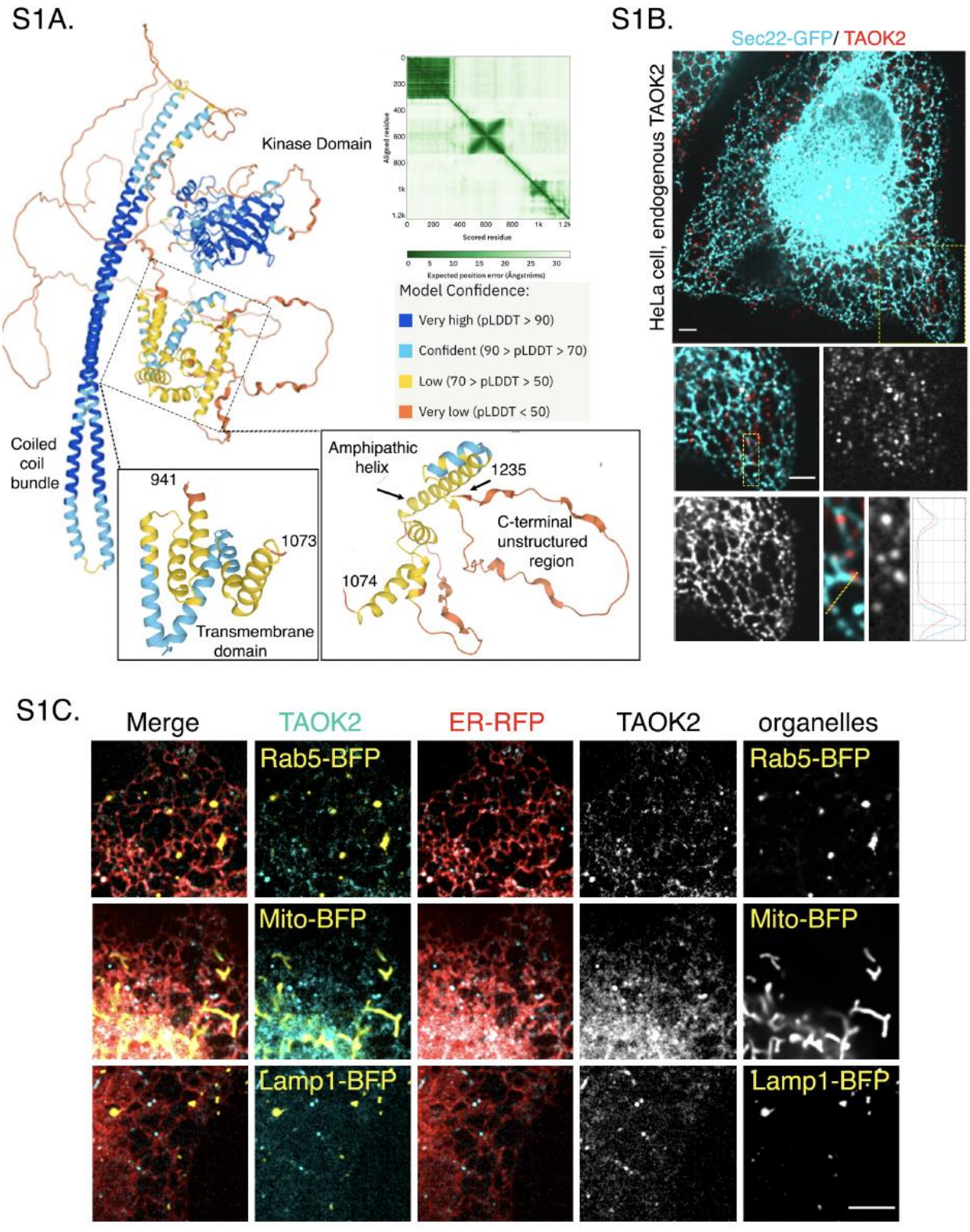
S1A.
Kinase Domain
Coiled coil bundle
941
1073
Transmembrane domain
Amphipathic helix
1235
C-terminal unstructured region
1074
Aligned residue
Scored residue
Expected position error (Ångströms)
Model Confidence:
Very high (pLDDT > 90)
Confident (90 > pLDDT > 70)
Low (70 > pLDDT > 50)
Very low (pLDDT < 50)
S1B.
Sec22-GFP/ TAOK2
HeLa cell, endogenous TAOK2
S1C.
Merge
TAOK2
ER-RFP
TAOK2
organelles
Rab5-BFP
Mito-BFP
Lamp1-BFP

Figure 3.S1. TAOK2 localizes to the ER membrane

(A) Model of TAOK2 structure as determined by AlphaFold2.0 protein structure and folding prediction algorithm. Structure is for the TAOK2α isoform (1-1235 amino acids). Kinase domain (top center), coiled coil bundle (left), transmembrane domains (941-1073) and C terminal tail (1074-1235) spanning the amphipathic domain and microtubule binding domain are shown (middle center, zoom in bottom). Expected position error at each residue is plotted for the entire length of the protein. Structure is color coded according to confidence of the algorithm in the prediction.

(B) Confocal image of HeLa cell expressing EGFP-Sec22b (cyan) and immunostained for TAOK2 (red). Scale bar is 5μm (top) and 1μm (bottom). RGB profile of fluorescence intensity peaks of TAOK2 (red) and EGFP-Sec22b (cyan).

(C) Confocal images of HeLa cells expressing GFP-tagged TAOK2 (cyan), ER-mRFP (red) along with the indicated organellar constructs (yellow). Endosomes visualized through expression of BFP-Rab5, mitochondria marked by BFP-mito, and lysosomes are marked by BFP-Lamp1. Greyscale images for TAOK2 and organelles is displayed on right. Scale bar is 3μm.

TAOK2 associates directly with assembled microtubules via its conserved Cterminal tail

TAOK2 has previously been shown to colocalize with microtubules (Mitsopoulos et al., 2003), however mechanism underlying this observation is unknown. We found that when GFP-TAOK2 or truncated C-terminal TAOK2 constructs were overexpressed, they led to bundling of microtubules, and these microtubule bundles were extensively decorated with GFP-TAOK2 (Figure 3.2A-B). Colocalization of truncated C-terminal GFP-tagged TAOK2 with tubulin immunostaining allowed us to map the microtubule-binding domain to 40 amino acids (1196-1235) in the extreme C-terminal tail of TAOK2 (Figure 3.2A-B). A truncation construct lacking this domain (1-1195) did not associate with microtubules (Figure 3.2A). Consistent with strong microtubule binding, expression of truncation construct containing the microtubule binding domain, led to increase in acetylated microtubules while constructs lacking microtubule binding domain did not affect microtubule acetylation level (Figure 3.S2A). We next tested whether TAOK2 can bind microtubules directly using a biochemical binding assay with purified components. We bacterially purified GST tagged TAOK2 C-terminal tail protein (residues 1187-1235) (Figure 3.S2B). An in vitro microtubule binding assay was used to test whether purified GST-TAOK2-C could bind microtubules polymerized from purified tubulin protein. GST-TAOK2-C pelleted specifically with polymerized MTs on centrifugation, while the control GST protein remained in the supernatant (Figure 3.2C and 3.2D), suggesting TAOK2 can directly associate with microtubules via its C-terminal tail. Further, the affinity of the TAOK2-microtubules interaction was assessed by determining the fraction of microtubule bound TAOK2-C at increasing concentration of tubulin. We found that the C terminal tail of TAOK2 associates with microtubules with a K_D of 0.67 ± 0.19μM (Figure 3.2E and

3.2F). These results show that TAOK2 can directly bind microtubules through its cytoplasm facing C-terminal tail.

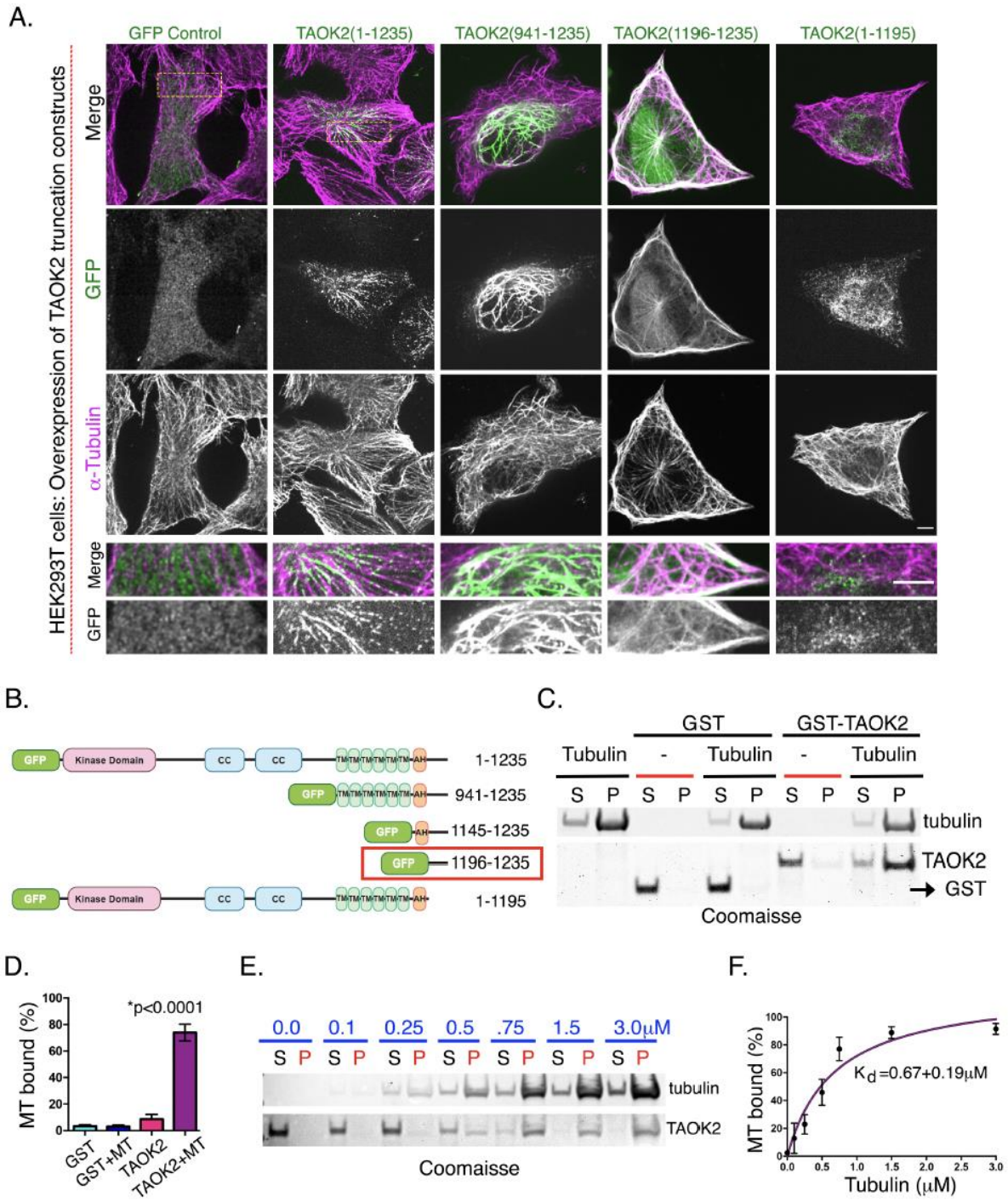

Figure 3.2. Direct binding of TAOK2 to microtubules through its C-terminal tail

(A) Confocal images of HEK293T cells transiently transfected with the indicated GFP-tagged TAOK2 construct immunostained for α-tubulin. Scale bar is 3μm. Magnified

images are shown in the bottom row to highlight the overlap of GFP-tagged TAOK2 with microtubules immunostained for α-tubulin. Scale bar is 5μm.

(B) Schematic representation of GFP-tagged deletion constructs used to map the microtubule binding domain. Coiled coil (CC), transmembrane (TMD); amphipathic helix (AH) domains are marked. Domain necessary and sufficient for microtubule localization is indicated by the red box.

(C) Coomassie stained SDS-page gel shows co-sedimentation of indicated proteins with polymerized tubulin. Microtubule binding assay was performed with 5μg of GST or GSTTAOK2-C (1187-1235) protein in the presence of taxol polymerized microtubules. Binding is assessed by the fraction of protein pelleted with microtubules (P) while unbound protein is in supernatant (S).

(D) Percent protein bound to microtubules is plotted for each protein as indicated. Error bars indicate standard error of mean, n=3, $p<0.0001$, one-way ANOVA.

(E) Coomassie stained SDS-page gel shows the amount of purified GST-TAOK2-(11871235) unbound (S) or co-sedimented with polymerized microtubules (P) with increasing concentrations of tubulin as indicated.

(F) Strength of microtubule association was determined from dissociation constant K_D derived by Michaelis-Menten equation. Error bars indicate standard error of mean, n=3 replicates.

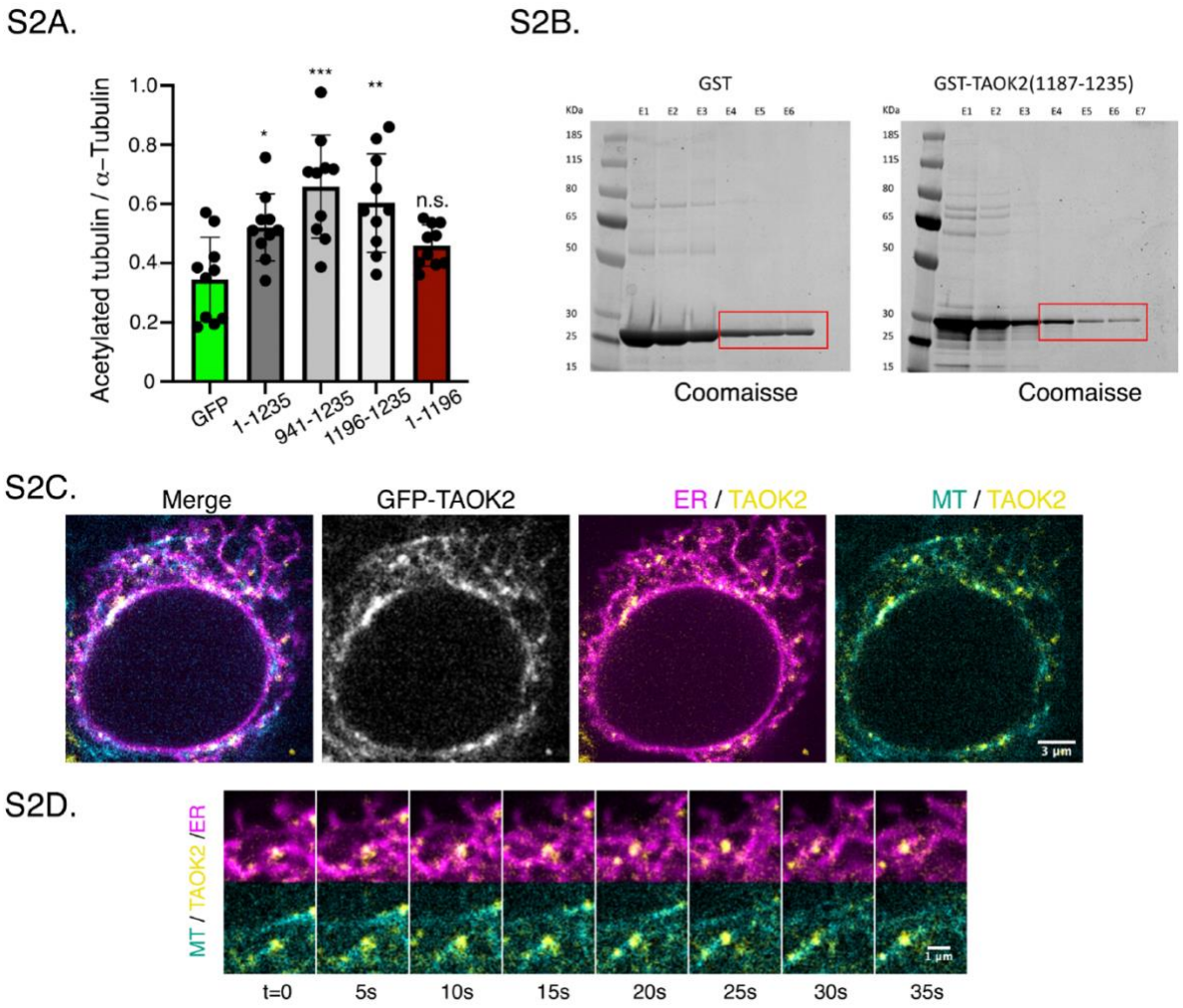

Figure 3.S2. TAOK2 is an ER-microtubule tether (related to main figure 2 and 3)

(A) Fraction of acetylated tubulin relative to α-tubulin for TAOK2 domain dissection constructs. Values indicate mean, error bars depict S.E.M., n=10 cells for each construct. Ordinary one-way ANOVA with multiple comparisons, where p values are denoted by *<0.05, **<0.001, ***<0.0005 and ****<0.0001.

(B) Coomassie stained gels showing eluate fractions obtained after affinity purification of GST (left) and GST-TAOK2-C (right) proteins. Fraction E4 was concentrated and used for downstream microtubule binding assays. Molecular weight proteins ladder is shown on the left.

(C) Confocal images of HEK293T cells expressing GFP-TAOK2 (yellow), ER-mRFP (magenta) and live-stained with microtubule dye (cyan). Scale bar is 3μm.

(D) Montage of confocal time lapse images shows TAOK2 (yellow) punctae colocalized with both ER membrane (magenta) and microtubules (cyan). Scale bar is 1μm.

ER membrane tethering to the microtubule cytoskeleton is mediated by TAOK2

Our finding that TAOK2 is an ER kinase with the ability to directly bind microtubules led us to hypothesize that this kinase can act as a molecular tether linking the ER membrane to microtubules (Figure 3.3A). To evaluate this possibility, we performed live cell imaging with simultaneous visualization of the ER membrane and microtubule cytoskeleton. Cells transfected with full length GFP-TAOK2 and ER-mRFP were incubated with a cell permeable microtubule binding dye, and three color time-lapse confocal microscopy was performed. TAOK2 punctae were often localized at the end of ER tubules where the tubules made contact with microtubules (Figure 3.3B and 3.3C). Indeed, 87% of GFP-TAOK2 punctae localized at the points of contact between the ER and the microtubule cytoskeleton (Figure 3.3D). These punctae tracked with the movement of the ER membrane on microtubules (Figure 3.S2C, D). To determine the functional consequences of TAOK2 depletion on ER-MT tethering, we generated two independent TAOK2 knockout (KO) HEK293T cell lines using CRISPR/Cas9 mediated gene editing. Genetic knockout and loss of protein was validated using genome sequencing and western blot respectively (Figure 3.3E, Figure 3.S3A-C). HEK293T control and TAOK2 knockout (KO) cells were transfected with microtubule binding protein EGFP-ensconsin and ER-mRFP to visualize microtubules and ER membranes respectively. The ER in control cells extended from the nuclear envelope to the cell periphery and made extensive contacts with the microtubules (Figure 3.3F). In contrast in TAOK2 KO cells, while the nuclear envelope and the sheet like perinuclear ER was unaffected, the ER density and morphology was perturbed at the cell periphery (Figure 3.3F, inset). For instance, the ER density at the cell periphery was significantly reduced compared to control cells (Figure 3.3H). Further the area of the ER that overlapped with the microtubules was significantly

decreased (Figure 3.3G). Next, we ascertained the domains within TAOK2 that conferred the tethering function of TAOK2 by expressing distinct deletion constructs in the TAOK2 KO HEK293T cells. Expression of construct that retained the ER localization and microtubule binding elements (amino acid 941-1235), but lacked the N-terminal kinase and coiled coil domains (Figure 3I) led to aberrant over-tethering of the ER to the MT perturbing ER morphology, such that the ER appeared bundled alongside perinuclear microtubule cables. As expected, expression of just the microtubule binding domain (1196-1235) or the construct lack the microtubule binding domain (1-1195) did not lead to ectopic tethering of the ER to microtubules. These data together show that TAOK2 indeed is an ER localized microtubule tether that is important for the extensive interaction of the peripheral ER with the microtubule cytoskeleton. We define the domains through which TAOK2 mediates its tethering function. Importantly, these findings also imply that additional domains of TAOK2 outside the tethering elements regulate the coupling dynamics of the ER to the microtubule cytoskeleton.

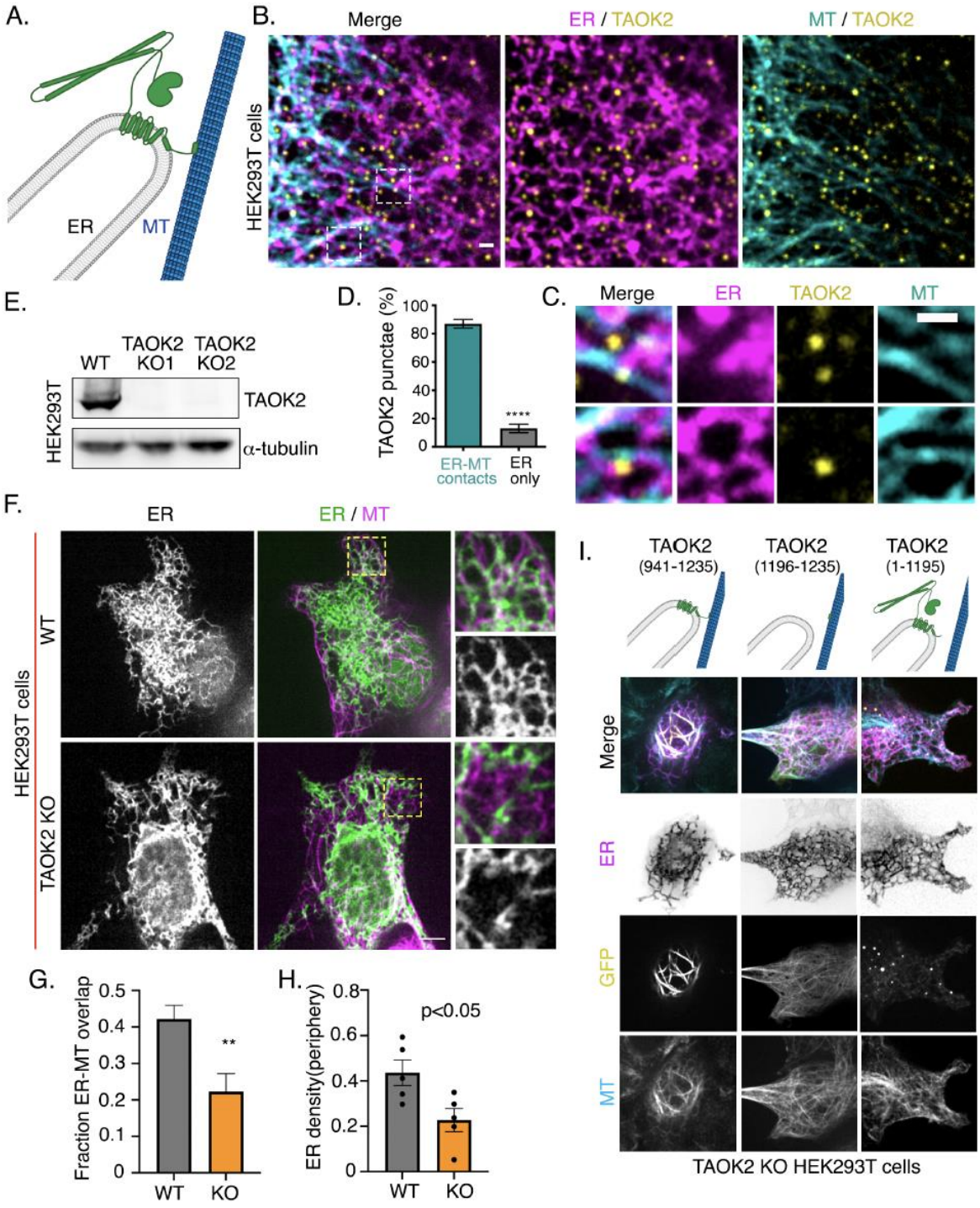

Figure 3.3. TAOK2 is an ER-microtubule tethering protein kinase

(A) TAOK2 (green) schematically depicted as a multipass transmembrane protein on the ER (grey). TAOK2 has an N-terminal cytoplasm facing kinase domain, is anchored to

the ER membrane through six transmembrane helices and an amphipathic region, and the C-terminal cytoplasmic tail directly binds microtubules (blue).

(B) Confocal images of HEK293T cells transfected with GFP-TAOK2 (yellow), ER-mRFP (magenta) and live-stained with microtubule dye (cyan). Scale bar is 1µm.

(C) Magnified images of inset in B displays two individual TAOK2 (yellow) punctae on ER tubules as it makes contacts with and microtubules (cyan). Scale bar is 1µm.

(D) Percent TAOK2 puncta colocalized with ER and microtubules in HEK293T cells is plotted. Values indicate mean and error bars indicate S.E.M., n=10 cells where at least 50 punctae per cell were analyzed.

(E) Western blot of lysate from wildtype and TAOK2 (knock out) KO cell lines generated using CRISPR/Cas9 mediated gene editing.

(F) Confocal images of WT and TAOK2 KO HEK293T cells transiently transfected with ER-mRFP (green) and mEmerald-ensconsin (magenta) to visualize microtubules. Yellow inset region of peripheral ER is magnified, and shown in the panels on the right for both WT and TAOK2 KO cells. Scale bar is 5µm.

(G) The ratio of peripheral ER area in contact with microtubules to the total peripheral ER area in a 100µm^2 region in the cell periphery is plotted for wildtype and TAOK2 knockout HEK293T cells. Values indicate mean, error bars indicate S.E.M., n=6, t-test with Welch's correction.

(H) ER density is calculated as fraction of ER area in a 100 µm2 region in the cell periphery measured in wildtype and TAOK2 knockout HEK293T cells. Values indicate mean, error bars indicate S.E.M., n=6, t-test with Welch's correction.

(I) Schematic depicts the topology of each of the three TAOK2 deletion constructs. Representative confocal images of HEK293T KO cells expressing the indicated TAOK2 constructs are shown where TAOK2 (yellow), ER-mRFP (magenta) and microtubules (cyan) are shown in merged and grayscale. Scale bar is 5μm.

S3A

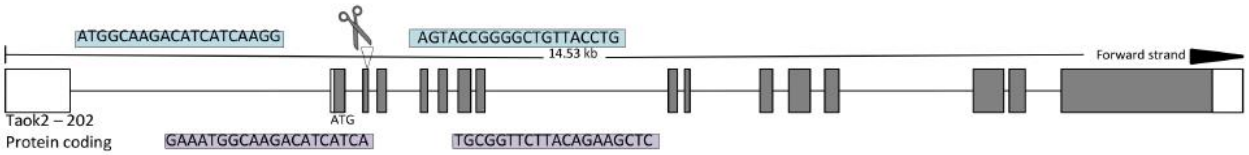

Guide	Sequence
# 1	GAAATGGCAAGACATCATCA
# 2	ATGGCAAGACATCATCAAGG
# 3	TGCGGTTCTTACAGAAGCTC
# 4	AGTACCGGGGCTGTTACCTG

S3B

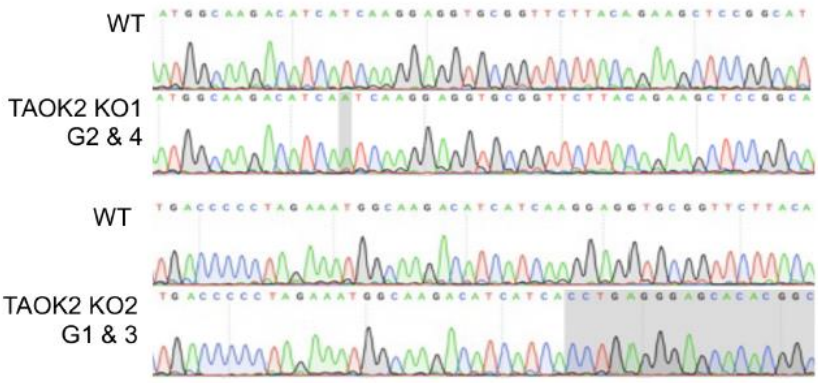

S3C

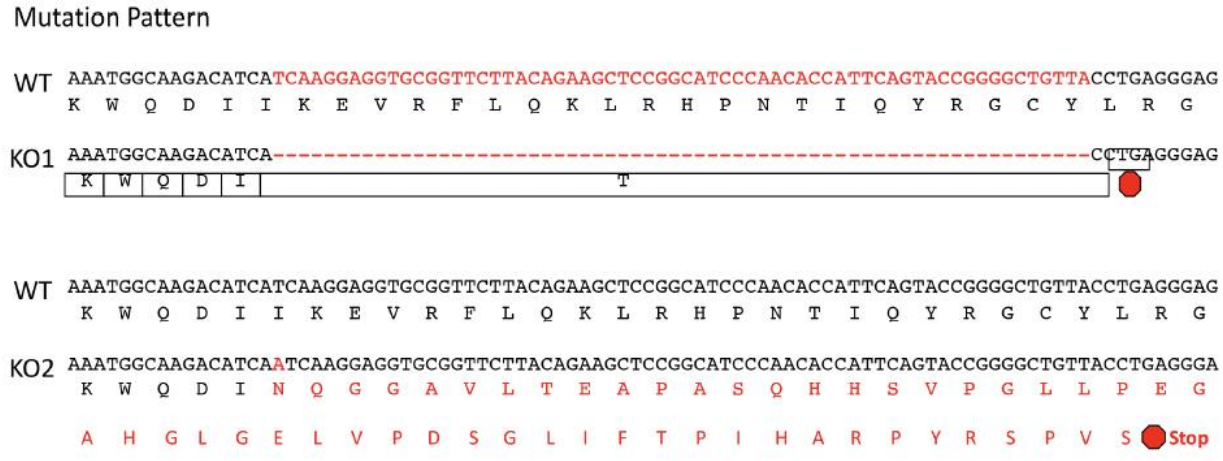

Figure 3.S3. Generation of TAOK2 knockout HEK293 cell lines using genome editing

(A) Genomic structure of TAOK2 as visualized through the UCSC genomic browser, shows the exons in gray, and region targeted by RNA guides (purple and blue) is marked by scissors. RNA guide sequences used for generation of TAOK2 knockout are shown.

(B) Sequence peaks show the result of DNA sequencing in wildtype and two separate KO cell lines performed after PCR of the surrounding genomic region. The change in nucleotide

(C) sequence is shown in gray.

(D) Genome editing leads to frameshift mediated early termination. Resulting changes in protein sequence for both TAOK2 knockout cell lines is depicted.

TAOK2 is required for ER microtubule plus end motility but not motor mediated movement

To test whether loss of TAOK2 mediated tethering would impact overall motility of the ER membranes, we measured ER membrane movement over time. Wildtype and TAOK2 KO cells were transfected with the ER marker EGFP-Sec22b and time-lapse confocal microscopy allowed us to visualize ER dynamics. ER motility in TAOK2 KO cells was significantly increased compared to WT cells (Figure 3.4A). Average normalized pixel differences over time allowed us to calculate the ER motility index which increased from 0.287±0.012 in WT cells to 0.351±0.017 (n=9, p=0.0098) in TAOK2 KO cells (Figure 3.4B). We next determined whether TAOK2 and microtubule interaction affected the motility of ER membrane on microtubules. To further investigate how absence of TAOK2 might affect ER motility, we performed simultaneous confocal imaging of ER (EGFP-Sec22b) and microtubule end binding protein mCherry-EB3 (Figure 3.4C). We found that in WT cells both TAC movements on microtubule plus end, as well as rapid ER movements independent of EB3 comets were observed, however, in TAOK2 KO cells TAC movements were severely disrupted, and almost all observed movements were rapid and not associated with EB3 comets. Thus, loss of TAOK2 specifically disrupts TAC movements of ER membrane on MT growing plus ends (Figure 3.4C and 3.4D). Next, we determined whether absence of TAOK2 would impact microtubule dynamics. We found while the number of microtubule plus ends marker by EB3-mCherry were unaffected in TAOK2 KO cells (Figure 3.4E), microtubule growth assessed by measuring EB3 velocity was significantly increased in TAOK2 KO cells (Figure 3.4G). Further, in TAOK2 knockout cells, EB3 comet tracks were less directed exhibiting increased curvature and paused more frequently compared to control WT cells (Figure 3.4F and 3.4H). These data show

that TAOK2 mediated ER-MT tethering is essential for the dynamics of ER membranes. Additionally, loss of tethering of microtubules to the ER membranes impacts several aspects of microtubule dynamics, such as EB3 velocity, the directional persistence, and pause time of growing microtubules suggesting that microtubule growth and dynamics are fundamentally regulated by their interaction with the endoplasmic reticulum.

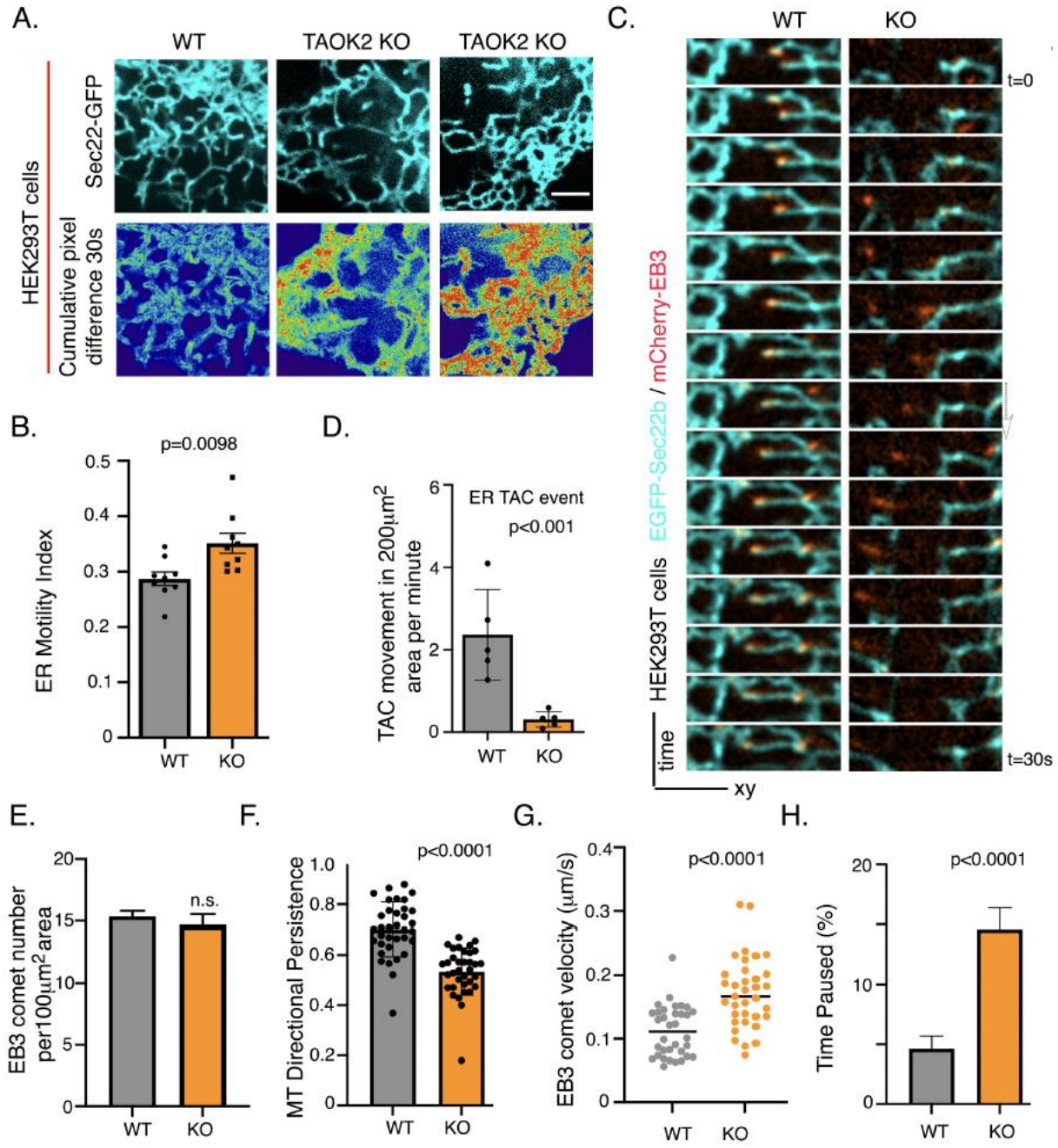

Figure 3.4. TAOK2 knockout disrupts ER-microtubule dynamics

(A) Confocal images of peripheral ER in wildtype and TAOK2 KO cells expressing ER marker EGFP-Sec22b at a single time point (left column). Sum slice projection of cumulative pixel difference in successive frames over 30s time period (right), where

images were acquired every 3sec. Fluorescence intensity is pseudocolor coded, red regions representing increased ER motility. Scale bar is 3µm.

(B) ER motility index calculated by averaging the normalized pixel difference between successive time frame over 30s is plotted for wildtype and TAOK2 KO cells. Error bars indicate S.E.M, n=9 cells, t-test.

(C) Montage of images acquired every 2s, of wildtype and TAOK2 KO cells expressing EGFP-Sec22b and mCherry-EB3 shows movement of ER membranes (cyan) associated

(D) with microtubule plus tips (red) in wildtype but not KO cells.

(E) Time-lapse confocal images of cells expressing EGFP-Sec22b and mCherry-EB3 were analyzed and ER membrane movements that classified as slow MT plus tip associated-TAC (colocalized with EB3 comet) in 200µm^2 area of the cell over one minute time period are plotted. Mean values are plotted, n=5 cells for each condition, two tailed t-test with Welch's correction.

(F) EB3 comet number in a 100µm^2 area in wildtype and knockout HEK293T cells is depicted. Values indicate mean, scale bars indicate S.E.M, n=10 cells, t-test with

(G) Welch's correction.

(H) Microtubule directional persistence, calculated as a fraction of perpendicular distance between start/end points and the length of the actual path taken is plotted for wildtype and TAOK2 knockout cells. Values indicate mean ± S.E.M., n=9 cells with at least 5 comet paths measured per cell, two tailed t-test.

(I) Percent total time spent by EB3 comet pausing (no growth) is plotted for wildtype and TAOK2 KO cells. Values indicate mean ± S.E.M., n=9 cells with at least 5 comet paths measured per cell, two tailed t-test.

(J) EB3 comet tracks generated using the Manual tracking function in Fiji were used to measure EB3 comet velocity by dividing the total distance traveled over time. Mean values for wildtype and TAOK2 KO cells are plotted, error bars indicate S.E.M, n=9 cells with 5 comets per cell, two tailed t-test.

TAOK2 regulates STIM1 mediated ER movement on microtubule growing ends

We further probed how TAOK2 kinase might contribute to the ER tip associated movement or TAC. Microtubule plus-end associated movement of ER has been previously shown to be mediated by interaction of the ER transmembrane protein STIM1 with the end binding proteins EB1 that bind the growing plus end of microtubules (Grigoriev et al., 2008). As TAOK2 knockout HEK293T cells exhibit defects in movement of ER on microtubule plus end, we next tested whether TAOK2 contributes to the STIM1 mediated TAC movements, or whether it constituted a distinct mechanism of TAC movement. We first tested if the expression of STIM1 and EB1 proteins were affected in TAOK2 knockout cells. We found no changes in protein levels of STIM1 and EB1 in two independent TAOK2 knockout HEK293 cells (Figure 3.S4A). Further, immunostaining for endogenous EB1 in control and TAOK2 KO HEK293 cells revealed no differences in the density of EB1 comets (Figure 3.S4B). If TAOK2 regulated Stim1 mediated TAC movements, then we hypothesized that STIM1-EB movements would be disrupted in absence of TAOK1. Therefore, we transfected control and TAOK2 knockout HEK293T cells with Stim1-YFP, the ER marker Sec61-BFP, and microtubule plus tip marker EB3mCherry. In control cells, we found that Stim1-YFP was ER localized and overlapped with Sec61-BFP as expected, but importantly was also concentrated at the contact points between ER tubules and MT plus ends (Figure 3.5A). However, in TAOK2 knockout cells while Stim1-YFP still co-distributed with Sec61-BFP, its concentration at MT plusends marked by EB3-mCherry was dramatically reduced (Figure 3.5A). Time lapse imaging revealed numerous TAC movements where STIM1-YFP coincided with EB3mCherry comets that moved together over time, while both accumulation of STIM1 at

MT plus-ends, and ER TAC movements were absent in TAOK2 knockout cells (Figure 5B and 5C). While the percent of EB3/STIM1 comets mediating TAC movement declined drastically, the number of EB3 comets making no contact with STIM1 significantly increase in TAOK2 KO HEK293T cells (Figure 3.5C). The association of STIM1 and EB proteins is direct through interaction of the Ser-x-Ile-Pro (SxIP) motif in the C-terminal tail of Stim1, with a well-defined hydrophobic cavity in the C-terminal end binding homology domain of EB1 and EB3 (Honnappa et al., 2009). We next tested whether EB binding motifs would be present in TAOK2. Indeed, we found that the C-terminal tail of TAOK2 harbored a highly conserved SxIP motif (amino acids 1192-1195) which is found in many other EB binding proteins including CLASP1 and STIM1 (Figure 3.5D). The SxIP motif is typically present in a region rich in basic amino acids, which is also the case for TAOK2 (Figure 3.5D, highlighted in red). Therefore, we tested whether TAOK2 localized with EB1 on microtubule plus end. Immunostaining for endogenous TAOK2 and EB1 proteins in HeLa cells transfected with Sec22-GFP revealed that TAOK2 punctae colocalized with 34.7% of EB1 comets (Figure 3.5E and 3.5H). Further, to test whether TAOK2 and EB1 interact biochemically, we immunoprecipitated EB1 from HeLa cell lysate and then probed for TAOK2 and STIM1. TAOK2 and STIM1 both co-immunoprecipitated with EB1 (n=3 experiments, Figure 3.5F). To test whether the SxIP motif is important for the binding of TAOK2 to EB1 on microtubule plus ends, we expressed the C-terminal tail of TAOK2 containing the SxIP motif and microtubule binding domain (1162-1235) along with EB3mCherry in TAOK2 KO HEK293T cells. This construct localized to the microtubules as well as accumulated at the microtubles plus ends decorated by Eb3-mCherry. Further, the construct TAOK2 C-terminal tail construct which lacks the SxIP motif can still bind

microtubules but not plus tips. Therefore, deletion of SxIP motif was sufficient to disrupt localization of TAOK2 to the plus tips but did not affect its microtubule binding properties (Figure 3.5G).

To further determine the spatial distribution of endogenous TAOK2 and EB1 on microtubule plus ends and ER respectively, we analyzed the co-distribution of these proteins in fixed HeLa cells expressing ER marker Sec22b and immunostained for endogenous TAOK2 and EB1. Every TAOK2 punctae was on the ER membrane as expected, of which 22% were co-localized on EB1 comets (Figure 3.5H). Next, we tested the co-distribution of endogenous TAOK2 and STIM1 in HeLa cells transfected with ER marker GFP-Sec22b. Both TAOK2 and STIM1 punctae were beautifully localized to the ER membrane marked by GFP-Sec22b (Figure 3.S4D). We found that about 18% of all TAOK2 punctae colocalized with STIM1 punctae, and 19% of total STIM1 punctae colocalized with TAOK2 (Figure 3.S4C). Interestingly 56% of EB1 comets appeared to be in contact with the ER membrane. Of these ER contacting plus tips, 62.5% were positive for TAOK2 punctae (Figure 3.5H). These analyses reveal a high degree of interaction between the growing microtubule plus tips and the ER membrane. We show that TAOK2 is important for TAC mediated ER motility, and that TAOK2 binds growing microtubule ends through interaction with EB1 mediated by the SxIP motif. Importantly, we found that the microtubule binding and EB binding properties of TAOK2 were distinct, and one could be abolished without affecting the other.

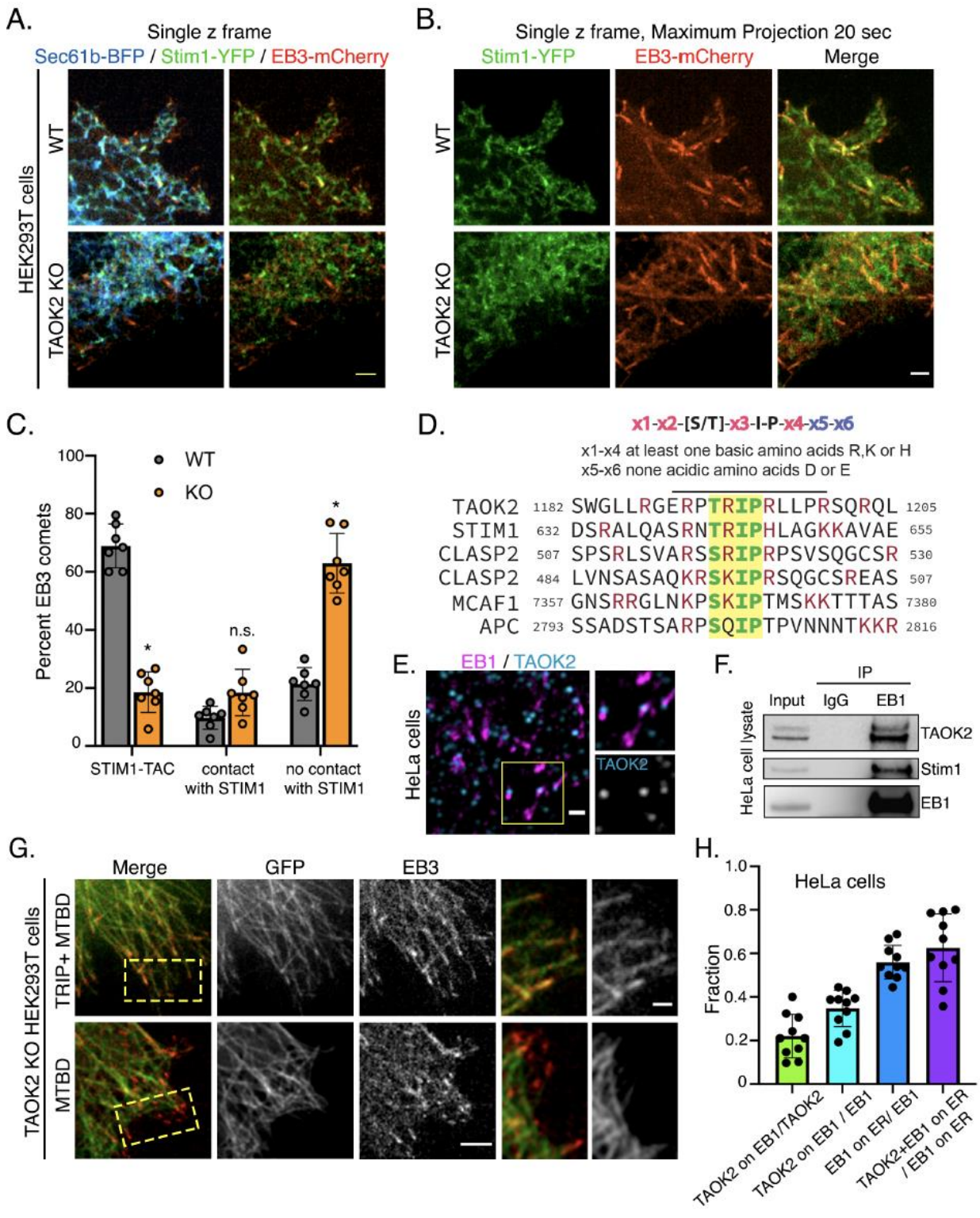

Figure 3.5 TAOK2 regulates ER TAC movement and interacts with EB1 via SxIP motif

(A) Representative single z-frame confocal images of WT and KO HEK293T cells transiently expressing ER marker Sec61-BFP (blue), STIM1-YFP (green) and EB3mcherry (red). Scale bar is 3μm.

(B) Maximum projection of single z frames shown in (A) over a period of 20 sec to visualize movement and path of EB3 and STIM1 over time in WT and TAOK2 KO

(C) HEK293T cells. STIM1-YFP (green) and EB3-mcherry (red). Scale bar is 3μm. (C) Percentage of EB3 comets in 200μm^2 area were classified as 1. Comets interacting with STIM1/ER and performing TAC, 2. Comets interacting with STIM1 transiently but not performing TAC, and 3. Comets not contacting STIM1/ER. Value indicates mean, error bar indicates S.E.M. n=7 cells, two-way ANOVA.

(D) Schematic depicting the conserved binding motif of microtubule plus tip interacting proteins that associate with EB proteins. The SxIP-9 amino acid consensus and associated rules are shown. Yellow highlighted region shows aligned SxIP motifs of TAOK2 and known EB interacting proteins, bold green depicts conserved residues, and the basic amino acids are highlighted in red.

(E) Confocal image of wildtype HeLa cells immunostained for EB1 (magenta) and TAOK2 (blue). Yellow inset region is magnified on the right. Scale bar is 1 μm.

(F) Representative western blot (n=3) shows coimmunoprecipitation of TAOK2 and STIM1 when EB1 is immunoprecipitated using anti-EB1 antibodies from HeLa cell lysates. 1% input is shown for comparison in the left lane.

(G) Representative confocal images of KO HEK293T cells transiently transfected with EB3-mcherry (red) and TAOK2 C terminal tail microtubule binding domain with and without the TRIP (SxIP) motif that confers EB1 binding. Scale bar is 3μm. Yellow inset

region is magnified and shown on right to highlight the colocalization of EB3 with TAOK2 in the presence of the TRIP (SxIP) sequence.

(H) Wildtype HEK293T cells expressing ER-marker EGFP-Sec22b were immunostained for endogenous EB1 and TAOK2. Images of EB1 comets were analyzed to quantify the fractions of EB1 positive TAOK2 puncta to total TAOK2 puncta, number of TAOK2 positive EB1 puncta compared to total EB1 puncta, number of EB1 puncta on ER compared to total EB1 puncta, and number of TAOK2 positive EB1 puncta on ER compared to total number of EB1 on the ER. Puncta were counted in 100μm^2 ROI in the cell periphery. Values indicate mean, error bars indicate S.E.M., n=10 cells.

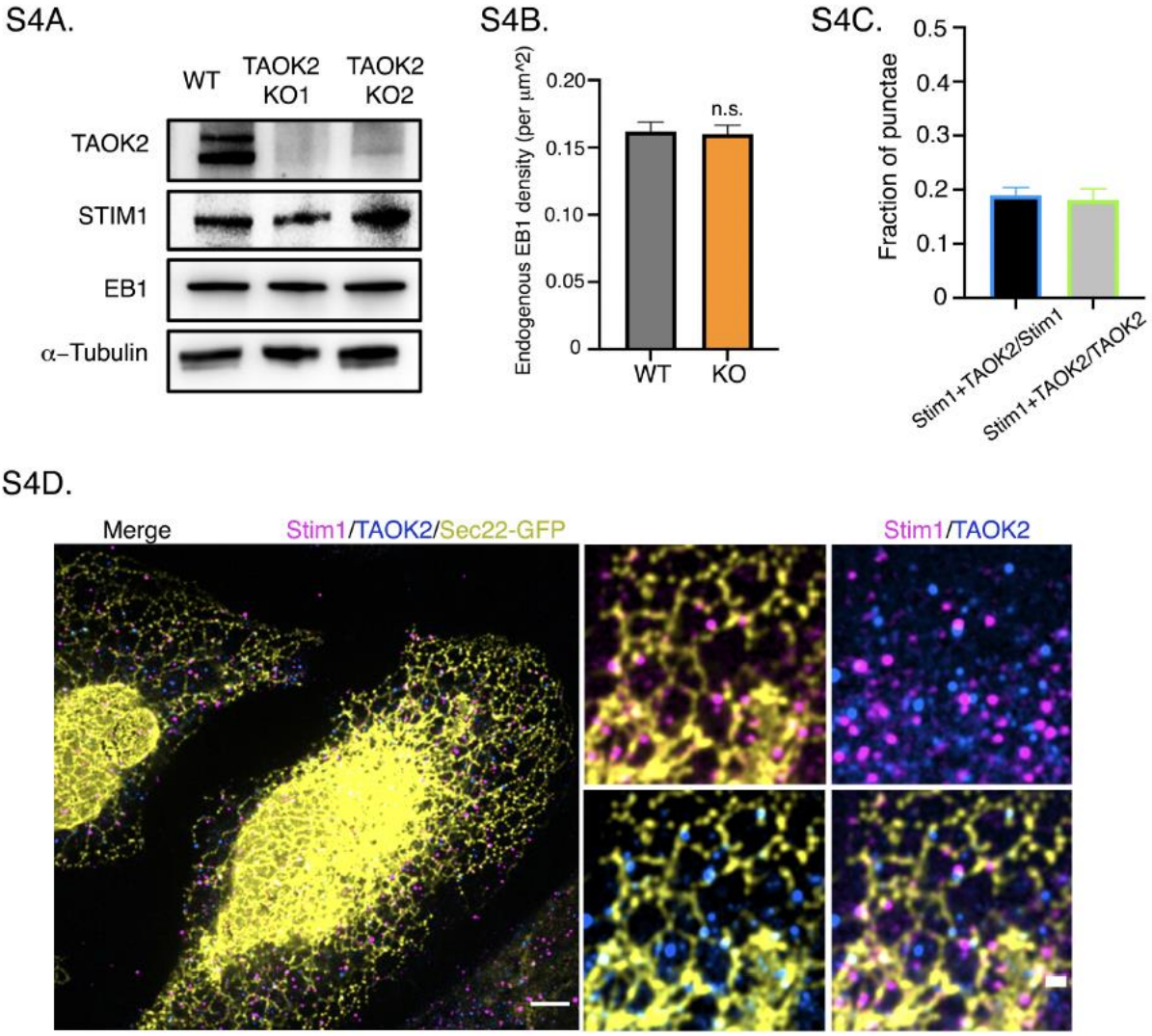

Figure 3.S4. Role of TAOK2 in ER motility on microtubule plus tips

(A) Western blot of HEK293T WT and TAOK2 KO (1 and 2) cell lysate. Probed for TAOK2, EB1, STIM1 and α-tubulin.

(B) Endogenous EB1 density over 100 µm2 region in cell periphery of WT and TAOK2 KO HEK293T cells. Values indicate mean, error bars indicate S.E.M., t-test.

(C) Fraction of TAOK2 punctae positive for STIM1 and fraction of STIM1 puncta positive for TAOK2. Values indicate mean, error bars indicate S.E.M., t-test.

(D) Confocal image of HeLa cell expressing EGFP-Sec22b (yellow) and immunostained for TAOK2 (blue) and STIM1 (magenta). Scale bar is 3μm (top) and 1μm (right).

Aberrant TAOK2 tethering disrupts ER restructuring during mitosis

The endoplasmic reticulum undergoes dynamic restructuring during cell division (Carlton et al., 2020). During metaphase, as the mitotic spindle aligns the chromosomes at the metaphase plate, the ER is anchored at each end to the spindle poles but largely absent from chromosomes and the area between the spindle poles. Defects in ER clearance from the chromosomes and spindle elicit mitotic defects (Schlaitz et al., 2013). Given the extensive association of ER with MT during cell division, we investigated the role of TAOK2 in ER restructuring during mitosis. We performed super resolution confocal microscopy to visualize GFP-TAOK2 localization in mitotic cells. We found that GFP-TAOK2 was present in close apposition to the spindle poles at sites where the ER membranes converged (Figure 3.6A). TAOK2 localized at discrete punctate sites throughout the curvilinear peripheral ER surrounding the mitotic cell, as well as at the points of contact between ER membrane and the mitotic spindle (Figure 3.6A). To test, whether TAOK2 was important for ER structural remodeling during cell division, we imaged WT and TAOK2-KO HEK293T mitotic cells expressing EGFP-Sec22b and mCherry-EB3 to visualize ER membranes and mitotic spindle. WT cells exhibited the characteristic ER morphology where ER membranes accumulated at spindle poles and fenestrated curvilinear peripheral ER surrounded the mitotic spindle. In contrast, TAOK2KO cells had abnormal morphology with increased peripheral curvilinear ER membranes, and a striking decrease in ER association with spindle poles (Figure 3.6B-C). To determine if this aberrant ER morphology affected cell division, we immunostained WT and TAOK2 KO cells with tubulin and DAPI. While 95.6% WT cells showed normal bipolar spindle, only 44.8% KO cells had a normal bipolar spindle. KO mitotic cells displayed a chromosomal misalignment defect, where 39.3% KO cells had a bipolar

spindle with misaligned chromosomes, and 15.8% KO cells had multipolar spindle (Figure 6D). While loss of TAOK2 induced defects in ER association with mitotic spindle, we next queried whether these defects could be rescued by expression of TAOK2. We quantified three distinct parameters namely, number of mitotic cells with 1) normal bipolar spindle, 2) ER associated with spindle poles, and 3) ER dissociated from mitotic spindle. Expression of the full length TAOK2 in KO HEK293T cells abrogated the mitotic spindle defects and defects in ER association with the spindle pole (Figure 3.6E, top row and 3.6F). Expression of the truncated TAOK2 lacking the N-terminal kinase and coiled coil domains in TAOK2 KO HEK 293T cells, induced a dramatic collapse of the ER membranes on the mitotic spindle. TAOK2 binding to microtubules created an extremely short and stable MT-ER bridge between the spindle poles. The chromosomes were displaced from the metaphase plate and instead formed a rosette around the ER-MT spindle (Figure 3.6E-F, middle row). These cells failed to divide. Additionally, the TAOK2 microtubule binding domain when expressed in TAOK2 KO HEK293 cells localized to the mitotic spindle and not the ER as expected, and also did not cause the ER to collapse on the spindle. The number of normal bipolar cells increased from 49.3% in KO cells to 99% on expression of WT-TAOK2 in the TAOK2 KO cells. Only 5.8% of TAOK2 KO cells expressing the abnormal tether construct TAOK2 (941-1235) had a normal bipolar spindle, while 78.3% cells expressing the TAOK2 microtubule binding domain (1196-1235) had a bipolar spindle. Moreover, expression of the TAOK2 microtubule binding domain (1196-1235) failed to rescue the defect in ER-spindle pole association observed in TAOK2 KO cells (Figure 3.6F). These data collectively show that TAOK2 mediates ER tethering to the spindle poles during cell division. Association of TAOK2 to the spindle

poles is important for ER accumulation at the poles during mitosis. Further, the dissociation of TAOK2 from microtubules of the mitotic spindle is critical for the disengagement of ER from the mitotic spindle without which cell division is arrested.

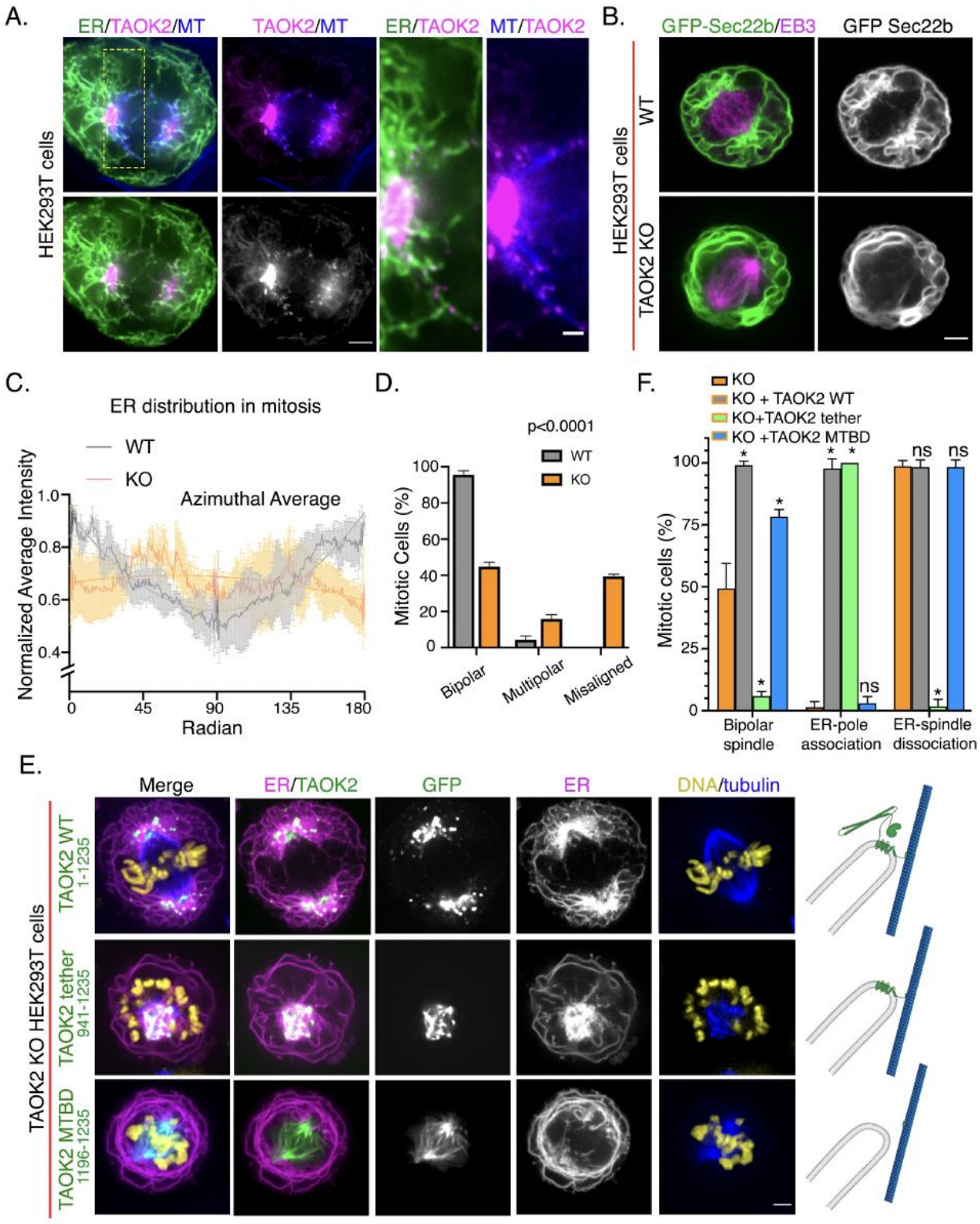

Figure 3.6 TAOK2 localizes to the mitotic spindle and regulates mitotic ER remodeling

(A) SoRa superresolution confocal image of HEK293T mitotic cell expressing GFPTAOK2 (magenta) and ER-mRFP (green) and stained with microtubule dye (blue), scale bar is 2μm. Magnified view of the ER-MT tethering sites on the spindle is shown on the right, scale bar is 0.5μm.

(B) Representative confocal images of WT and TAOK2 KO mitotic HEK293T cells transiently transfected with EGFP-Sec22b (green) and mCherry-EB3 (magenta). ER morphology in WT and TAOK2 KO cells is shown in grayscale on right. Scale bar is 5μm.

(C) ER distribution in mitotic cells is measured using Azimuthal Average of normalized fluorescence intensity in each hemisphere demarcated by the mitotic spindle (where 0 and 180 correspond to the spindle poles) is plotted for WT (gray) and TAOK2 KO (orange) cells. Average means are plotted, error bars are S.E.M., and n=3 cells. (D) Percent mitotic WT (grey) and TAOK2 KO (orange) cells that exhibit bipolar, multipolar or misaligned mitotic spindles are plotted. Values indicate mean ± S.E.M., n>45 mitotic cells from three different experiments, $p<0.0001$ one-way ANOVA.

(D) Representative confocal images of mitotic TAOK2 KO HEK293T cells expressing the indicated TAOK2 constructs (green), ER-mRFP (magenta), DNA (yellow) and microtubules (blue) are shown. Localization of TAOK2 construct and corresponding effect on ER morphology is shown in grayscale as well. Scale bar is 5μm. Schematic (right) depicts topology of GFP-TAOK2 deletion constructs.

(E) Percent of mitotic TAOK2 KO HEK293T cells transiently expressing the indicated constructs were scored on the basis of 1) exhibiting normal bipolar spindle, 2) ER association with spindle poles and 3) ER dissociation from mitotic spindle. Values indicate mean ± S.E.M., n=75 cells from 3 different experiments.

Catalytic autoregulation of TAOK2 mediated ER-MT coupling

What might be the mechanism through which TAOK2 regulates its function as an ER-MT tether? We tested whether the kinase activity of TAOK2 regulates its microtubule association. First, we introduced a kinase-dead mutation within the catalytic domain of TAOK2 at residue K57A, which disrupts the autophosphorylation at the critical residue S181 in the activation loop (Moore et al., 2000), and hence the catalytic activity of TAOK2 (Figure 3.7A). Next, we expressed either GFP tagged-TAOK2 WT or TAOK2K57A along with ER-mRFP in TAOK2 KO HEK293 cells to determine how catalytic activity might impact microtubule tethering and ER motility. Comparative analysis of overlap between ER membrane and microtubules in cells expressing WT and kinasedead TAOK2 in TAOK2 KO HEK293 cells, revealed that loss of kinase activity increased the association of ER with microtubules from 42.9% to 75.4% while the peripheral ER density was unaffected (Figure 3.7B-D). To test if increased association with microtubules resulted in stronger ER-MT tethering and hence reduced motility, we measured ER motility in TAOK2 KO HEK293 cells expressing kinase dead TAOK2-K57A and ER marker EGFP-Sec22b. A substantial decrease in ER membrane motility was found in cells expressing TAOK2-K57A as opposed to TAOK2-WT (Figure 3.7E and F). The ER motility index calculated from mean normalized pixel differences over time, was found to decrease from 0.35±0.02 in TAOK2-WT to 0.26±0.03 (n=9, p=0.0019) in K57-TAOK2 expressing cells (Figure 3.7E-F). Further, we found that TAOK2 kinase activity was important for microtubule growth rates determined by measuring EB3 comet velocity. EB3 velocity averaged at 0.21µm/s in TAOK2-WT expressing KO HEK293 cells and was decreased significantly to 0.14µm/s in KO HEK293 cells expressing kinase dead TAOK2 (Figure 3.7G). Next, we used a pharmacological TAOK kinase inhibitor CP43, to acutely inhibit the kinase activity of

TAOK2 and test its effect on ER-MT coupling. HeLa cells incubated with 250nM CP43 for 2 hours led to a strong reduction in its kinase activity, both in terms of autophosphorylation as well as its ability to phosphorylate Septin7, a known substrate (Figure 3.S5A). We measured ER motility index in HeLa cells transfected with EGFP-Sec22b incubated with DMSO or 250nM CP43 and found that ER motility was decreased from 0.27±0.02 to 0.16±0.05 (n=9, p=0.002) in the presence of CP43 (Figure 3.S5B). Additionally, measurement of EB3 velocity in HeLa cells showed that velocity was decreased from 0.33±0.017μm/s in DMSO treated cells to 0.24±0.04μm/s on addition CP43 inhibitor (Figure 3.S5C). These data indicate that catalytic activity of TAOK2 regulates its ER-MT tethering function. While TAOK2 kinase activity negatively regulates its association with microtubules, it positively regulates microtubule growth and dynamics.

Next, we assessed whether TAOK2 catalytic activity was regulated during mitosis and found that TAOK2 was highly activated during mitosis. Immunostaining interphase and mitotic cells with phospho-S181 antibody revealed a 2-fold increase in mitotic cells compared to interphase (Figure 3.7I). Western blot analysis showed high ratio of pS181-TAOK2/TAOK2 in lysates from synchronized mitotic cells compared to asynchronous cell lysate (Figure 7H). Therefore, we tested if perturbation of TAOK2 kinase activity would impact mitosis or ER segregation during cell cycle. We expressed in TAOK2 KO HEK293 cells either the TAOK2-WT or TAOK2-K57A construct along with ER-mRFP, and then used a 405nm-DNA dye and 673nm-MT dye to enable four-color imaging of TAOK2, ER membrane, chromosomes, and mitotic MT spindle. We found that while in TAOK2-WT expressing KO cells, both TAOK2 and the ER membranes were enriched at the spindle poles, and a majority of the ER membrane was dissociated from the spindle microtubules

(Figure 3.7J). However, in KO cells expressing TAOK2-K57A kinase dead mutant, TAOK2 association with the spindle MT was markedly increased and ER membranes were extensively associated with the mitotic spindle MT (Figure 3.7J). A failure of ER membranes to disengage from the spindle MT led to severe mitotic defects in K57A expressing cells including monopolar (25.5%), multipolar (23.5%) and aberrant spindles (20.8%). Accordingly, the number of mitotic cells exhibiting a normal bipolar spindle deceased from 92.8% in TAOK2 KO cells expressing TAOK2-WT to about 30% in TAOK2-K57A expressing cells (Figure 3.7K). These data demonstrate that the increased kinase activity of TAOK2 is important for dynamic regulation of ER-MT tethering during cell division, and perturbation of its catalytic activity leads to failure of ER disengagement from the mitotic spindle, ultimately inducing mitotic defects.

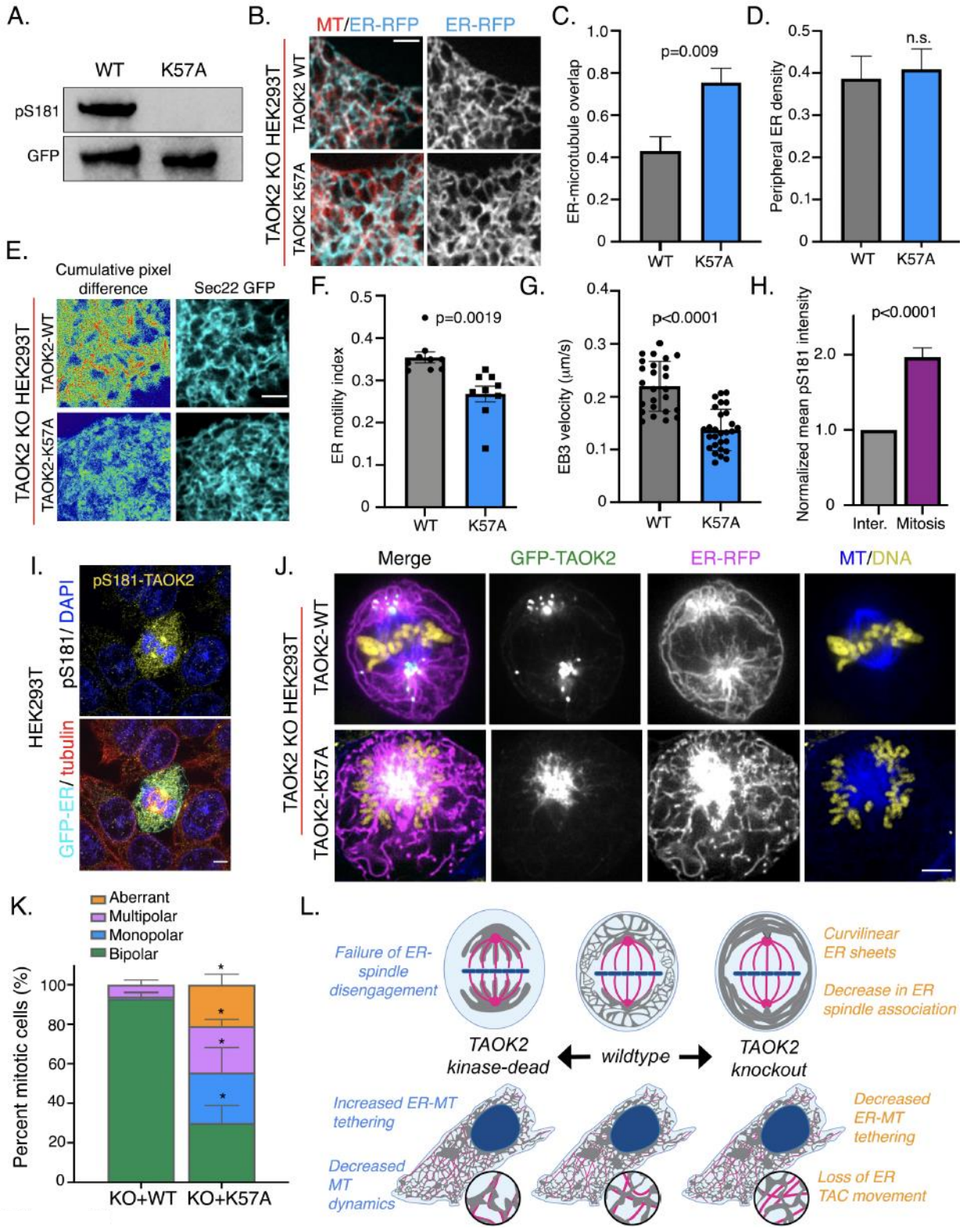

Figure 3.7 ER-microtubule tethering is regulated by catalytic activity of TAOK2

(A) Catalytic activity of GFP-TAOK2 WT and GFP-TAOK2 K57A was measured in an in vitro kinase reaction using autophosphorylation at S181 as the readout. Western blot probed with phospho-S181 antibody to measure kinase activity and anti-GFP represent the total amount of TAOK2.

(B) Confocal images of TAOK2 KO HEK293T cells expressing TAOK2-WT or TAOK2K57A along with ER-mRFP (cyan) and live-stained with microtubule dye (red). Scale bar is 3μm.

(C) The ratio of peripheral ER area in contact with microtubules to the total peripheral ER area in a 100μm^2 region in the cell periphery is plotted for TAOK2 KO HEK293T cells expressing either TAOK2-WT or TAOK2-K57A. Values indicate mean, error bars indicate S.E.M., n=6, t-test with Welch's correction.

(D) ER density is calculated for TAOK2 KO HEK293T cells expressing either TAOK2-WT or TAOK2-K57A by measuring the fraction of ER area in a 100μm^2 region in the cell periphery. Values indicate mean, error bars indicate S.E.M., n=6, t-test with Welch's correction.

(E) Confocal images of peripheral ER in TAOK2 KO HEK293T cells expressing TAOK2 WT or TAOK2 K57A along with ER marker EGFP-Sec22b at a single time point (left column). Sum slice projection of cumulative pixel difference in successive frames over 30s, where images were acquired every 3s are shown. Fluorescence intensity is pseudocolor coded, red regions representing increased ER motility. Scale bar is 3μm.

(F) ER motility index is calculated by averaging the normalized pixel difference between successive time frame over 30s. Mean ER motility for TAOK2 KO HEK293T cells

expressing either TAOK2-WT or TAOK2-K57A expressing cells is plotted. Error bars indicate S.E.M, n=9 cells, two tailed t-test.

(G) EB3 comet tracks generated using the Manual Tracking function in Fiji were used to measure EB3 comet velocity by dividing the total distance travelled over time. Mean values for TAOK2 KO cells expressing TAOK2-WT, and TAOK2-K57A are plotted, error bars indicate S.E.M, n=5 cells with 5 comets per cell, two tailed t-test.

(H) Average intensity of phospho-S181 staining in mitotic cells normalized by average interphase intensity is plotted. Error bars indicate S.E.M, n=10 cells, t-test with Welch correction.

(I) Confocal images of mitotic and interphase HEK293T cells stained with phospho-S181 and tubulin antibodies to label active TAOK2 and microtubules respectively. DNA stained with DAPI.

(J) Confocal images of TAOK2 KO HEK293T mitotic cells expressing either GFP-TAOK2 WT or GFP-TAOK2 K57A (green) along with ER-mRFP (magenta) was stained with DNA dye (yellow) and microtubules dye (blue). Scale bar is 5µm.

(K) Mitotic defects in TAOK2 KO HEK293T cells expressing either GFP-TAOK2 WT or GFP-TAOK2 K57A are plotted as the percent of total mitotic cells. Values indicate mean ± S.E.M., n=85 cells from 3 different experiments.

(L) Schematic representation of the pleiotropic function of TAOK2 in maintaining ER - microtubule tethering, microtubule dynamics and ER remodeling during interphase and mitosis. Distinct effects of TAOK2 depletion (TAOK2 knockout) compared to those due to kinase dysfunction (TAOK2 kinase dead) in interphase and mitotic cells are shown. The divergent effects of TAOK2 kinase dead mutation and TAOK2 knockout suggest

pleiotropic roles of TAOK2 mediated by distinct functional domains in addition to its kinase domain.

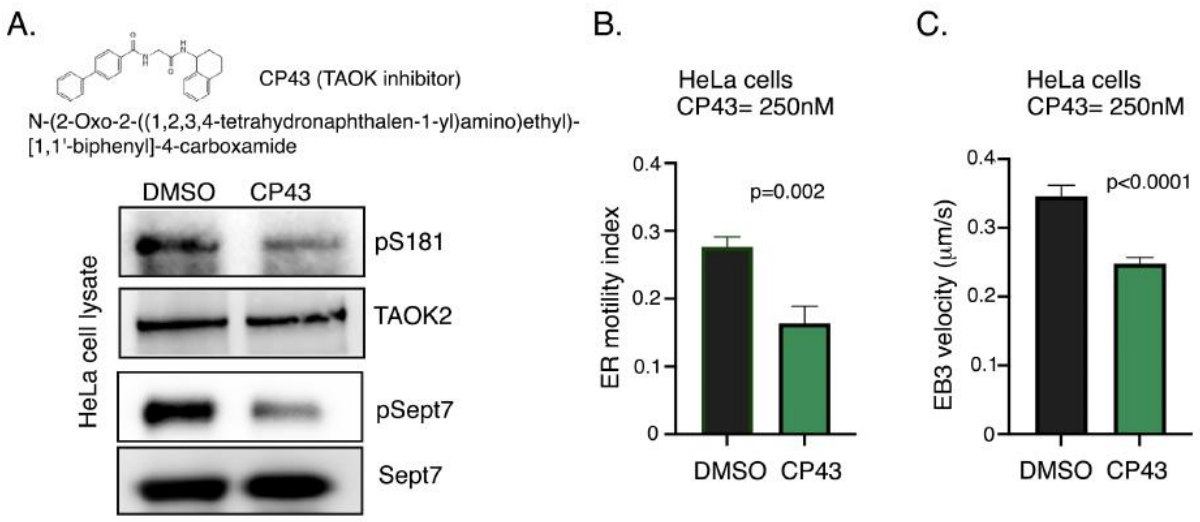

Figure 3.S5. Effect of TAOK2 kinase inhibition on ER and microtubule dynamics

(A) Kinase activity of endogenous TAOK2 was measured in the presence of DMSO and 250nM CP43 using an in vitro kinase reaction with autophosphorylation at S181 and septin7 phosphorylation as the readout. Western blot probed with: phospho-S181 antibody to measure kinase autophosphorylation activity, TAOK2 to measure immunoprecipitated TAOK2, pSept7 to measure substrate phosphorylation, and Septin7 (GST) represent the total amount of purified Septin7 c-terminal coiled coil-GST added.

(B) ER motility index calculated by averaging the normalized pixel difference between successive time frame over 30s is plotted for DMSO and CP43 treated HeLa cells. Error bars indicate S.E.M, n=10 cells, two tailed t-test.

(C) EB3 comet tracks generated using the Manual tracking function in Fiji were used to measure EB3 comet velocity by dividing the total distance traveled over time. Mean values for DMSO and CP43 treated HeLa cells. Error bars indicate S.E.M, n=10 cells with 5 comets per cell, two tailed t-test.

3.4 - Discussion

Our study identifies TAOK2 as an ER resident kinase that functions as a molecular tether linking the ER membranes to microtubule cytoskeleton. TAOK2 is a large multifunctional protein of 1235 amino acids (Chen et al., 1999). At the molecular level, we show that distinct structural domains within TAOK2 confer its catalytic activity, ER localization and microtubule association. Importantly, we demonstrate that, while the ER-microtubule tethering function of TAOK2 is structurally dissociated from its kinase domain, the catalytic activity of TAOK2 negatively regulates ER-microtubule tethering. Our results show that knockout of TAOK2 and expression of kinase-dead TAOK2 have opposing effects on ER-microtubule tethering and dynamics in both interphase and mitotic cells (Figure 3.7L). Thus, TAOK2 possesses the unique capacity to oppositely autoregulate ER-microtubule tethering through its kinase activity. We provide two key pieces of evidence in support of opposing autoregulation of tethering by TAOK2. First, we show that the kinase dead TAOK2 is a stronger ER-microtubule tether. Second, TAOK2 kinase activity is increased in mitosis, which correlates with a dramatic decrease in the tethering of ER membranes with the mitotic spindle microtubules. Perturbation of TAOK2 kinase activity in interphase cells causes increased ER-microtubule interaction and inhibiting kinase activity in mitotic cells leads to failure of ER-disengagement from the mitotic spindle causing mitotic defects.

Our study also revealed another function of TAOK2 in regulating ER membrane tracking on MT plus tips. TAOK2 contains a conserved four residue motif SxIP that allows interaction with microtubule plus end proteins EB (end binding). The SxIP motifs are typically embedded within basic and proline/serine-rich sequence regions and are characteristic features of other +TIPs such as APC, MACF, CLASP, STIM1, and MCAK

(Honnappa et al., 2009). Similarly, we found that SxIP motif within TAOK2 was part of the C terminal intrinsically disordered region and was surrounded by basic and serine residues. A previous proteome wide identification of mammalian SxIP-containing +TIPs led to the identification of several uncharacterized EB partners that have the capacity to accumulate at the growing microtubule ends. TAOK2 was identified in this study bioinformatically as an EB binding protein based on its SxIP motif, and was also detected in a biotinylation pulldown assay as an EB1 and EB3 (but not EB2) binding partner (Jiang et al., 2012).

Identification of TAOK2 as a unique kinase that also functions as an ER-MT tether, adds to the short list of two other multifunctional ER enzymes, Spastin and Atlastin that bind microtubules. Hereditary spastic paraplegia protein, Spastin, is a microtubule severing AAA ATPase enzyme that localizes to the ER and remodels microtubules via its C terminus domain (Hazan et al., 1999; Roll-Mecak and Vale, 2008). The other is Atlastin, an ER localized GTPase required for ER tubule fusion (Orso et al., 2009). In addition to these enzymes, several other ER proteins associate with the microtubule cytoskeleton directly or indirectly and are each likely to serve a particular physiological function through tethering (Wang et al., 2016). Perhaps the most well studied, Stim1, is an ER protein that interacts with microtubule growing tips indirectly by binding EB1 proteins (Grigoriev et al., 2008; Pavez et al., 2019). Climp63 is an ER protein thought to instruct the luminal width of ER sheets (Nikonov et al., 2007; Vedrenne et al., 2005) and can directly associate with microtubules (Klopfenstein et al., 1998). It is important to note, that unlike the abovementioned microtubule binding ER proteins, TAOK2 has the unique ability to interact with both microtubules and plus end proteins EB, and additionally can

bidirectionally autoregulate its microtubule association through its catalytic activity. Whether and how TAOK2 can catalytically regulate ER TAC movement remains to be tested.

In light of our findings, TAOK2 appears to be a unique serine/threonine kinase, as no other multipass membrane serine/threonine kinase has been reported to date. Two other kinases with a single transmembrane domain reside in the ER membrane, Ire1(Cox et al., 1993; Morl et al., 1993) and PERK (Harding et al., 1999). Both Ire1 and PERK kinases have a cytosol facing kinase domain similar to TAOK2. The C-terminal tailsof Ire1 and PERK project into the luminal domain where they have important functions associated with sensing ER stress (Ron and Walter, 2007). In contrast, the C-terminal tail of TAOK2 faces the cytoplasm and directly binds microtubules. The intrahelical loops between with the transmembrane helices are predicted to be extremely short (4-6 amino acids), and it is unlikely that TAOK2 serves a role as an ER stress sensor within the ER lumen. However, it is conceivable that TAOK2 is activated during ER stress indirectly through other ER stress sensors. Our data suggests that the punctate localization of TAOK2 within distinct ER subdomains is conferred by an amphipathic helical domain following the sixth transmembrane helix. Investigating the molecular identity of these ER subdomains in terms of its lipid and protein constituents would likely reveal important insight into TAOK2 regulation. Based on the findings of this study, we predict that increased activation in conditions of cellular stress might negatively regulate its function as an ER-MT tether and will be an important area of future inquiry.

Little is known about upstream mechanisms that mediate TAOK2 activation. Early studies on the family of TAO kinases suggest that they might function as intermediate signaling

kinases that link certain heterotrimeric G protein-coupled receptors to the p38 MAPK pathway. Among ligands that induce TAOK2 activation, nocodazole, sorbitol and the muscarinic agonist carbachol were found to increase TAOK2 activity from 1.5-3 fold on stimulation (Chen et al., 2003). Members of the TAO family can be activated by ATM kinase is response to genotoxic stress (Raman et al., 2007), however, whether TAOK2 is phosphorylated is unknown. TAOK2 is phosphorylated by the Hippo kinase mammalian homolog MST3 at residue T468 proximal to the kinase domain (Ultanir et al., 2014). Whether phosphorylation by MST3 increases TAOK2 catalytic activity has not been demonstrated. Further, in neurons, the secreted semaphorin molecule Sema3a has been shown to increase TAOK2 kinase activity in neurons through interaction with its receptor Neuropilin 1 (de Anda et al., 2012). Therefore, several independent signaling pathways might impinge on TAOK2 kinase to achieve distinct context-dependent cellular outcomes. As a kinase highly expressed in neurons, and one critical for neurodevelopment, the role of TAOK2 as an autoregulated ER-MT tether is likely to serve specific physiological functions in neurons. Neuronal development, connectivity and plasticity are dependent on the presence of ER membranes within fine neuronal processes such as spines, axons and dendrites where they are transported along and tethered to microtubules. TAOK2 is critical for dendritic spine development (Ultanir et al., 2014; Yadav et al., 2017), axon elongation and basal dendrite branching (de Anda et al., 2012; Richter et al., 2018). TAOK2 knockout mouse models exhibit cognitive and socialbehavioral deficits, and show structural changes in brain size (Richter et al., 2018), mechanisms of which are unknown. Further, de novo mutations in TAOK2 have been found through whole-genome and exome sequencing of patients with autism spectrum disorder (Richter et al., 2018). Our

findings provide a hitherto unknown mechanism for kinase mediated control of ER tethering to microtubule cytoskeleton. Elucidating TAOK2 function in specialized cell types such as neurons that respond to physiological stimuli by remodeling ER-microtubules tethering is likely to expand on our current understanding of the importance and dynamics of communication between cellular organelles and the cytoskeleton.

Acknowledgement

We are grateful for research funding provided by National Institute of Mental Health, R00 MH108648 and R01 MH121674 to SY, the Brain and Behavior Research Foundation's NARSAD Young Investigator Award (27818) to SY. KN was supported by the NIH predoctoral Pharmacological Sciences Training Program T32GM007750. We thank Dan Fong (Nikon) for technical assistance on the Nikon CSU-W1 SoRa superresolution microscope. We are grateful to Brian Beliveau (UW), Cole Trapnell (UW) and Jay Shendure (UW, HHMI) for use of their Nikon CSU-W1 SoRa superresolution microscope funded by HHMI. Thanks to John D. Scott (UW), Ning Zheng (UW, HHMI) and Shao-En Ong (UW) for comments and suggestions on the manuscript.

Author contribution

K.N. designed and performed TAOK2 domain dissection experiments, all biochemical characterization experiments/analyses, bioinformatic sequence analyses, confocal microscopy, and image analysis/quantification. K.N. contributed to writing the manuscript. AF designed, generated and characterized the TAOK2 KO lines; designed and performed molecular biology experiments, and analyzed EB3 dynamics and ER TAC

motility. MB performed molecular biology experiments. Manuscript written by KN and SY and edited by all authors. All aspects of this work were supervised by SY.

3.5 - Methods

Antibodies and Plasmids

Antibodies used in this study are as follows: alpha-Tubulin (Mouse, Sigma, T9026100UL), GAPDH (Mouse, Invitrogen, MA5-151738), Calreticulin (Mouse, Abcam, ab22683), TAOK2, Rabbit, Sigma, HPA010650), Rtn3a (Rabbit, ProteinTech,12055-2AP), Acetylated alpha Tubulin (Mouse, Sigma, T6793), GST (Mouse, Invitrogen), GM130 (Mouse, BD Labs, 610822), TAOK2-Cterm (Rabbit), Tom20 (Mouse, Santa Cruz Biotech, sc-17764), Stim1 (Mouse, Santa Cruz Biotech, sc-166840), GFP (Mouse, Roche, 11 814 460 001), Phospho-TAO2 (S181) (Rabbit, R&D Systems, PPS037). EB1 (Mouse, Santa Cruz Biotech sc-47704), Alpha Tubulin (Rabbit, Cell Signaling, 2144S). Addgene Plasmids used in this study are as follows: mCh-Sec61 beta (#49155), sfGFP-C1 (#54579), ER-mRFP (#62236), EGFP-Sec22b (#101918), BFP-Sec61 (#49154), Stim1-YFP (#19754), EB3-mcherry (), mito-BFP (#49151), mTagBFP2-Lysosomes20 (#55308), Rab5-BFP (#49147) and mEmerald Ensconsin-C-18 (#62753).

Molecular Cloning

Full length human TAOK2 was PCR amplified from pCMV-Sp6-TAOK2 plasmid described previously (Ultanir et al., 2014), and inserted in vector sfGFP-C1 (Addgene #54579) using restriction sites HindIII and MfeI. Domain dissection mutants were subcloned from sfGFP-TAOK2 using restriction enzymes HindIII and MfeI (New England Biolabs). All resultant plasmids were verified by sequencing. GST-TAOK2-(1187-1235) was subcloned from the sfGFP-TAOK2 into the pGEX4T1 vector using sites SalI and NotI. BFP-STIM1 was created by subcloning BFP from BFP-Rab5 (#49147) and inserting into STIM-YFP (#19754) using restriction sites SalI and NotI.

CRISPR/Cas9 genome editing

Two independent TAOK2 knockout cell lines were generated using CRISPR/Cas9 genome editing in HEK293T cells. Four guides were designed using Synthego guide design tool (https://www.synthego.com) to target coding exon 2. Guides were cloned into plasmid CrisprV2pSpCas9(BB)-2A-Puro (PX459) V2.0 (Addgene Plasmid #62988) which has Puromycin resistance. Cells were passaged in single cell suspension and plated at 50% confluence. Cultures were then transfected with lipofectamine 2000 reagent (Invitrogen 11668-030) and 2mg of each of the 2 guides used per KO line. Cells were then selected with Puromycin for 2 days to select for transfected cells. Non-Homology End Joining (NHEJ) repair created a deletion around the gRNA cutting site. Edited cells were then passaged into single cells and expanded into single cell colonies. Genomic DNA was extracted and the region around the cutting site was PCR amplified to send for sequencing. Knockout of the gene TAOK2 was confirmed by Sanger sequencing analysis, and absence of encoded protein was validated using western blot.

Cell Culture and Maintenance

All experiments were performed in HEK293T and HeLa cells, which were grown in DMEM media (Thermo Fisher, Gibco) with 10% fetal bovine serum (Axenia BioLogix) and 1% Pen-Strep (Invitrogen). Cells were maintained at 5% CO2 and 37°C and passaged every 3-4 days.

Immunofluorescence and Western Blotting

Cells were fixed with 4% paraformaldehyde and 4% sucrose for 20 minutes at room temperature, followed by 3 washes with phosphate-buffered saline (PBS). One-hour incubation with blocking buffer (200mM Glycine pH 7.4, 0.25% TritonX-100, 10% Normal Donkey Serum, in PBS) was followed by overnight incubation with primary antibody at a

1:1000 dilution in blocking buffer. After three 5min washes in PBS, cells were incubated with secondary antibody at 1:1000 dilution in blocking buffer for 3hr. Coverslips were washed and then mounted onto slides with FluoromontG. Endogenous TAOK2 staining was performed similarly, except cells were fixed with cold methanol incubated on ice for 20 minutes instead of PFA. Endogenous EB1 staining was adapted from (Grigoriev et al., 2008) with specified changes. Briefly, cells were fixed with -20C methanol on ice for 15 minutes and subsequently 4% PFA with 4% Sucrose for 15 minutes. Coverslips were washed with PBS and permeabilized with PBS and 1% TritonX-100. Blocking, washing and antibody dilution steps were performed using PBS with 1% bovine serum albumin and 0.15% Tween-20. Samples for western blot analysis were treated with 4X LDS Sample Buffer (Thermo Fisher) with 125 mM DTT and subsequently heated for 10 minutes at 95C. Samples were electrophoresed on NuPAGE 4-12% Bis-Tris Polyacrylamide gels (Thermo Fisher) with NuPAGE MOPS running buffer (Thermo Fisher). Western blot transfer to ImmobilonP PVDF membrane (Millipore-Sigma) with Transfer Buffer (25mM Tris, 192mM Glycine, 20% (v/v) Methanol, 0.05% SDS) at 100V for 60min. Resultant blot was blocked in 5% milk or BSA blocking buffer and subjected to primary antibody and HRP conjugated secondary antibody before visualization with Pierce™ ECL Western Blotting Substrate (Thermo Fisher). Western blot images were obtained using the ChemiDoc Imager (BioRad).

Image Analysis and quantification

MT growth analysis was performed using the ImageJ plugin for manually tracking objects (Manual Tracking). Single frame time lapse image stacks were processed to measure the distance traveled by EB3 comets in each frame. Velocity was calculated by dividing the total distance traveled by the time taken. Curvature was calculated by dividing the

minimum linear path (from beginning to end) by the length of the actual distance the EB3 comet traveled. Time paused was calculated by measuring the number of times the EB3 comet did not change coordinates multiplied by time between each frame (2s). Percent time paused is calculated by divided by the total time the comet was tracked. TAC - EB3 comet quantification was done by counting the number of EB3 comets showing different EB and STIM1 properties during first 10 frames of images acquired every 2 seconds apart. “Stim1-TAC” contacts was counted as percent of EB3 that were positive for STIM1 and where the ER/STIM1 extended along EB3. “Contact with STIM1” showed initial EB3-STIM1 contact but no extension of the ER occurred. “No contact with STIM1” represents EB3 comets that did not colocalize with the STIM1/ER during the studied frames. Number of EB3 comets was measured by counting comets in images obtained as z-stacks with 0.1 micron slicing whole cell expressing EB3-mcherry and dividing by the area of the cell. Endogenous EB1 comet number was measured by counting comets in a 100-micron ROI in cells immunostained for EB1.

ER motility was measured from single-z frame image stacks acquired from imaging the ER markers (EGFP-Sec22 or ER-mRFP) using ImageJ. Substacks were created corresponding to frames 6s apart and pixel differences every 6s were calculated using the Stack Difference function to determine a change in fluorescence (ΔF). ΔF was then divided by the mean fluorescence (F) of the earliest time point frame from which it was derived. (i.e., ΔF between frames 3 and 4 would be divided by frame 3) These ΔF/F values were taken for each time point and averaged over 2 minutes to determine ER motility for each cell. To obtain the cumulative pixel difference the substack obtained from

using the Stack Difference function was z-projected with the ‘sum slices’ option, and then pseudocolored using the physics LUT. This method to calculate ER motility index is an adaptation from Dong et al. (2018) (Dong et al., 2018) with specified changes. Manders’ Overlap Coefficient (MOC) (MANDERS et al., 1993) was measured using Just Another Colocalization Plugin (JACoP) (BOLTE and CORDELIÈRES, 2006). TAOK2 puncta overlap with EB1 and STIM1 was analyzed using a single frame 100micron ROI in the cell periphery by counting independent and overlapping puncta. The ratio of acetylated tubulin to total a-tubulin was measured from images of immunostained cells acquired as z-stacks with 0.1micron z-steps. Maximum zprojections were thresholded and analyzed for area of acetylated tubulin and a-tubulin respectively. Ratios were determined by dividing the area of acetylated tubulin by that of a-tubulin in each cell.

ER-microtubule overlap was measured using single frames of images cropped to a 100-micron ROIs at the cell periphery, split into respective channels and thresholded. Total area of ER and microtubules was measured using “analyze particles” option on imageJ. Overlapping area was determined by using the ‘image calculator’ AND function on thresholded images of ER and microtubules; resultant area was measured using “analyze particles.” Overlap was measured as the ratio of area of overlap to the area of the ER. ER density was subsequently measured as the area of the ER divided by the area of the ROI. These analyses were performed on WT and TAOK2 KO HEK293T cells expressing mEmerald-ensconsin and ER-mRFP, as well as TAOK2 KO HEK293T cells expressing ER-mRFP, TAOK2 WT and K57A respectively, stained with Viafluor microtubule live imaging dyes (Biotum, #70064, #70063). To assess mitotic defects, four color images were acquired as z-stacks with 0.3micron spacing such that the entire mitotic cell was

captured. Mitotic defects were scored manually by visualizing the entire z stack, based on the spindle morphology, ER morphology and chromosomal localization.

Differential Centrifugation Assay

HEK293T cells were grown to confluence in four 10cm dishes using DMEM media with 10% fetal bovine serum and 1% Pen-Strep. Cells were washed once with Dulbecco's PBS, collected in ice cold PBS and pelleted by centrifugation at 200g. Pellet was resuspended in 2 mL of homogenization buffer (250mM sucrose, 10mM HEPES, 1mM EDTA, protease inhibitors (Roche), 1mM PMSF, and 1mM DTT) and homogenized with a 25-gauge syringe needle. Homogenate was subsequently spun at 800g to pellet nuclear fraction. Post nuclear supernatant (S1) was diluted in homogenization buffer to split between two 2mL ultracentrifuge tubes. Heavy membrane fraction (P2) was obtained by centrifuging S1 at 27,000g for 30 minutes at 4 °C. Light membrane fraction (P3) was obtained by centrifuging S2 at 100,00g for 30 minutes. P3 was resuspended in either 200uL: homogenization buffer (control), or detergent buffer (1% NP-40, 1% TritonX-100, 0.1% SDS) and incubated on ice for 30 minutes before spinning at 200,000g for 60 minutes at 4 °C. Resultant high speed pellets (P4) were resuspended in 4x sample buffer with 125mM DTT. Resultant supernatants S4 and cytosolic supernatant fraction S3 were precipitated with ice cold 10% trichloroacetic acid by incubating on ice for 15 minutes followed by centrifugation at 21,000g. Precipitates were washed with icecold acetone, and pelleted at 21,000g for 5 minutes and resuspended in 4x sample buffer with 125 mM DTT. All samples were run on SDS-PAGE gels and transferred to PVDF membrane for western blot analysis.

ER Membrane Isolation

HEK293T cells were grown to confluence in four 10cm dishes. Cells were washed once with Dulbecco's PBS, collected in ice cold PBS and pelleted by centrifugation at 200g. Pellet was resuspended in 1mL of isolation buffer (225mM mannitol, 75mM sucrose, 30mM Tris-HCl pH 7.4, 0.1mM EGTA and protease inhibitors (Roche), and homogenized with a 25G needle at 4°C. The homogenate was subsequently subjected to a series of spins at 4°C, retaining the pellet from each and continuing with supernatant to the next spin. The centrifugation schema was as follows (adapted from Hoyer et al. 2018): 2 spins at 600g for 5 minutes to pellet both cell debris and nuclei (P1 and P2), 3 spins at 7000g for 5 minutes each to pellet mitochondria (P3, P4, and P5), and a 20,000g spin for 20 minutes to pellet the crude ER fraction (P6). The supernatant from the last spin yielded the cytosol, and P6 was washed with isolation buffer devoid of EGTA and subject to a 20,000g spin for 15 minutes at 4°C to re-pellet. P1-6 were resuspended in resuspension buffer (50mM HEPES, 2.5mM $MgCl_2$, 200mM KCl, 5% glycerol, 1% TritonX-100). Protein concentrations of resuspended P1-6 and cytosolic fraction were quantified by BCA assay, and subsequently 4X sample buffer with 0.125M DTT was added. This method of crude organellar separation was adapted from Hoyer et al., (2018) (Hoyer et al., 2018). Normalized samples were analyzed by western blot.

Microscopy

Superresolution imaging was performed using the Nikon-CSU-W1 Spinning Disk equipped with a microlensed SoRa emission disk that achieves Super Resolution by Optical Pixel Reassignment with a xy resolution of 120nm. Images were acquired on an inverted Nikon Eclipse Ti2 microscope (Nikon Instruments) attached to a Yokogawa spinning disk unit (CSU-W1 SoRa, Yokogawa Electric) using a 1.49 100x Apo TIRF oil

immersion objective lens. Images were captured by an Andor Sona 4.2B-11 camera using the 2.8x SoRa relay, resulting in an effective pixel size of ~40 nm. 405, 488, and 561 nm laser lines were used for excitation. All other live and fixed cell imaging was performed on a Nikon Ti2 Eclipse-CSU-X1 confocal spinning disk microscope equipped with four laser lines 405nm, 488nm, 561nm and 670nm and an sCMOS Andor camera for image acquisition. The microscope was caged within the OkoLab environmental control setup enabling temperature and CO_2 control during live imaging. Imaging was performed using Nikon 1.49 100x Apo 100X or 60X oil objectives. Live imaging for ER motility and EB3 comet velocity was performed on fibronectin coated MatTek dishes
(MatTek, P35G-1.5-14-C), and images at a single confocal z frame were captured every 2sec. Fixed cell image acquisition was performed as a z stack of images with z distance of 0.3micron. Viafluor microtubule live imaging dyes (Biotum, #70064, #70063) were used to visualize microtubules during live imaging. Cells were incubated for 30 minutes at 37 degrees C with (1:2000) dye in culture media. Subsequently, dye treated media is replaced with live imaging media with (1:10000) tubulin dye. DNA was stained with NucBlue™ Live ReadyProbes™ Reagent (Hoechst 33342) (Invitrogen), two drops/mL live imaging media incubated for 15 minutes at room temperature before imaging.

Protein Purification

TAOK2 C-terminal amino acids 1187-1235 were cloned into pGEX4T1 vector and transformed into BL21 E. coli to bacterially express the GST-tagged TAOK2 1187-1235. A 25ml starter culture grown from a single colony overnight was used to inoculate 1L culture, which was allowed to grow to an O.D, of 0.6 at 37°C. Protein expression was induced by IPTG at a final concentration of 0.4mM for 18 hours at 18°C. Bacteria were collected by a 15min spin at 5000g, washed with ice cold PBS, and the pellet was

resuspended in ice cold lysis buffer (50mM Tris pH 8.0, 5mM EDTA, 150mM NaCl, 20% glycerol, 5mM DTT, protease inhibitors and PMSF). Addition of 4mg lysozyme (Sigma) was followed by 30min incubation with 0.5% TritonX-100 and sonication on ice. The supernatant was collected after a 60min spin at 25,000g, and incubated with prewashed GST beads (Thermo Fisher) for 1 hour. Beads were washed with wash buffer (PBS + 1mM DTT + 0.1% tween 20) followed by wash buffer without detergent. Bound protein was eluted and collected in fractions by glutathione elution buffer at pH8.0 (50mM Tris pH8.0, 250mM KCl, 1mM DTT, 10% glycerol and 30mM glutathione).

Microtubule co-sedimentation assay

Microtubules were prepared by polymerizing porcine tubulin (Cytoskeleton inc.) in general tubulin buffer (80mM PIPES pH 6.9, 2mM $MgCl_2$, 0.4mM EGTA, Roche Protease Inhibitors) in the presence of 1mM GTP for 20 minutes at 35^{o}C and then diluted further. To prevent depolymerization, microtubules were treated with 40 μM Taxol. Microtubules and 5 μg purified protein were incubated at room temperature, and pelleted at 100,000g over a 60% glycerol cushion buffer (80mM PIPES pH 7.0, 1 mM MgCl2, 1 mM EGTA, 60% Glycerol, protease inhibitor). The supernatant (top layer above cushion) and the pellet were removed and treated with 4X Sample Buffer with 250mM DTT and 5% beta-mercaptoethanol. Resultant samples were subject to SDS-PAGE and colloidal Coomassie blue staining (Invitrogen).

Mitotic cell lysate

HEK293T cells were synchronized by treatment with 1.67μM nocodazole for 12-16 hours. Rounded cells were dislodged by shaking and collected with media. Concurrently, untreated asynchronously growing HEK293T cells were scraped and collected in DPBS. Both tubes of cells were separately pelleted, washed in DPBS, and lysed in HKT buffer

(25mM HEPES pH7.2, 150mM KCl, 1% Triton X-100, 1mM DTT, 1 mM EDTA, Protease Inhibitors (Roche, Complete), Halt Phosphatase Inhibitors (Thermo Fisher). Lysate was cleared of cell debris by centrifugation and protein concentrations were determined via BCA assay (Thermo Fisher). Sample Buffer with 125mM DTT was added to equalized amounts of protein and subject to western blot analysis as described above.

Immunoprecipitation Kinase Assay

HEK293T cells transfected with sfGFP-TAOK2 WT and sfGFP-TAOK2 K57A were lysed with HKT buffer (25mM HEPES pH7.2, 150mM KCl, 1% Triton X-100, 1mM DTT, 1 mM EDTA, Protease Inhibitors (Roche, Complete)). Lysate was precleared with Pierce ProteinG Agarose (Thermo Fisher), and immunoprecipitated with Roche anti-GFP Mouse antibody bound on Pierce protein G agarose. Beads were washed twice with HKT, once for 10 minutes with HKT with 1mM NaCl, and finally washed with HK buffer (25mM HEPES pH 7.2, 150mM KCl, 1mM DTT, 1 mM EDTA, Protease Inhibitors (Roche, Complete EDTA free)). Beads were washed once with the Kinase Buffer (25mM Tris pH 7.5, 10mM MgCl2, 1mM DTT) prior to the in vitro kinase assay. Kinase assay was then performed by incubating with 0.5mM ATP and Halt protease/phosphatase inhibitors (Thermo Fisher) for 45 minutes at 30°C on a shaking heat block. Samples were then subjected to western blot analysis detailed above to detect autophosphorylation of TAOK2 at S181 using the rabbit antibody (R&D Systems, PPS037).

CP43 Kinase Assay: Endogenous TAOK2 was immunoprecipitation from untransfected HeLa cells using the TAOK2 Sigma antibody. CP43 (500nM) was added to kinase assay along with 0.5mM ATP, Halt protease/phosphatase inhibitors (Thermo Fisher) and GSTSeptin 7 C-terminal coiled coil tail (321-438 amino acids) [Purified as described in Yadav et al., 2017)] as a substrate for 45 minutes at 30°C on a shaking heat block.

Immunoprecipitation of endogenous EB1 was adapted from (Hoogenraad et al., 2000). Briefly, HeLa cells were lysed with HKT buffer (25mM HEPES pH7.2, 100mM KCl, 0.5% Triton X-100, 1mM DTT, 1 mM EDTA, Protease Inhibitors (Roche, Complete)). Lysate was precleared with Pierce Protein-G Agarose (Thermo Fisher), and immunoprecipitated with anti-GFP Mouse (control), anti-EB1 mouse and anti-STIM1 antibodies separately bound on Pierce protein G agarose. Beads were washed thrice with HKT and washed thrice with HK buffer (25mM HEPES pH 7.2, 100mM KCl, 1mM DTT, 1 mM EDTA) then treated with 4X Sample Buffer with 250mM DTT and 5% beta-mercaptoethanol. Resultant samples were subject to SDS-PAGE.

Statistics

All statistics were performed in GraphPad software Prism9.0. Multiple groups were analyzed using ANOVA, while two group comparisons were made using unpaired t-test unless otherwise stated. Statistically p value less that 0.05 was considered significant. All experiments were done in triplicate, and experimental sample size and p values are indicated with the corresponding figures.

CHAPTER 4: ELUCIDATING TAOK2 INTERACTORS THROUGH BIOID2 PROXIMITY LABELING

4.1 - Introduction

The cell is jam-packed with a plethora of various molecules of different sizes creating contextual 'neighborhoods' wherein contacts are made, and reactions occur. Understanding the function of a protein and the biological processes in which it contributes can often come down to understanding its interaction network. Over the years many different tools and methods have been created to study molecular contacts through an engineered or modified enzyme that is able to label interactors within a known radius either fused or targeted to the protein of interest (Qin et al., 2021). Proximity labeling enzymes are of two general groups: peroxidases, and biotin ligases. The peroxidases of this group are activated by peroxide to convert biotin-phenols into highly reactive radical species which, on the scale of seconds, are able to tag proteins within a 1-10nm radius with biotin, which then can be captured on streptavidin beads (Li et al., 2014; Rhee et al., 2013). Horseradish peroxidase (HRP) and engineered ascorbate peroxidase (APEX) were originally fused to proteins of interest to act as reporters in electron microscopy (Hopkins et al., 2000; Martell et al., 2012); but have since evolved into the world of proximity labeling (Li et al., 2014; Rhee et al., 2013). APEX was further engineered to APEX2, which is more active in cells than its predecessor (Lam et al., 2015). It is worth noting that a pitfall of this approach that the peroxidase-based proximity labeling reactions require presence of hydrogen peroxide which is toxic to cells (Nindl et al., 2004).

The other group of engineered enzymes for proximity labeling are biotin ligases, which utilize promiscuous point mutants of bacterial biotin ligases to biotinylate proteins within 10nm of the protein of interest (Branon et al., 2018; Kim et al., 2016; Roux et al., 2012). The first of these proteins to be generated was BioID which utilizes BirA*, a promiscuous

point mutant of 35kDa E. coli biotin ligase as a labeling enzyme (Roux et al., 2012). The second generation of the biotin-ligase based proximity labeling enzymes, BioID2, employs a smaller, 27kDa, biotin ligase from A. aeolicus that does not bind DNA but is highly efficient (Kim et al., 2016). Both BioID and BioID2 require around 18 hours, to effectively biotinylate neighboring proteins (Roux et al., 2012; Kim et al., 2016). More recently, directed evolutions of BioID known as TurboID and miniTurbo have gained use due to their 10 minute reaction time, and in the case of miniTurbo, 28 kDa protein size (Branon et al., 2018). These molecules are invaluable tools for studying protein-protein interactions and can be used to shed light on protein involvement in numerous pathways and processes.

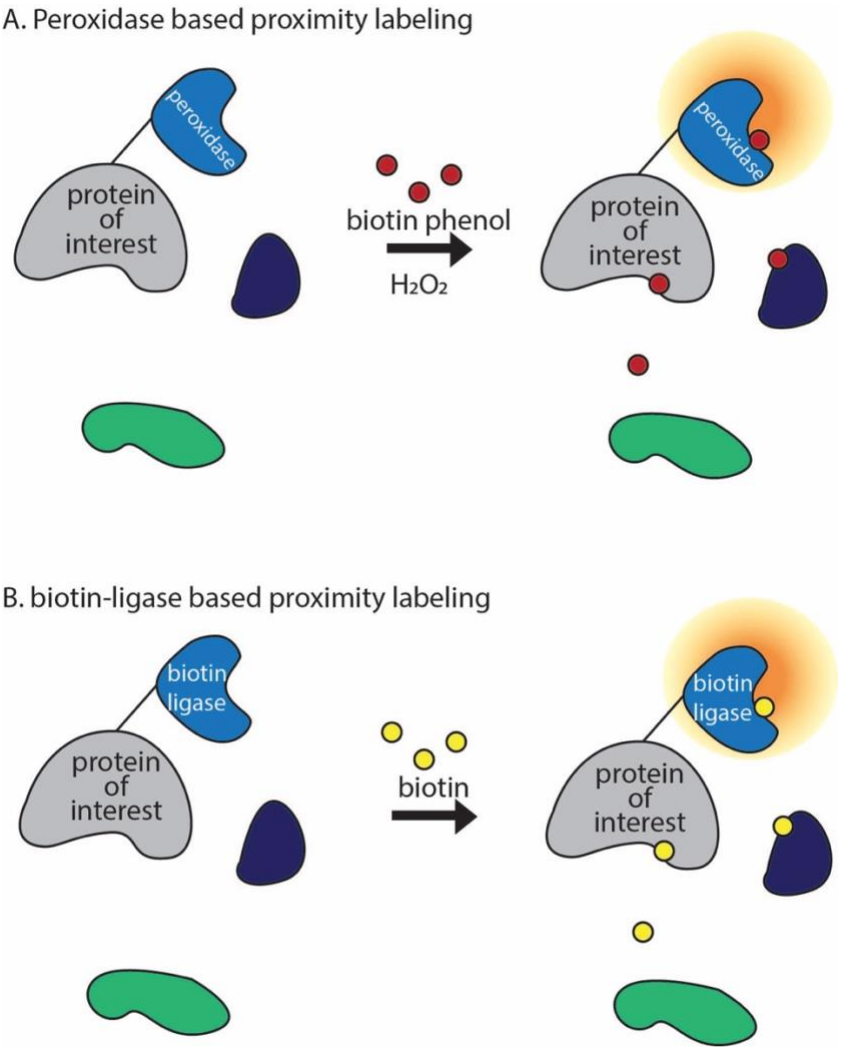

Figure 4.1 – Schematic representation of the two classes of biotin ligase.

(A) Shows peroxidases using biotin-phenol to biotinylate proteins within a proximal radius of the protein of interest (POI).

(B) Depicts biotin ligases biotinylating proteins with a proximal radius of the POI in the presence of increased biotin.

Our lab previously uncovered several potential substrates through chemical genetic substrate identification (Yadav et al., 2017). Of these substrates, Septin 7 is the only one that has been validated as a bona fide substrate (Yadav et al., 2017). Given the essential role of TAOK2 in several aspects of neuronal development, and the lack of known regulators/interactors of TAOK2, unbiased identification of proteins that associate with TAOK2, will likely yield important insight into its function. In order to uncover TAOK2 interactors, I have chosen to use BioID2 due to its smaller protein size and long reaction time. Due to the large size of TAOK2 (138kDa) (Chen et al., 1999), a small biotin ligase such as BioID2 (Kim et al., 2016) will be more favorable to avoid steric hindrance. Further, a longer reaction time will allow for the labeling of interactors from numerous contexts rather than a 10-minute period which is more appropriate and useful for transient interactions.

4.2 - Methods

Cloning

Myc-tagged BioID2 was subcloned from pcDNA3.1 myc-bioid2-MCS (addgene# 74223) using myc-BioID2_AgeI_F and myc-BioID2_BglII_R (see table below) digested with AgeI and BglII (New England Biolabs)(Platinum SuperFi Polymerase, Thermofisher Scientific). sfGFP-TAOK2 (previously described in Chapter 3 methods) was digested with AgeI and BglII to remove super-folded GFP. Digested vector and subcloned fragment were ligated using T4-ligase (New England Biolabs). Resultant plasmid pcDNA3.1 myc-bioid2-TAOK2 was sequenced using sanger sequencing.

pZIP-hEF1a-myc-bioid2-TAOK2 and pZIP-hEF1a-zsgreen-myc-bioid2-TAOK2 were cloned from pZIP- hEF1a-zsgreen-puromycin and pcDNA3.1 myc-bioid2-TAOK2 using

primers listed in the chart below by Gibson Assembly (New England Biolabs, NEBuilder® HiFi DNA Assembly Master Mix, E2621S) (Platinum SuperFi Polymerase, Thermofisher Scientific).

PRIMER NAME	SEQUENCE 5' TO 3'
myc-BioID2_AgeI_F	GGTGGTACCGGTATGGAACAAAAACTCATCTCAGA
myc-BioID2_BglII_R	GGTGGTAGATCTGCTTCTTCTCAGGCTGAACTCG
FRAG1_PZIP_FWD	GACGGATCGGGAGATCCTCGCGC
FRAG1_PZIP_REV	CGGAGCCTCACGTATCGATAAACT
FRAG2_PZIP_FWD	AGTTTATCGATACGTGAGGCTCCG
FRAG2_PZIP_REV	GATGAGTTTTTGTTCCATGGTATTATCGTGTTTTTCAA
FRAG3_MYCBIOIDTAOK2_FWD	AACACGATAATACCATGGAACAAAAACTCATCTCAGAAGAGGAT
FRAG3_MYCBIOIDTAOK2_REV	TCCAGAGGTTGATTTCACCTCCAGGGGGG
FRAG4_PZIP_FWD	CCCCCCTGGAGGTGAAATCAACCTCTGGA
FRAG4_PZIP_REV	GCGCGAGGATCTCCCGATCCGTC
FRAG 2.1_PZIP_REV	TGAGTTTTTGTTCCATTGGACCGGGCACGAC
FRAG3.1_MYCBIOIDTAOK2_FWD	GCCCGGTCCAATGGAACAAAAACTCATCTCAGAA
FRAG3.1_MYCBIOIDTAOK2_REV	GAGGTTGATTGTTTCACCTCCAGGGGGGCAGG
FRAG 4.1_PZIP_FWD	CCCCCCTGGAGGTGAAACAATCAACCTCTGGA

Antibodies/Reagents

Anti-c-Myc (Sigma #C3956), Streptavidin-HRP (Abcam #ab7403), Neutravidin-DyLight 550 (Invitrogen).

Cell Culture

Experiments were performed in HEK293T and HeLa cells, which were grown in DMEM media (Thermo Fisher, Gibco) with 10% fetal bovine serum (Axenia BioLogix) and 1% Pen-Strep (Invitrogen). Cells were maintained at 5% CO2 and 37°C and passaged every 3-4 days)

BioID2 Experiments: Briefly, HEK293T cells grown on 10 cm plates were transfected with myc-BioID2-TAOK2 (JetOptimus, PolyPlus). After 12-24 hours, media was replaced in half of the plates with media containing 50uM Biotin. Remaining plates served as a control receiving 0.1% DMSO. Cells incubated for 18 hours in DMSO or biotin media and were subsequently washed with 25 mL room temperature DPBS (Gibco)/plate. Cells were collected in respective tubes and lysed on ice in HKTDS lysis buffer (25 mM HEPES pH 7.2, 150 mM KCl, 1% Triton X 100, 0.5% deoxycholate, 0.1% SDS, 1mM EDTA, 1mM DTT with roche c0mplete protease inhibitors) and spun down 10 min at 16,500 × g, 4°C. Lysate was incubated on streptavidin beads overnight. Beads were washed extensively: 3x with HKTDS, 3x with 2M Urea in 10mM Tris pH 8.0 and 3x with 20mM Tris pH 7.5. 10% of the sample was analyzed by western blot (as described in chapter 3), remaining 90% underwent sample preparation and subsequent mass spectrometry. Immunocytochemistry and confocal microscopy were performed as described in Chapter 3.

Sample Preparation

Beads were resuspended in 3x bead volumes of 8M Urea/10 mM Tris pH 8.0. Disulfide bonds were reduced by adding TCEP to a final concentration of 1 mM and incubating at room temperature for 30 minutes. Chloroacetamide (CAM) to final concentration of 3 mM. and incubated for 10 minutes at room temperature to alkylate cysteines. CAM was quenched by adding TCEP to 1mM. Sample pH was ensured at pH 8 and then incubated 1:100 with LysC for 2 hours at 37°C. After adding TEAB to dilute urea to less than or equal 2M, trypsin was added and incubated 37°C for 12-16 hrs with gentle agitation.

Digestion was stopped by using TFA until sample reads pH 2.0. Samples were then loaded onto C18 StageTips.

Data Analysis and Quantification

Data was analyzed in Perseus 1.6.5.0. String11.5 analysis was performed on string-db.org. Gene Ontology analysis was performed using dice-database.org.

4.3 - Pilot Experiment: Preliminary Results and Interpretation

myc-BioID2-TAOK2 expressed in HEK293T cells localizes in the same microtubular pattern as observed previously (Fig 3.2 A Figure 4.2). Biotinylation occurs in a spatially precise fashion surrounding the myc-BioID2-TAOK2 signal (Figure 4.2). Lysate from HEK293T cells expressing myc-BioID2-TAOK2 treated with 50uM biotin or DMSO show changes in the amount of the biotinylated proteins, this is reflected in the streptavidin pull down (Figure 4.3). We do not see myc-BioID2 TAOK2 enriched in the pull down, which was not expected. I hypothesize is that this construct is not taken up into enough cells to express high levels.

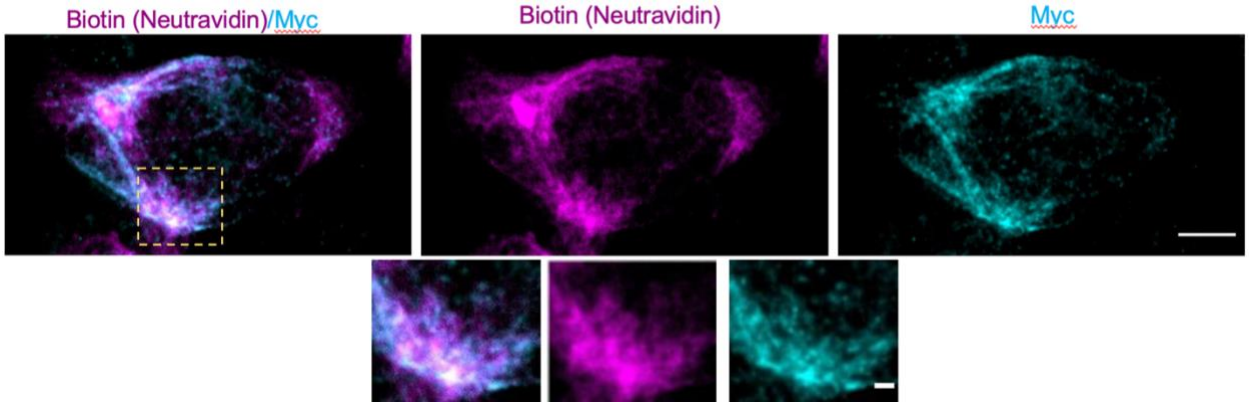

Figure 4.2 – Confocal microscope images of HEK293T cells expressing myc-BioID2-TAOK2 treated with 50uM biotin.

Myc-BioID2-TAOK2 (cyan) is visualized using a c-myc antibody. Biotinylated proteins (Magenta) are depicted using Neutravidin-Dylight 550.

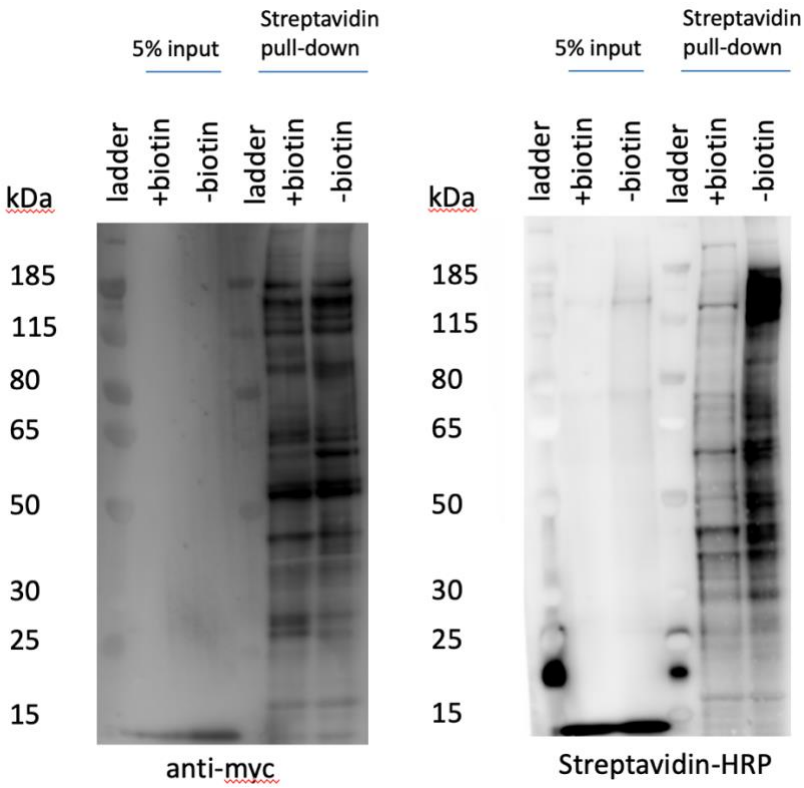

Figure 4.3 – BioID2 Western blots

(A) Western blots of +biotin and -biotin streptavidin pull-down samples and 5% input samples. Right side shows blot against biotinylated proteins using streptavidin-HRP. Left shows blot against c-myc.

Note: The data beyond this point were generated from the pilot mass spectrometry run from this project. This run was not perfect in its experimental design and sample prep as there was approximately 5-fold more raw material in the +biotin condition than the -biotin/DMSO only condition. Further, these samples were not loaded onto more than one C18 StageTip each, therefore, we have only one value per run and cannot calculate significance from these data. Due to the single replicate, I was not able to create a volcano plot with the logarithm of the fold change on the X axis, and the logarithm of the significance on the Y axis.

I have plotted the ratio of enrichment here (Figure 4.4) which shows that there were numerous proteins highly enriched in the +biotin condition as compared to -biotin condition. This graph is not descriptive of significance of these values or fold change. Without significance values it is impossible to pick out hits from this large dataset, therefore the STRING11.5 analysis (Figure 4.5) and Gene Ontology analysis of biological processes (Figure 4.6) are unintelligible. In future datasets with proper internal replicates, hits will be picked out and focused on in these further analyses to elucidate TAOK2 interactors.

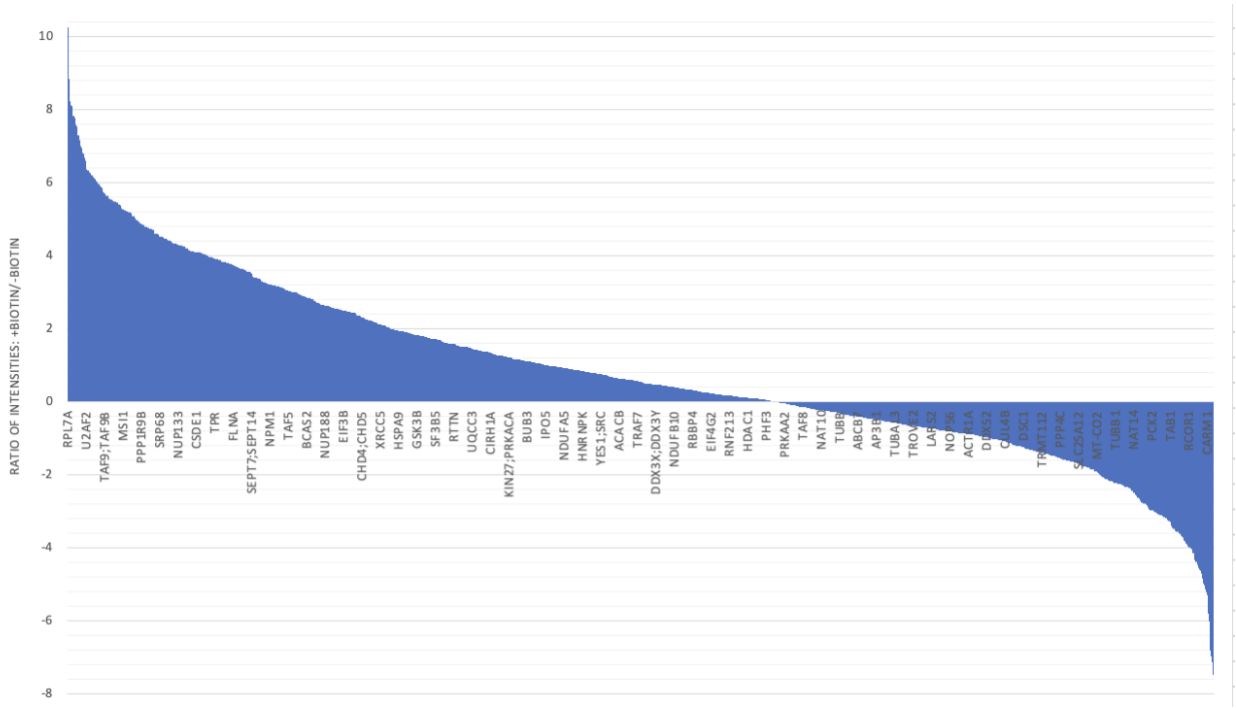

Figure 4.4 – Graph comparing enrichment of proteins between +Biotin/-Biotin samples.

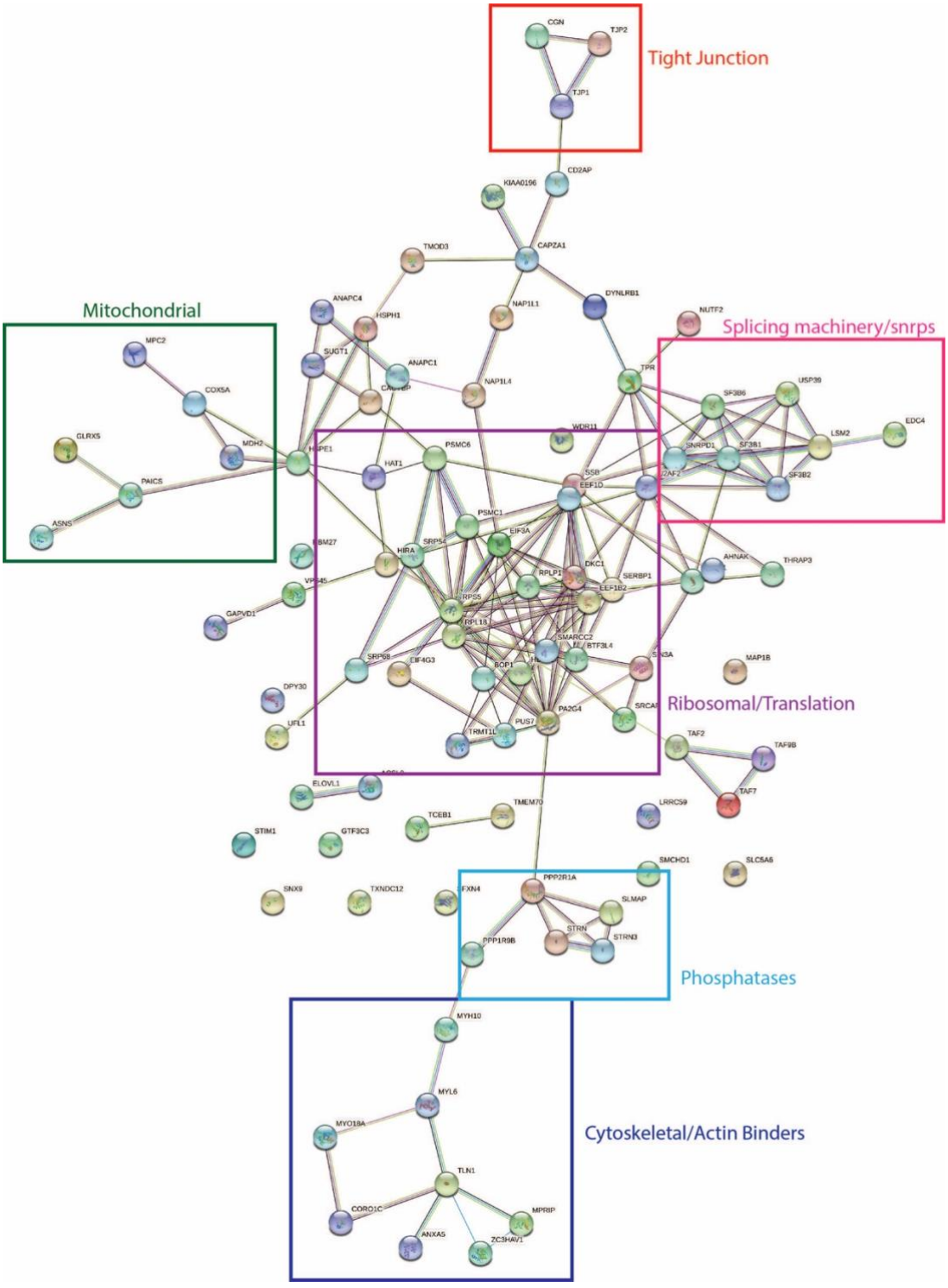

Figure 4.5 – STRING 11.5 analysis of top 100 potential TAOK2 interactors identified by BioID2 proximity biotinylation and mass spectrometry. Gene groups labeled by squares.

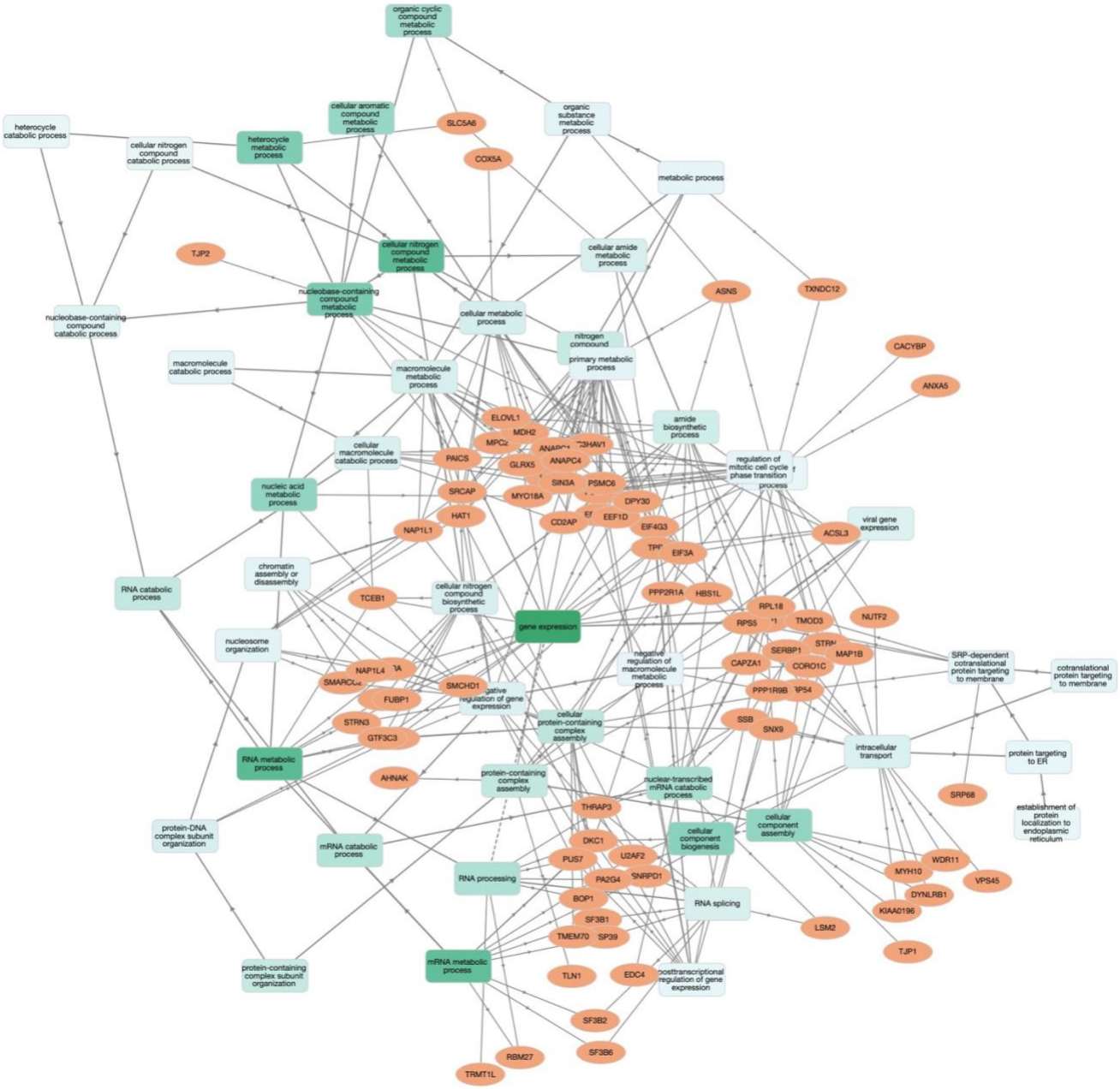

Figure 4.6 – Gene Ontology analysis network of biological processes based on top 100 potential TAOK2 interactors identified by BioID2 proximity biotinylation and mass spectrometry. Genes are in orange, biological processes in green. Saturation of green denotes strength of association.

4.4 - Future Directions

Determining and validating TAOK2 interactors in HEK293T cells has proven challenging thus far. Expression level of the protein has been moderate, and transfection efficiency have been difficult to judge due to a lack of fluorescent tag. Further, the HEK293T cells have been a great starting point to optimize the proximity labeling technique but are not the most relevant cell type to study neurodevelopment. Moving forward, I propose to use rat primary cortical neurons as the context in which to perform proximity biotinylation experiments and further understand TAOK2's role in biological processes necessary for neuronal development. Regarding the difficulties with transfection, I have cloned two myc-bioid2-TAOK2 lentiviral transfer vectors, one of which is bicistronic, expressing zs-green to alleviate difficulties determining efficiency of horizontal gene transfer. The vector itself can be used direct transfection in HEK293T cells or can be used to make virus to transduce other cell types such as neurons which are difficult to transfect efficiently.

Another limitation in this process has been the mixed specificity of our c-myc antibody, which is able to label both c-myc and myc-tagged proteins. In the future, an antibody against only myc-tagged proteins should be used for cleaner western blots and immunocytochemistry. Once data from mass spectrometry runs with proper replicates have been collected, data should be processed by paired t-test in Perseus 1.6.5.0 to create a volcano plot depicting log (fold change) vs. log(p-value). Potential interactors will have high log(p-value) and high log (fold change) values and can be further analyzed using string analysis STRING11.5 and Gene Ontology analysis in dice-database.org. Potential interactors can be verified by coimmunoprecipitation.

Limitations and Alternative Approaches: There is potential for BioID2 to not yield specific or significant results. In this case another proximity labeling method such as APEX or

miniTurbo should be considered to circumvent difficulties with this proximity labeling enzyme. Furthermore, co-immunoprecipitation mass spec can be performed as an alternative or in addition to proximity labeling to ensure validity of the data.

CHAPTER 5: DISCUSSION AND FUTURE DIRECTIONS

5.1 - Molecular and cellular functions of TAOK2 kinase

Through the experimental work in chapter 3, we demonstrated that TAOK2 is a large multidomain ER-localized kinase that directly binds to microtubules, thereby acting as an ER-microtubule tether. Further, we revealed that TAOK2 localized at microtubule plus-ends and that TAOK2 depletion results in disturbed STIM1/EB1 mediated TAC movement. Additionally, we uncovered that TAOK2 interacts with EB1 via a conserved SxIP motif to facilitate TAC movement, independently from its microtubule-binding activity. We determined that TAOK2 is highly enriched at the mitotic spindle poles acting as an anchoring point for ER-spindle interactions. Interestingly, we found that TAOK2 microtubule binding is regulated by its catalytic activity, loss of kinase activity resulting in increased ER-microtubule tethering. In chapter 4, I have detailed the experimental blueprint for determining TAOK2 interactors using proximity biotinylation enzyme BioID2. Identification of TAOK2 as a distinctive ER-microtubule tethering kinase has opened up many new questions to comprehend TAOK2's role in neuronal development (Figure 5.1).

Determining that TAOK2 localizes to discrete ER domains of high curvature in the cell periphery was an interesting finding as it required six transmembrane domains and amphipathic helix to confer its localization. However, when only the 6 transmembrane helices are expressed TAOK2 localizes continuously throughout the ER membrane rather than these distinct areas. The question remains as to what area of the ER to which TAOK2 localizes and to what biological process TAOK2 contributes. One potential subdomain of the ER that TAOK2 may localize to is the Rab10 subdomain of phospholipid biosynthesis (English and Voeltz, 2013). Rab10 is an ER-localized GTPase that moves along microtubules in active subdomains pinpointed at the tip of approximately 50% of ER

tubules (English and Voeltz, 2013). Fascinatingly, these Rab10 subdomains contain two integral ER enzymes, phosphatidylinositol synthase (PIS) and choline/ethanolamine phosphotransferase (CEPT1) (English and Voeltz, 2013), which are necessary for the synthesis of phosphatidylinositol, phosphatidylcholine, and phosphatidylethanolamine respectively (Antonsson, 1997; Henneberry et al., 2002). The presence of Rab10 in this subdomain is important for ER tubule extension and fusion (English and Voeltz, 2013), which could make Rab10, PIS, and CEPT1 interesting potential interactors for TAOK2.

Earlier in this thesis study, I showed TAOK2 knockout reveals changes in ER density in the ER periphery. It is highly likely that TAOK2 could be interacting with proteins that shape the ER membrane such as reticulons, a class of transmembrane that form a hairpin-like structure in the membrane acting as a wedge in areas of high curvature (Voeltz et al., 2006). Interestingly, loss of reticulons results in decreased ER tubules, but increased ER sheet structures (Anderson and Hetzer, 2008; Craene et al., 2006; Voeltz et al., 2007). Another group of ER shaping proteins that TAOK2 could be interacting with are REEP1-4 which promote ER tubules, and REEP5/6 (also known as DP1/Yop1) which similarly to reticulons form wedges on the ER membrane that stabilize the membrane curvature (Hu et al., 2009). Loss of members of this group of proteins leads to unbranched tubular extensions of the ER (Hu et al., 2009), which can upset ER density which could make these proteins noteworthy in our quest for understanding TAOK2 in the context of ER shape. Another distinct subdomain of ER are the sites of interaction with distinct organelles such as mitochondria, endosomes, peroxisomes as well as membrane-less organelles such as the p-body. Whether TAOK2 localizes at any of these organellar contact sites remains to be tested.

In chapter 3 we explored the impact of TAOK2 on ER morphology and movement, however, the implications of TAOK2 on ER function remain largely unknown. Given TAOK2 is activated in response to cellular stress (Chen et al., 1999; Chen et al., 2003; Fang et al., 2020), it follows that TAOK2 may play a role in the ER stress response and maintenance of homeostasis. Further studies are necessary to understand the role of TAOK2 on ER function, calcium storage, and cellular stress.

5.2 - Implications of TAOK2 ER-MT tethering for neuronal development

Direct microtubule binding and ER-microtubules tethering by TAOK2 are remarkable functions of TAOK2 which has enumerated more lines of questioning for this kinase. We now know that TAOK2 is one of several proteins that act as ER-microtubule tethers and also regulates STIM1 mediated ER-TAC movement through its association with EB1. An aspect of this signaling pathway that we have not yet explored is whether the catalytic activity of TAOK2 regulates ER-TAC movement. Based on our data, expression of TAOK2 kinase-dead results in increased microtubule binding of TAOK2, stronger ER microtubule tethering, increased ER density, decreased ER motility, and decreased EB3 velocity. We could speculate that TAC movement would occur slower than it does under wildtype conditions. Toward understanding if catalytic activity regulates TAC, an important next step is to test how TAOK2 is interacting with TAC machinery components EB1 and STIM1. We know that TAOK2 and EB1 associate, but whether TAOK2 phosphorylates EB1 or STIM1 and whether that regulated its binding to the EB1/STIM1 complex has not been investigated. It is conceivable that TAOK2 phospho-regulates STIM1 as it has been shown that STIM1 phosphorylation leads to exclusion of the ER from the spindle during mitosis (Smyth et al., 2012). Finally, with regards to TAOK2 microtubule binding, it is still not understood mechanistically how TAOK2 catalytic

activity regulates its association with microtubules. Given the potential that this could be an autophosphorylation event, in future studies, it would be interesting to map potential phospho-sites in the TAOK2 C-terminal microtubule binding. Understanding how TAOK2 catalytic activity contributes to regulating TAC, EB1/STIM1 localization, and microtubule-binding would shed light on how the mechanism by which TAOK2 mediates ER-microtubule motility.

Given that TAOK2 is a regulator of several aspects of neuronal morphology including axon elongation, dendritic arborization, and spine formation, many questions remain about TAOK2 mediated ER-microtubule tethering in neuronal development. TAOK2 is now added to the list of proteins that regulate ER microtubule contacts such as M1 Spastin CLIMP-63, p180, and STIM1 (Grigoriev et al., 2008; Klopfenstein et al., 1998; Ogawa-Goto et al., 2007; Park et al., 2010) which play various roles in neuronal development. Several of these proteins are involved in the remodeling of microtubules. For instance, Spastin specifically decreases the microtubule network in the axon by severing microtubules (Sherwood et al., 2004), but does promote microtubule regrowth (Kuo et al., 2019). In addition, depletion of p180 in cultured neurons results in decreased microtubule stability through reduction of acetylated tubulin (Farias et al., 2019). Other ER-microtubule tethering proteins such as CLIMP-63 play a role in the distribution of smooth ER tubules throughout axons via dynein and kinesin-mediated sliding events (Faras et al., 2019). Finally, STIM1 is important for ER-TAC movement by its interactions with EB1/3 decorated microtubule plus ends, depletion of EB1/3 results in decreased smooth ER-tubules distribution to dendrites but does not change the distribution in the axon (Farías et al., 2019). These data suggest that ER-microtubule tethering is important

for the ER insertion and distribution into neurites. How TAOK2 contributes to ER distribution through its ER-microtubule tethering ability is yet to be understood.

TAOK2 depletion studies have shown a decrease in basal dendrite complexity, but no change in apical dendrites (de Anda et al., 2012; Richter et al., 2018). There is little known about the ER distribution in basal dendrites of pyramidal neurons. Further studies are necessary to understand how TAOK2 and ER impact basal dendrite formation and elaboration.

ER insertion into the dendritic spines is important for synaptic plasticity local translation (Holbro et al., 2009; Ostroff et al., 2017). Further, ER inserted into dendritic spines forms a specialized organelle important for long term potentiation, known as the spine apparatus (Perez-Alvarez et al., 2020). There are still lapses in our collective knowledge of ER insertion into dendritic spines. TAOK2 interacts with actin motor protein, Myosin Va on phosphorylation at T440 by MST3 kinase, and this regulates the recruitment of Myosin Va into the dendrites (Ultanir et al., 2014). In Purkinjje neurons, Myosin Va is responsible for ER transport into dendritic spines (Wagner et al., 2011). Myosin Va accumulates at the tip of the ER tubule as it moves into spines, and blocking Myosin Va actin-based movement reduces ER translocation into dendritic spines. It is likely that TAOK2 modulates this process and may act as a linking point between the ER and Myosin Va. Further research is required to better understand how TAOK2 and Myosin Va interplay are implicated in this process.

Axonal growth is dependent on dynamic ER tubules enriched in the axonal growth cone that push forward the extension of the plasma membrane during neuronal development (Dailey and Bridgman, 1989; Farías et al., 2019) Interestingly, the ER is

translocated into the axonal growth cone filopodia during development by STIM1 (Pavez et al., 2019). Given that TAOK2 is highly enriched in the axonal growth cone during development, and depletion of TAOK2 results in impairments in axonal guidance (de Anda et al., 2012), it would be incredibly interesting to study if and how TAOK2 plays a role in neuronal ER insertion into the axonal growth cone and the impact on axonal development.

Perhaps one of the most interesting aspects of studying TAOK2 has been its linkage to autism spectrum disorder (ASD) (Weiss et al., 2008; Richter et al., 2018). Further, TAOK2 is encoded in the 16p11.2 genomic locus, copy number variations (CNVs) of which are associated strongly with ASD and schizophrenia (Kumar et al., 2007; McCarthy et al., 2009; Weiss et al., 2008). Due to the association of gene dosage changes of TAOK2 with brain size changes in mice and head circumference in patients (Luo et al., 2012; Richter et al., 2018), ER-microtubule coupling should be examined in models of these CNVs to determine a potential cellular basis of disease. Of the 24 TAOK2 variants found by GWAS studies, only two of them show changes in kinase activity (Richter et al., 2018). TAOK2 A135P is the only one of these mutations found in the kinase domain and is the only mutation which abolishes kinase activity (Richter et al., 2018). The remainder of these mutations do not have a clear pathophysiology but remain as ASD-linked unstudied mutants. In our study, we have uncovered TAOK2 ER localization and mapped the C-terminal microtubule-binding domain. These findings serve as a firm basis for further study and understanding of the impacts of these TAOK2 ASD variants on TAOK2 function in ER microtubule tethering, TAC movement of the ER, and potential interactors (Figure 5.1).

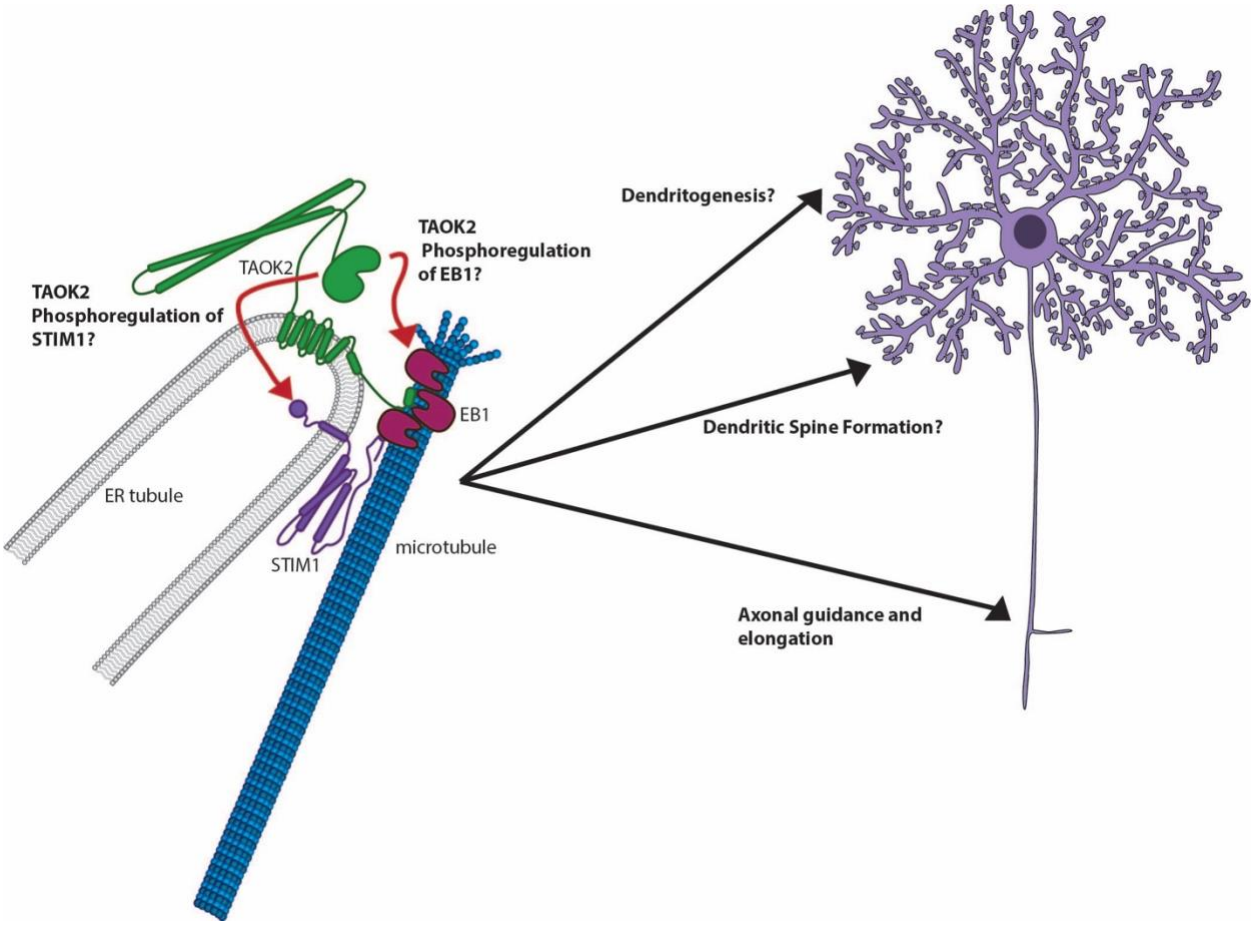

Figure 5.1 Schematic of TAOK2, an ER resident protein that binds microtubules, acting as a microtubule tether and its potential interactors.

TAOK2 binds EB1, but how it interacts with STIM1 is unknown. It remains unknown if TAOK2 phosphoregulates STIM1 or EB1. There is still a great amount to be learned as to how TAOK2 contributes to dendrite formation, dendritic spine formation and axonal elongation

REFERENCES

Aizawa, H., Hu, S.-C., Bobb, K., Balakrishnan, K., Ince, G., Gurevich, I., Cowan, M., and Ghosh, A. (2004). Dendrite Development Regulated by CREST, a Calcium-Regulated Transcriptional Activator. Science 303, 197–202.

Akita, T., Aoto, K., Kato, M., Shiina, M., Mutoh, H., Nakashima, M., Kuki, I., Okazaki, S., Magara, S., Shiihara, T., et al. (2018). De novo variants in CAMK2A and CAMK2B cause neurodevelopmental disorders. Ann Clin Transl Neur 5, 280–296.

Allen, K.M., Gleeson, J.G., Bagrodia, S., Partington, M.W., MacMillan, J.C., Cerione, R.A., Mulley, J.C., and Walsh, C.A. (1998). PAK3 mutation in nonsyndromic X-linked mental retardation. Nat Genet 20, 25–30.

Amenduni, M., Filippis, R.D., Cheung, A.Y.L., Disciglio, V., Epistolato, M.C., Ariani, F., Mari, F., Mencarelli, M.A., Hayek, Y., Renieri, A., et al. (2011). iPS cells to model CDKL5-related disorders. Eur J Hum Genet 19, 1246–1255.

Anda, F.C. de, Rosario, A.L., Durak, O., Tran, T., Gräff, J., Meletis, K., Rei, D., Soda, T., Madabhushi, R., Ginty, D.D., et al. (2012). Autism spectrum disorder susceptibility gene TAOK2 affects basal dendrite formation in the neocortex. Nat Neurosci 15, 1022–1031.

Anderson, D.J., and Hetzer, M.W. (2008). Shaping the endoplasmic reticulum into the nuclear envelope. J Cell Sci 121, 137–142.

Antonsson, B. (1997). Phosphatidylinositol synthase from mammalian tissues1Dedicated to Professor Eugene Kennedy.1. Biochimica Et Biophysica Acta Bba - Lipids Lipid Metabolism 1348, 179–186.

Bahi-Buisson, N., Villeneuve, N., Caietta, E., Jacquette, A., Maurey, H., Matthijs, G., Esch, H.V., Delahaye, A., Moncla, A., Milh, M., et al. (2012). Recurrent mutations in the CDKL5 gene: Genotype–phenotype relationships. Am J Med Genet A 158A, 1612–1619.

Baltussen, L.L., Rosianu, F., and Ultanir, S.K. (2017). Kinases in synaptic development and neurological diseases. Prog Neuro-Psychopharmacology Biological Psychiatry 84, 343–352.

Baltussen, L.L., Negraes, P.D., Silvestre, M., Claxton, S., Moeskops, M., Christodoulou, E., Flynn, H.R., Snijders, A.P., Muotri, A.R., and Ultanir, S.K. (2018). Chemical genetic identification of CDKL 5 substrates reveals its role in neuronal microtubule dynamics. Embo J 37.

Bantscheff, M., Eberhard, D., Abraham, Y., Bastuck, S., Boesche, M., Hobson, S., Mathieson, T., Perrin, J., Raida, M., Rau, C., et al. (2007). Quantitative chemical proteomics reveals mechanisms of action of clinical ABL kinase inhibitors. Nat Biotechnol 25, 1035–1044.

Barford, D., Das, A.K., and Egloff, M.-P. (1998). THE STRUCTURE AND MECHANISM OF PROTEIN PHOSPHATASES: Insights into Catalysis and Regulation. Annu Rev Bioph Biom 27, 133–164.

Barnes, A.P., and Polleux, F. (2009). Establishment of Axon-Dendrite Polarity in Developing Neurons. Annu Rev Neurosci 32, 347–381.

Becker, L.E., Armstrong, D.L., and Chan, F. (1986). Dendritic atrophy in children with Down's syndrome. Ann Neurol 20, 520–526.

Berman, K.S., Hutchison, M., Avery, L., and Cobb, M.H. (2001). kin-18, a C. elegans protein kinase involved in feeding. Gene 279, 137–147.

Bidinosti, M., Botta, P., Krüttner, S., Proenca, C.C., Stoehr, N., Bernhard, M., Fruh, I., Mueller, M., Bonenfant, D., Voshol, H., et al. (2016). CLK2 inhibition ameliorates autistic features associated with SHANK3 deficiency. Science 351, 1199–1203.

Blethrow, J.D., Glavy, J.S., Morgan, D.O., and Shokat, K.M. (2008). Covalent capture of kinase-specific phosphopeptides reveals Cdk1-cyclin B substrates. Proc National Acad Sci 105, 1442–1447.

Blizinsky, K.D., Diaz-Castro, B., Forrest, M.P., Schürmann, B., Bach, A.P., Martin-de-Saavedra, M.D., Wang, L., Csernansky, J.G., Duan, J., and Penzes, P. (2016). Reversal of dendritic phenotypes in 16p11.2 microduplication mouse model neurons by pharmacological targeting of a network hub. Proc National Acad Sci 113, 8520–8525.

Boggiano, J.C., Vanderzalm, P.J., and Fehon, R.G. (2011). Tao-1 Phosphorylates Hippo/MST Kinases to Regulate the Hippo-Salvador-Warts Tumor Suppressor Pathway. Dev Cell 21, 888–895.

BOLTE, S., and CORDELIÈRES, F.P. (2006). A guided tour into subcellular colocalization analysis in light microscopy. J Microsc-Oxford 224, 213–232.

Bon, B.W.M. van, Coe, B.P., Bernier, R., Green, C., Gerdts, J., Witherspoon, K., Kleefstra, T., Willemsen, M.H., Kumar, R., Bosco, P., et al. (2016). Disruptive de novo mutations of DYRK1A lead to a syndromic form of autism and ID. Mol Psychiatr 21, 126–132.

Bradke, F., and Dotti, C.G. (1999). The Role of Local Actin Instability in Axon Formation. Science 283, 1931–1934.

Branon, T.C., Bosch, J.A., Sanchez, A.D., Udeshi, N.D., Svinkina, T., Carr, S.A., Feldman, J.L., Perrimon, N., and Ting, A.Y. (2018). Efficient proximity labeling in living cells and organisms with TurboID. Nat Biotechnol 36, 880.

Butler, M.G., Dasouki, M.J., Zhou, X.-P., Talebizadeh, Z., Brown, M., Takahashi, T.N., Miles, J.H., Wang, C.H., Stratton, R., Pilarski, R., et al. (2005). Subset of individuals with autism spectrum disorders and extreme macrocephaly associated with germline PTEN tumour suppressor gene mutations. J Med Genet 42, 318.

Calabrese, B., and Halpain, S. (2005). Essential Role for the PKC Target MARCKS in Maintaining Dendritic Spine Morphology. Neuron 48, 77–90.

Campbell, D.B., D'Oronzio, R., Garbett, K., Ebert, P.J., Mirnics, K., Levitt, P., and Persico, A.M. (2007). Disruption of cerebral cortex MET signaling in autism spectrum disorder. Ann Neurol 62, 243–250.

Carlton, J.G., Jones, H., and Eggert, U.S. (2020). Membrane and organelle dynamics during cell division. Nat Rev Mol Cell Bio 21, 151–166.

Chen, Z., Hutchison, M., and Cobb, M.H. (1999). Isolation of the Protein Kinase TAO2 and Identification of Its Mitogen-activated Protein Kinase/Extracellular Signal-regulated Kinase Kinase Binding Domain. J Biol Chem 274, 28803–28807.

Chen, Z., Raman, M., Chen, L., Lee, S.F., Gilman, A.G., and Cobb, M.H. (2003). TAO (Thousand-and-one Amino Acid) Protein Kinases Mediate Signaling from Carbachol to p38 Mitogen-activated Protein Kinase and Ternary Complex Factors*. J Biol Chem 278, 22278–22283.

Cheung, Z.H., Chin, W.H., Chen, Y., Ng, Y.P., and Ip, N.Y. (2007). Cdk5 Is Involved in BDNF-Stimulated Dendritic Growth in Hippocampal Neurons. Plos Biol 5, e63.

Chiocchetti, A.G., Yousaf, A., Bour, H.S., Haslinger, D., Waltes, R., Duketis, E., Jarczok, T., Sachse, M., Biscaldi, M., Degenhardt, F., et al. (2018). Common functional variants of the glutamatergic system in Autism spectrum disorder with high and low intellectual abilities. J Neural Transm 125, 259–271.

Cline, H.T. (2001). Dendritic arbor development and synaptogenesis. Curr Opin Neurobiol 11, 118–126.

Cobb, M.H. (1999). MAP kinase pathways. Prog Biophysics Mol Biology 71, 479–500.

Cochran, J.N., Hall, A.M., and Roberson, E.D. (2013). The dendritic hypothesis for Alzheimer's disease pathophysiology. Brain Res Bull 103, 18–28.

Cohen, P. (2002). Protein kinases — the major drug targets of the twenty-first century? Nat Rev Drug Discov 1, 309–315.

Combet, C., Blanchet, C., Geourjon, C., and Deléage, G. (2000). NPS@: Network Protein Sequence Analysis. Trends Biochem Sci 25, 147–150.

Congdon, E.E., and Sigurdsson, E.M. (2018). Tau-targeting therapies for Alzheimer disease. Nat Rev Neurol 14, 399–415.

Cooper, G.M., Coe, B.P., Girirajan, S., Rosenfeld, J.A., Vu, T., Baker, C., Williams, C., Stalker, H., Hamid, R., Hannig, V., et al. (2011). A Copy Number Variation Morbidity Map of Developmental Delay. Nat Genet 43, 838–846.

Costa, M.R., Wen, G., Lepier, A., Schroeder, T., and Götz, M. (2007). Par-complex proteins promote proliferative progenitor divisions in the developing mouse cerebral cortex. Development 135, 11–22.

Courcet, J.-B., Faivre, L., Malzac, P., Masurel-Paulet, A., Lopez, E., Callier, P., Lambert, L., Lemesle, M., Thevenon, J., Gigot, N., et al. (2012). The DYRK1A gene is a

cause of syndromic intellectual disability with severe microcephaly and epilepsy. J Med Genet 49, 731.

Coutadeur, S., Benyamine, H., Delalonde, L., Oliveira, C. de, Leblond, B., Foucourt, A., Besson, T., Casagrande, A.-S., Taverne, T., Girard, A., et al. (2015). A novel DYRK1A (Dual specificity tyrosine phosphorylation-regulated kinase 1A) inhibitor for the treatment of Alzheimer's disease: effect on Tau and amyloid pathologies in vitro. J Neurochem 133, 440–451.

Cox, J.S., Shamu, C.E., and Walter, P. (1993). Transcriptional induction of genes encoding endoplasmic reticulum resident proteins requires a transmembrane protein kinase. Cell 73, 1197–1206.

Craene, J.-O.D., Coleman, J., Martin, P.E. de, Pypaert, M., Anderson, S., Yates, J.R., Ferro-Novick, S., and Novick, P. (2006). Rtn1p Is Involved in Structuring the Cortical Endoplasmic Reticulum. Mol Biol Cell 17, 3009–3020.

Crosson, S., and Moffat, K. (2002). Photoexcited Structure of a Plant Photoreceptor Domain Reveals a Light-Driven Molecular Switch. Plant Cell 14, 1067–1075.

Cruz, J.C., and Tsai, L.-H. (2004). Cdk5 deregulation in the pathogenesis of Alzheimer's disease. Trends Mol Med 10, 452–458.

Cui-Wang, T., Hanus, C., Cui, T., Helton, T., Bourne, J., Watson, D., Harris, K.M., and Ehlers, M.D. (2012). Local Zones of Endoplasmic Reticulum Complexity Confine Cargo in Neuronal Dendrites. Cell 148, 309–321.

Dagda, R.K., Pien, I., Wang, R., Zhu, J., Wang, K.Z.Q., Callio, J., Banerjee, T.D., Dagda, R.Y., and Chu, C.T. (2014). Beyond the mitochondrion: cytosolic PINK1 remodels dendrites through Protein Kinase A. J Neurochem 128, 864–877.

Dailey, M., and Bridgman, P. (1989). Dynamics of the endoplasmic reticulum and other membranous organelles in growth cones of cultured neurons. J Neurosci 9, 1897–1909.

Dalva, M.B., Takasu, M.A., Lin, M.Z., Shamah, S.M., Hu, L., Gale, N.W., and Greenberg, M.E. (2000). EphB Receptors Interact with NMDA Receptors and Regulate Excitatory Synapse Formation. Cell 103, 945–956.

Dang, T., Duan, W.Y., Yu, B., Tong, D.L., Cheng, C., Zhang, Y.F., Wu, W., Ye, K., Zhang, W.X., Wu, M., et al. (2017). Autism-associated Dyrk1a truncation mutants impair neuronal dendritic and spine growth and interfere with postnatal cortical development. Mol Psychiatr 23, 747–758.

DasBanerjee, T., Dagda, R.Y., Dagda, M., Chu, C.T., Rice, M., Vazquez-Mayorga, E., and Dagda, R.K. (2017). PINK1 Regulates Mitochondrial Trafficking in Dendrites of Cortical Neurons through Mitochondrial PKA. J Neurochem 142, 545–559.

Deshpande, A., Yadav, S., Dao, D.Q., Wu, Z.-Y., Hokanson, K.C., Cahill, M.K., Wiita, A.P., Jan, Y.-N., Ullian, E.M., and Weiss, L.A. (2017). Cellular Phenotypes in Human iPSC-Derived Neurons from a Genetic Model of Autism Spectrum Disorder. Cell Reports 21, 2678–2687.

DeVos, S.L., Corjuc, B.T., Oakley, D.H., Nobuhara, C.K., Bannon, R.N., Chase, A., Commins, C., Gonzalez, J.A., Dooley, P.M., Frosch, M.P., et al. (2018). Synaptic Tau Seeding Precedes Tau Pathology in Human Alzheimer's Disease Brain. Front Neurosci-Switz 12, 267.

Dierssen, M. (2012). Down syndrome: the brain in trisomic mode. Nat Rev Neurosci 13, 844–858.

Dolmetsch, R., and Geschwind, D.H. (2011). The Human Brain in a Dish: The Promise of iPSC-Derived Neurons. Cell 145, 831–834.

Dong, R., Zhu, T., Benedetti, L., Gowrishankar, S., Deng, H., Cai, Y., Wang, X., Shen, K., and Camilli, P.D. (2018). The inositol 5-phosphatase INPP5K participates in the fine control of ER organization. J Cell Biol 217, 3577–3592.

Dulovic-Mahlow, M., Trinh, J., Kandaswamy, K.K., Braathen, G.J., Donato, N.D., Rahikkala, E., Beblo, S., Werber, M., Krajka, V., Busk, Ø.L., et al. (2019). De Novo Variants in TAOK1 Cause Neurodevelopmental Disorders. Am J Hum Genetics 105, 213–220.

Emoto, K. (2011). The growing role of the Hippo–NDR kinase signalling in neuronal development and disease. J Biochem 150, 133–141.

Emoto, K., He, Y., Ye, B., Grueber, W.B., Adler, P.N., Jan, L.Y., and Jan, Y.-N. (2004). Control of Dendritic Branching and Tiling by the Tricornered-Kinase/Furry Signaling Pathway in Drosophila Sensory Neurons. Cell 119, 245–256.

Emoto, K., Parrish, J.Z., Jan, L.Y., and Jan, Y.-N. (2006). The tumour suppressor Hippo acts with the NDR kinases in dendritic tiling and maintenance. Nature 443, 210–213.

English, A.R., and Voeltz, G.K. (2013). Endoplasmic Reticulum Structure and Interconnections with Other Organelles. Csh Perspect Biol 5, a013227.

Ethell, I.M., Irie, F., Kalo, M.S., Couchman, J.R., Pasquale, E.B., and Yamaguchi, Y. (2001). EphB/Syndecan-2 Signaling in Dendritic Spine Morphogenesis. Neuron 31, 1001–1013.

Ewers, H., Tada, T., Petersen, J.D., Racz, B., Sheng, M., and Choquet, D. (2014). A Septin-Dependent Diffusion Barrier at Dendritic Spine Necks. Plos One 9, e113916.

Fabbro, D., Cowan-Jacob, S.W., and Moebitz, H. (2015). Ten things you should know about protein kinases: IUPHAR Review 14. Brit J Pharmacol 172, 2675–2700.

Fang, C.-Y., Lai, T.-C., Hsiao, M., and Chang, Y.-C. (2020). The Diverse Roles of TAO Kinases in Health and Diseases. Int J Mol Sci 21, 7463.

Farías, G.G., Fréal, A., Tortosa, E., Stucchi, R., Pan, X., Portegies, S., Will, L., Altelaar, M., and Hoogenraad, C.C. (2019). Feedback-Driven Mechanisms between Microtubules and the Endoplasmic Reticulum Instruct Neuronal Polarity. Neuron 102, 184-201.e8.

Fink, C.C., Bayer, K.-U., Myers, J.W., Ferrell, J.E., Schulman, H., and Meyer, T. (2003). Selective Regulation of Neurite Extension and Synapse Formation by the β but not the α Isoform of CaMKII. Neuron 39, 283–297.

Florio, M., and Huttner, W.B. (2014). Neural progenitors, neurogenesis and the evolution of the neocortex. Development 141, 2182–2194.

Forrest, M.P., Parnell, E., and Penzes, P. (2018). Dendritic structural plasticity and neuropsychiatric disease. Nat Rev Neurosci 19, 215–234.

Frese, C.K., Mikhaylova, M., Stucchi, R., Gautier, V., Liu, Q., Mohammed, S., Heck, A.J.R., Altelaar, A.F.M., and Hoogenraad, C.C. (2017). Quantitative Map of Proteome Dynamics during Neuronal Differentiation. Cell Reports 18, 1527–1542.

Friedman, J.R., Webster, B.M., Mastronarde, D.N., Verhey, K.J., and Voeltz, G.K. (2010). ER sliding dynamics and ER–mitochondrial contacts occur on acetylated microtubules. J Cell Biol 190, 363–375.

Fuchs, C., Trazzi, S., Torricella, R., Viggiano, R., Franceschi, M.D., Amendola, E., Gross, C., Calzà, L., Bartesaghi, R., and Ciani, E. (2014). Loss of CDKL5 impairs survival and dendritic growth of newborn neurons by altering AKT/GSK-3β signaling. Neurobiol Dis 70, 53–68.

Gan, L., Cookson, M.R., Petrucelli, L., and Spada, A.R.L. (2018). Converging pathways in neurodegeneration, from genetics to mechanisms. Nat Neurosci 21, 1300–1309.

Gautier, R., Douguet, D., Antonny, B., and Drin, G. (2008). HELIQUEST: a web server to screen sequences with specific α-helical properties. Bioinformatics 24, 2101–2102.

Geiger, T., Cox, J., Ostasiewicz, P., Wisniewski, J.R., and Mann, M. (2010). Super-SILAC mix for quantitative proteomics of human tumor tissue. Nat Methods 7, 383–385.

Geschwind, D.H., and Levitt, P. (2007). Autism spectrum disorders: developmental disconnection syndromes. Curr Opin Neurobiol 17, 103–111.

Ghosh, A., and Greenberg, M. (1995). Calcium signaling in neurons: molecular mechanisms and cellular consequences. Science 268, 239–247.

Giacobini, E., and Gold, G. (2013). Alzheimer disease therapy—moving from amyloid-β to tau. Nat Rev Neurol 9, 677–686.

Giacomini, C., Koo, C.-Y., Yankova, N., Tavares, I.A., Wray, S., Noble, W., Hanger, D.P., and Morris, J.D.H. (2018). A new TAO kinase inhibitor reduces tau phosphorylation at sites associated with neurodegeneration in human tauopathies. Acta Neuropathologica Commun 6, 37.

Glibert, P., Meert, P., Steendam, K.V., Nieuwerburgh, F.V., Coninck, D.D., Martens, L., Dhaenens, M., and Deforce, D. (2015). Phospho-iTRAQ: Assessing Isobaric Labels for the Large-Scale Study Of Phosphopeptide Stoichiometry. J Proteome Res 14, 839–849.

Golkowski, M., Vidadala, R.S.R., Lombard, C.K., Suh, H.W., Maly, D.J., and Ong, S.-E. (2017). Kinobead and Single-Shot LC-MS Profiling Identifies Selective PKD Inhibitors. J Proteome Res 16, 1216–1227.

Golkowski, M., Lau, H.-T., Chan, M., Kenerson, H., Vidadala, V.N., Shoemaker, A., Maly, D.J., Yeung, R.S., Gujral, T.S., and Ong, S.-E. (2020). Pharmacoproteomics Identifies Kinase Pathways that Drive the Epithelial-Mesenchymal Transition and Drug Resistance in Hepatocellular Carcinoma. Cell Syst 11, 196-207.e7.

Götz, M., and Huttner, W.B. (2005). The cell biology of neurogenesis. Nat Rev Mol Cell Bio 6, 777–788.

Grigoriev, I., Gouveia, S.M., Vaart, B. van der, Demmers, J., Smyth, J.T., Honnappa, S., Splinter, D., Steinmetz, M.O., Putney, J.W., Hoogenraad, C.C., et al. (2008). STIM1 Is a MT-Plus-End-Tracking Protein Involved in Remodeling of the ER. Curr Biol 18, 177–182.

Grueber, W.B., and Sagasti, A. (2010). Self-avoidance and Tiling: Mechanisms of Dendrite and Axon Spacing. Csh Perspect Biol 2, a001750.

Grueber, W.B., Jan, L.Y., and Jan, Y.N. (2003). Different Levels of the Homeodomain Protein Cut Regulate Distinct Dendrite Branching Patterns of Drosophila Multidendritic Neurons. Cell 112, 805–818.

Guo, Y., Li, D., Zhang, S., Yang, Y., Liu, J.-J., Wang, X., Liu, C., Milkie, D.E., Moore, R.P., Tulu, U.S., et al. (2018). Visualizing Intracellular Organelle and Cytoskeletal Interactions at Nanoscale Resolution on Millisecond Timescales. Cell 175, 1430-1442.e17.

Harding, H.P., Zhang, Y., and Ron, D. (1999). Protein translation and folding are coupled by an endoplasmic-reticulum-resident kinase. Nature 397, 271–274.

Harms, F.L., Kloth, K., Bley, A., Denecke, J., Santer, R., Lessel, D., Hempel, M., and Kutsche, K. (2018). Activating Mutations in PAK1, Encoding p21-Activated Kinase 1, Cause a Neurodevelopmental Disorder. Am J Hum Genetics 103, 579–591.

Hazan, J., Fonknechten, N., Mavel, D., Paternotte, C., Samson, D., Artiguenave, F., Davoine, C.-S., Cruaud, C., Dürr, A., Wincker, P., et al. (1999). Spastin, a new AAA protein, is altered in the most frequent form of autosomal dominant spastic paraplegia. Nat Genet 23, 296–303.

Henkemeyer, M., Itkis, O.S., Ngo, M., Hickmott, P.W., and Ethell, I.M. (2003). Multiple EphB receptor tyrosine kinases shape dendritic spines in the hippocampus. J Cell Biology 163, 1313–1326.

Henneberry, A.L., Wright, M.M., and McMaster, C.R. (2002). The Major Sites of Cellular Phospholipid Synthesis and Molecular Determinants of Fatty Acid and Lipid Head Group Specificity. Mol Biol Cell 13, 3148–3161.

Hering, H., and Sheng, M. (2001). Dentritic spines : structure, dynamics and regulation. Nat Rev Neurosci 2, 880–888.

Hertog, J. den (2003). Regulation of protein phosphatases in disease and behaviour. Embo Rep 4, 1027–1031.

Hertz, N.T., Berthet, A., Sos, M.L., Thorn, K.S., Burlingame, A.L., Nakamura, K., and Shokat, K.M. (2013). A Neo-Substrate that Amplifies Catalytic Activity of Parkinson's-Disease-Related Kinase PINK1. Cell 154, 737–747.

Hoeffer, C.A., and Klann, E. (2010). mTOR signaling: At the crossroads of plasticity, memory and disease. Trends Neurosci 33, 67–75.

Holbro, N., Grunditz, Å., and Oertner, T.G. (2009). Differential distribution of endoplasmic reticulum controls metabotropic signaling and plasticity at hippocampal synapses. Proc National Acad Sci 106, 15055–15060.

Honnappa, S., Gouveia, S.M., Weisbrich, A., Damberger, F.F., Bhavesh, N.S., Jawhari, H., Grigoriev, I., Rijssel, F.J.A. van, Buey, R.M., Lawera, A., et al. (2009). An EB1-Binding Motif Acts as a Microtubule Tip Localization Signal. Cell 138, 366–376.

Hoogenraad, C.C., Akhmanova, A., Grosveld, F., Zeeuw, C.I.D., and Galjart, N. (2000). Functional analysis of CLIP-115 and its binding to microtubules. J Cell Sci 113, 2285–2297.

Hoover, B.R., Reed, M.N., Su, J., Penrod, R.D., Kotilinek, L.A., Grant, M.K., Pitstick, R., Carlson, G.A., Lanier, L.M., Yuan, L.-L., et al. (2010). Tau Mislocalization to Dendritic Spines Mediates Synaptic Dysfunction Independently of Neurodegeneration. Neuron 68, 1067–1081.

Hopkins, C., Gibson, A., Stinchcombe, J., and Futter, C. (2000). Chimeric molecules employing horseradish peroxidase as reporter enzyme for protein localization in the electron microscope. Methods Enzymol 327, 35–45.

Horch, H.W., and Katz, L.C. (2002). BDNF release from single cells elicits local dendritic growth in nearby neurons. Nat Neurosci 5, 1177–1184.

Horn, S., Au, M., Basel-Salmon, L., Bayrak-Toydemir, P., Chapin, A., Cohen, L., Elting, M.W., Graham, J.M., Gonzaga-Jauregui, C., Konen, O., et al. (2019). De novo variants in PAK1 lead to intellectual disability with macrocephaly and seizures. Brain 142, 3351–3359.

Hosp, F., and Mann, M. (2017). A Primer on Concepts and Applications of Proteomics in Neuroscience. Neuron 96, 558–571.

Hotulainen, P., and Hoogenraad, C.C. (2010). Actin in dendritic spines: connecting dynamics to function. J Cell Biology 189, 619–629.

Hoyer, M.J., Chitwood, P.J., Ebmeier, C.C., Striepen, J.F., Qi, R.Z., Old, W.M., and Voeltz, G.K. (2018). A Novel Class of ER Membrane Proteins Regulates ER-Associated Endosome Fission. Cell 175, 254-265.e14.

Hu, C., Feng, P., Yang, Q., and Xiao, L. (2021). Clinical and Neurobiological Aspects of TAO Kinase Family in Neurodevelopmental Disorders. Front Mol Neurosci 14, 655037.

Hu, J., Shibata, Y., Voss, C., Shemesh, T., Li, Z., Coughlin, M., Kozlov, M.M., Rapoport, T.A., and Prinz, W.A. (2008). Membrane Proteins of the Endoplasmic Reticulum Induce High-Curvature Tubules. Science 319, 1247–1250.

Huang, E.J., and Reichardt, L.F. (2001). NEUROTROPHINS: Roles in Neuronal Development and Function1. Annu Rev Neurosci 24, 677–736.

Huang, S.-H., Wang, J., Sui, W.-H., Chen, B., Zhang, X.-Y., Yan, J., Geng, Z., and Chen, Z.-Y. (2013). BDNF-Dependent Recycling Facilitates TrkB Translocation to Postsynaptic Density during LTP via a Rab11-Dependent Pathway. J Neurosci 33, 9214–9230.

Huang, X., Shi, L., Cao, J., He, F., Li, R., Zhang, Y., Miao, S., Jin, L., Qu, J., Li, Z., et al. (2014). The Sterile 20-Like Kinase Tao Controls Tissue Homeostasis by Regulating the Hippo Pathway in Drosophila Adult Midgut. J Genet Genomics 41, 429–438.

Hutchison, M., Berman, K.S., and Cobb, M.H. (1998). Isolation of TAO1, a Protein Kinase That Activates MEKs in Stress-activated Protein Kinase Cascades*. J Biol Chem 273, 28625–28632.

Imai, F., Hirai, S., Akimoto, K., Koyama, H., Miyata, T., Ogawa, M., Noguchi, S., Sasaoka, T., Noda, T., and Ohno, S. (2006). Inactivation of aPKCλ results in the loss of adherens junctions in neuroepithelial cells without affecting neurogenesis in mouse neocortex. Development 133, 1735–1744.

Inoue, H., Nagata, N., Kurokawa, H., and Yamanaka, S. (2014). iPS cells: a game changer for future medicine. Embo J 33, 409–417.

Iossifov, I., O'Roak, B.J., Sanders, S.J., Ronemus, M., Krumm, N., Levy, D., Stessman, H.A., Witherspoon, K.T., Vives, L., Patterson, K.E., et al. (2014). The contribution of de novo coding mutations to autism spectrum disorder. Nature 515, 216–221.

Iqbal, K., Liu, F., and Gong, C.-X. (2016). Tau and neurodegenerative disease: the story so far. Nat Rev Neurol 12, 15–27.

Ittner, A., and Ittner, L.M. (2018). Dendritic Tau in Alzheimer's Disease. Neuron 99, 13–27.

Ittner, L.M., Ke, Y.D., Delerue, F., Bi, M., Gladbach, A., Eersel, J. van, Wölfing, H., Chieng, B.C., Christie, M.J., Napier, I.A., et al. (2010). Dendritic Function of Tau Mediates Amyloid-β Toxicity in Alzheimer's Disease Mouse Models. Cell 142, 387–397.

Jan, Y.-N., and Jan, L.Y. (2001). Dendrites. Gene Dev 15, 2627–2641.

Jan, Y.-N., and Jan, L.Y. (2010). Branching out: mechanisms of dendritic arborization. Nat Rev Neurosci 11, 316–328.

Jansen, L.A., Mirzaa, G.M., Ishak, G.E., O'Roak, B.J., Hiatt, J.B., Roden, W.H., Gunter, S.A., Christian, S.L., Collins, S., Adams, C., et al. (2015). PI3K/AKT pathway mutations cause a spectrum of brain malformations from megalencephaly to focal cortical dysplasia. Brain 138, 1613–1628.

Jaworski, J., Spangler, S., Seeburg, D.P., Hoogenraad, C.C., and Sheng, M. (2005). Control of Dendritic Arborization by the Phosphoinositide-3'-Kinase-Akt-Mammalian Target of Rapamycin Pathway. J Neurosci 25, 11300–11312.

Jaworski, J., Kapitein, L.C., Gouveia, S.M., Dortland, B.R., Wulf, P.S., Grigoriev, I., Camera, P., Spangler, S.A., Stefano, P.D., Demmers, J., et al. (2009). Dynamic Microtubules Regulate Dendritic Spine Morphology and Synaptic Plasticity. Neuron 61, 85–100.

Ji, J., Lee, H., Argiropoulos, B., Dorrani, N., Mann, J., Martinez-Agosto, J.A., Gomez-Ospina, N., Gallant, N., Bernstein, J.A., Hudgins, L., et al. (2015). DYRK1A haploinsufficiency causes a new recognizable syndrome with microcephaly, intellectual disability, speech impairment, and distinct facies. Eur J Hum Genet 23, 1473–1481.

Jiang, K., Toedt, G., Montenegro Gouveia, S., Davey, N.E., Hua, S., van der Vaart, B., Grigoriev, I., Larsen, J., Pedersen, L.B., Bezstarosti, K., et al. (2012). A Proteome-wide Screen for Mammalian SxIP Motif-Containing Microtubule Plus-End Tracking Proteins. Curr Biol 22, 1800–1807.

Johne, C., Matenia, D., Li, X., Timm, T., Balusamy, K., and Mandelkow, E.-M. (2008). Spred1 and TESK1—Two New Interaction Partners of the Kinase MARKK/TAO1 That Link the Microtubule and Actin Cytoskeleton. Mol Biol Cell 19, 1391–1403.

Jongsma, M.L.M., Berlin, I., and Neefjes, J. (2015). On the move: organelle dynamics during mitosis. Trends Cell Biol 25, 112–124.

Jossin, Y. (2020). Reelin Functions, Mechanisms of Action and Signaling Pathways During Brain Development and Maturation. Biomol 10, 964.

Jumper, J., Evans, R., Pritzel, A., Green, T., Figurnov, M., Ronneberger, O., Tunyasuvunakool, K., Bates, R., Žídek, A., Potapenko, A., et al. (2021). Highly accurate protein structure prediction with AlphaFold. Nature 596, 583–589.

Kapfhamer, D., Taylor, S., Zou, M.E., Lim, J.P., Kharazia, V., and Heberlein, U. (2013). Taok2 controls behavioral response to ethanol in mice. Genes Brain Behav 12, 87–97.

Kashani, A.H., Qiu, Z., Jurata, L., Lee, S.-K., Pfaff, S., Goebbels, S., Nave, K.-A., and Ghosh, A. (2006). Calcium Activation of the LMO4 Transcription Complex and Its Role in the Patterning of Thalamocortical Connections. J Neurosci 26, 8398–8408.

Kelava, I., and Lancaster, M.A. (2016). Dishing out mini-brains: Current progress and future prospects in brain organoid research. Dev Biol 420, 199–209.

Kernohan, K.D., McBride, A., Hartley, T., Rojas, S.K., Consortium, C.C., Dyment, D.A., Boycott, K.M., and Dyack, S. (2019). p21 protein-activated kinase 1 is associated with severe regressive autism, and epilepsy. Clin Genet 96, 449–455.

Khamrui, S., Ung, P.M.U., Secor, C., Schlessinger, A., and Lazarus, M.B. (2020). High-Resolution Structure and Inhibition of the Schizophrenia-Linked Pseudokinase ULK4. J Am Chem Soc 142, 33–37.

Kim, D.I., Jensen, S.C., Noble, K.A., KC, B., Roux, K.H., Motamedchaboki, K., and Roux, K.J. (2016). An improved smaller biotin ligase for BioID proximity labeling. Mol Biol Cell 27, 1188–1196.

King, I., Tsai, L.T.-Y., Pflanz, R., Voigt, A., Lee, S., Jackle, H., Lu, B., and Heberlein, U. (2011). Drosophila tao Controls Mushroom Body Development and Ethanol-Stimulated Behavior through par-1. J Neurosci 31, 1139–1148.

Klein, R. (2009). Bidirectional modulation of synaptic functions by Eph/ephrin signaling. Nat Neurosci 12, 15–20.

Klopfenstein, D.R.Ch., Kappeler, F., and Hauri, H. (1998). A novel direct interaction of endoplasmic reticulum with microtubules. Embo J 17, 6168–6177.

Koleske, A.J. (2013). Molecular mechanisms of dendrite stability. Nat Rev Neurosci 14, 536–550.

Konur, S., and Ghosh, A. (2005). Calcium Signaling and the Control of Dendritic Development. Neuron 46, 401–405.

Krahn, A.I., Wells, C., Drewry, D.H., Beitel, L.K., Durcan, T.M., and Axtman, A.D. (2020). Defining the Neural Kinome: Strategies and Opportunities for Small Molecule Drug Discovery to Target Neurodegenerative Diseases. Acs Chem Neurosci 11, 1871–1886.

Krogh, A., Larsson, B., Heijne, G. von, and Sonnhammer, E.L.L. (2001). Predicting transmembrane protein topology with a hidden markov model: application to complete genomes11Edited by F. Cohen. J Mol Biol 305, 567–580.

Krüger, M., Moser, M., Ussar, S., Thievessen, I., Luber, C.A., Forner, F., Schmidt, S., Zanivan, S., Fässler, R., and Mann, M. (2008). SILAC Mouse for Quantitative Proteomics Uncovers Kindlin-3 as an Essential Factor for Red Blood Cell Function. Cell 134, 353–364.

Kulkarni, V.A., and Firestein, B.L. (2012). The dendritic tree and brain disorders. Mol Cell Neurosci 50, 10–20.

Kumar, R.A., KaraMohamed, S., Sudi, J., Conrad, D.F., Brune, C., Badner, J.A., Gilliam, T.C., Nowak, N.J., Cook, E.H., Dobyns, W.B., et al. (2007). Recurrent 16p11.2 microdeletions in autism. Hum Mol Genet 17, 628–638.

Kuo, Y.-W., Trottier, O., Mahamdeh, M., and Howard, J. (2019). Spastin is a dual-function enzyme that severs microtubules and promotes their regrowth to increase the number and mass of microtubules. Proc National Acad Sci 116, 201818824.

Küry, S., Woerden, G.M. van, Besnard, T., Onori, M.P., Latypova, X., Towne, M.C., Cho, M.T., Prescott, T.E., Ploeg, M.A., Sanders, S., et al. (2017). De Novo Mutations in Protein Kinase Genes CAMK2A and CAMK2B Cause Intellectual Disability. Am J Hum Genetics 101, 768–788.

Kuwako, K., and Okano, H. (2018). The LKB1-SIK Pathway Controls Dendrite Self-Avoidance in Purkinje Cells. Cell Reports 24, 2808-2818.e4.

Kwon, C.-H., Zhu, X., Zhang, J., and Baker, S.J. (2003). mTor is required for hypertrophy of Pten-deficient neuronal soma in vivo. Proc National Acad Sci 100, 12923–12928.

Lagran, M.M. de, Benavides-Piccione, R., Ballesteros-Yañez, I., Calvo, M., Morales, M., Fillat, C., DeFelipe, J., Ramakers, G.J.A., and Dierssen, M. (2012). Dyrk1A Influences Neuronal Morphogenesis Through Regulation of Cytoskeletal Dynamics in Mammalian Cortical Neurons. Cereb Cortex 22, 2867–2877.

Lam, S.S., Martell, J.D., Kamer, K.J., Deerinck, T.J., Ellisman, M.H., Mootha, V.K., and Ting, A.Y. (2015). Directed evolution of APEX2 for electron microscopy and proteomics. Nat Methods 12, 51–54.

Lancaster, M.A., and Knoblich, J.A. (2012). Spindle orientation in mammalian cerebral cortical development. Curr Opin Neurobiol 22, 737–746.

Lang, B., Pu, J., Hunter, I., Liu, M., Martin-Granados, C., Reilly, T.J., Gao, G.-D., Guan, Z.-L., Li, W.-D., Shi, Y.-Y., et al. (2013). Recurrent deletions of ULK4 in schizophrenia: a gene crucial for neuritogenesis and neuronal motility. J Cell Sci 127, 630–640.

Lang, B., Zhang, L., Jiang, G., Hu, L., Lan, W., Zhao, L., Hunter, I., Pruski, M., Song, N.-N., Huang, Y., et al. (2016). Control of cortex development by ULK4, a rare risk gene for mental disorders including schizophrenia. Sci Rep-Uk 6, 31126.

Lauretti, E., Dincer, O., and Praticò, D. (2020). Glycogen synthase kinase-3 signaling in Alzheimer's disease. Biochimica Et Biophysica Acta Bba - Mol Cell Res 1867, 118664.

Leopold, A.V., Chernov, K.G., and Verkhusha, V.V. (2018). Optogenetically controlled protein kinases for regulation of cellular signaling. Chem Soc Rev 47, 2454–2484.

Li, K., Wei, Q., Liu, F.-F., Hu, F., Xie, A., Zhu, L.-Q., and Liu, D. (2018). Synaptic Dysfunction in Alzheimer's Disease: Aβ, Tau, and Epigenetic Alterations. Mol Neurobiol 55, 3021–3032.

Li, X.-W., Rees, J.S., Xue, P., Zhang, H., Hamaia, S.W., Sanderson, B., Funk, P.E., Farndale, R.W., Lilley, K.S., Perrett, S., et al. (2014). New Insights into the DT40 B Cell Receptor Cluster Using a Proteomic Proximity Labeling Assay*. J Biological Chem 289, 14434–14447.

Liao, L., Park, S.K., Xu, T., Vanderklish, P., and Yates, J.R. (2008). Quantitative proteomic analysis of primary neurons reveals diverse changes in synaptic protein content in fmr1 knockout mice. Proc National Acad Sci 105, 15281–15286.

Lin, Y.-C., and Koleske, A.J. (2010). Mechanisms of Synapse and Dendrite Maintenance and Their Disruption in Psychiatric and Neurodegenerative Disorders. Annu Rev Neurosci 33, 349–378.

Lipton, J.O., and Sahin, M. (2014). The Neurology of mTOR. Neuron 84, 275–291.

Lisman, J., Schulman, H., and Cline, H. (2002). The molecular basis of CaMKII function in synaptic and behavioural memory. Nat Rev Neurosci 3, 175–190.

Liu, M., Guan, Z., Shen, Q., Flinter, F., Domínguez, L., Ahn, J.W., Collier, D.A., O'Brien, T., and Shen, S. (2016). Ulk4 Regulates Neural Stem Cell Pool. Stem Cells 34, 2318–2331.

Liu, T., Rohn, J.L., Picone, R., Kunda, P., and Baum, B. (2010). Tao-1 is a negative regulator of microtubule plus-end growth. J Cell Sci 123, 2708–2716.

Locke, C., Machida, K., Tucker, C.L., Wu, Y., and Yu, J. (2018). Correction: Optogenetic activation of EphB2 receptor in dendrites induced actin polymerization by activating Arg kinase. Biol Open 7, bio034694.

Lom, B., and Cohen-Cory, S. (1999). Brain-Derived Neurotrophic Factor Differentially Regulates Retinal Ganglion Cell Dendritic and Axonal Arborization In Vivo. J Neurosci 19, 9928–9938.

Lugo, J.N., Smith, G.D., Arbuckle, E.P., White, J., Holley, A.J., Floruta, C.M., Ahmed, N., Gomez, M.C., and Okonkwo, O. (2014). Deletion of PTEN produces autism-like behavioral deficits and alterations in synaptic proteins. Front Mol Neurosci 7, 27.

Luo, R., Sanders, S.J., Tian, Y., Voineagu, I., Huang, N., Chu, S.H., Klei, L., Cai, C., Ou, J., Lowe, J.K., et al. (2012). Genome-wide Transcriptome Profiling Reveals the Functional Impact of Rare De Novo and Recurrent CNVs in Autism Spectrum Disorders. Am J Hum Genetics 91, 38–55.

Ma, S., Meng, Z., Chen, R., and Guan, K.-L. (2018). The Hippo Pathway: Biology and Pathophysiology. Annu Rev Biochem 88, 1–28.

MacLeod, D., Dowman, J., Hammond, R., Leete, T., Inoue, K., and Abeliovich, A. (2006). The Familial Parkinsonism Gene LRRK2 Regulates Neurite Process Morphology. Neuron 52, 587–593.

Maio, R.D., Hoffman, E.K., Rocha, E.M., Keeney, M.T., Sanders, L.H., Miranda, B.R.D., Zharikov, A., Laar, A.V., Stepan, A.F., Lanz, T.A., et al. (2018). LRRK2 activation in idiopathic Parkinson's disease. Sci Transl Med 10, eaar5429.

Mairet-Coello, G., Courchet, J., Pieraut, S., Courchet, V., Maximov, A., and Polleux, F. (2013). The CAMKK2-AMPK Kinase Pathway Mediates the Synaptotoxic Effects of Aβ Oligomers through Tau Phosphorylation. Neuron 78, 94–108.

MANDERS, E.M.M., VERBEEK, F.J., and ATEN, J.A. (1993). Measurement of co-localization of objects in dual-colour confocal images. J Microsc-Oxford 169, 375–382.

Manning, G., Whyte, D.B., Martinez, R., Hunter, T., and Sudarsanam, S. (2002). The Protein Kinase Complement of the Human Genome. Science 298, 1912–1934.

Martell, J.D., Deerinck, T.J., Sancak, Y., Poulos, T.L., Mootha, V.K., Sosinsky, G.E., Ellisman, M.H., and Ting, A.Y. (2012). Engineered ascorbate peroxidase as a genetically encoded reporter for electron microscopy. Nat Biotechnol 30, 1143–1148.

Martin-Belmonte, F., and Mostov, K. (2008). Regulation of cell polarity during epithelial morphogenesis. Curr Opin Cell Biol 20, 227–234.

Masters, C.L., Bateman, R., Blennow, K., Rowe, C.C., Sperling, R.A., and Cummings, J.L. (2015). Alzheimer's disease. Nat Rev Dis Primers 1, 15056.

Matus, A. (2000). Actin-Based Plasticity in Dendritic Spines. Science 290, 754–758.

McAllister, A.K. (2000). Cellular and Molecular Mechanisms of Dendrite Growth. Cereb Cortex 10, 963–973.

McAllister, A.K., Lo, D.C., and Katz, L.C. (1995). Neurotrophins regulate dendritic growth in developing visual cortex. Neuron 15, 791–803.

McAllister, A.K., Katz, L.C., and Lo, D.C. (1997). Opposing Roles for Endogenous BDNF and NT-3 in Regulating Cortical Dendritic Growth. Neuron 18, 767–778.

McCaffrey, L.M., and Macara, I.G. (2012). Signaling Pathways in Cell Polarity. Csh Perspect Biol 4, a009654.

McCarthy, S.E., Makarov, V., Kirov, G., Addington, A.M., McClellan, J., Yoon, S., Perkins, D.O., Dickel, D.E., Kusenda, M., Krastoshevsky, O., et al. (2009). Microduplications of 16p11.2 are associated with schizophrenia. Nat Genet 41, 1223–1227.

Meng, Y., Zhang, Y., Tregoubov, V., Janus, C., Cruz, L., Jackson, M., Lu, W.-Y., MacDonald, J.F., Wang, J.Y., Falls, D.L., et al. (2002). Abnormal Spine Morphology and Enhanced LTP in LIMK-1 Knockout Mice. Neuron 35, 121–133.

Mirzaa, G.M., Campbell, C.D., Solovieff, N., Goold, C.P., Jansen, L.A., Menon, S., Timms, A.E., Conti, V., Biag, J.D., Olds, C., et al. (2016). Association of MTOR Mutations With Developmental Brain Disorders, Including Megalencephaly, Focal Cortical Dysplasia, and Pigmentary Mosaicism. Jama Neurol 73, 836.

Mitsopoulos, C., Zihni, C., Garg, R., Ridley, A.J., and Morris, J.D.H. (2003). The Prostate-derived Sterile 20-like Kinase (PSK) Regulates Microtubule Organization and Stability. J Biol Chem 278, 18085–18091.

Mitz, A.R., Philyaw, T.J., Boccuto, L., Shcheglovitov, A., Sarasua, S.M., Kaufmann, W.E., and Thurm, A. (2018). Identification of 22q13 genes most likely to contribute to Phelan McDermid syndrome. Eur J Hum Genet 26, 293–302.

Møller, R.S., Kübart, S., Hoeltzenbein, M., Heye, B., Vogel, I., Hansen, C.P., Menzel, C., Ullmann, R., Tommerup, N., Ropers, H.-H., et al. (2008). Truncation of the Down Syndrome Candidate Gene DYRK1A in Two Unrelated Patients with Microcephaly. Am J Hum Genetics 82, 1165–1170.

Moore, T.M., Garg, R., Johnson, C., Coptcoat, M.J., Ridley, A.J., and Morris, J.D.H. (2000). PSK, a Novel STE20-like Kinase Derived from Prostatic Carcinoma That Activates the c-Jun N-terminal Kinase Mitogen-activated Protein Kinase Pathway and Regulates Actin Cytoskeletal Organization. J Biol Chem 275, 4311–4322.

Morl, K., Ma, W., Gething, M.-J., and Sambrook, J. (1993). A transmembrane protein with a cdc2+CDC28-related kinase activity is required for signaling from the ER to the nucleus. Cell 74, 743–756.

Navarrete-Perea, J., Yu, Q., Gygi, S.P., and Paulo, J.A. (2018). Streamlined Tandem Mass Tag (SL-TMT) Protocol: An Efficient Strategy for Quantitative (Phospho)proteome Profiling Using Tandem Mass Tag-Synchronous Precursor Selection-MS3. J Proteome Res 17, 2226–2236.

Nedivi, E., Wu, G.-Y., and Cline, H.T. (1998). Promotion of Dendritic Growth by CPG15, an Activity-Induced Signaling Molecule. Science 281, 1863–1866.

Nikonov, A.V., Hauri, H.-P., Lauring, B., and Kreibich, G. (2007). Climp-63-mediated binding of microtubules to the ER affects the lateral mobility of translocon complexes. J Cell Sci 120, 2248–2258.

Noble, W., Hanger, D.P., Miller, C.C.J., and Lovestone, S. (2013). The Importance of Tau Phosphorylation for Neurodegenerative Diseases. Front Neurol 4, 83.

Nolt, M.J., Lin, Y., Hruska, M., Murphy, J., Sheffler-Colins, S.I., Kayser, M.S., Passer, J., Bennett, M.V.L., Zukin, R.S., and Dalva, M.B. (2011). EphB Controls NMDA Receptor Function and Synaptic Targeting in a Subunit-Specific Manner. J Neurosci 31, 5353–5364.

Nourbakhsh, K., and Yadav, S. (2021). Kinase Signaling in Dendritic Development and Disease. Front Cell Neurosci 15, 624648.

Ogawa-Goto, K., Tanaka, K., Ueno, T., Tanaka, K., Kurata, T., Sata, T., and Irie, S. (2007). p180 Is Involved in the Interaction between the Endoplasmic Reticulum and Microtubules through a Novel Microtubule-binding and Bundling Domain. Mol Biol Cell 18, 3741–3751.

Okamoto, K.-I., Nagai, T., Miyawaki, A., and Hayashi, Y. (2004). Rapid and persistent modulation of actin dynamics regulates postsynaptic reorganization underlying bidirectional plasticity. Nat Neurosci 7, 1104–1112.

Okamoto, K.-I., Narayanan, R., Lee, S.H., Murata, K., and Hayashi, Y. (2007). The role of CaMKII as an F-actin-bundling protein crucial for maintenance of dendritic spine structure. Proc National Acad Sci 104, 6418–6423.

Okatsu, K., Oka, T., Iguchi, M., Imamura, K., Kosako, H., Tani, N., Kimura, M., Go, E., Koyano, F., Funayama, M., et al. (2012). PINK1 autophosphorylation upon membrane potential dissipation is essential for Parkin recruitment to damaged mitochondria. Nat Commun 3, 1016.

Oldach, L., and Zhang, J. (2014). Genetically Encoded Fluorescent Biosensors for Live-Cell Visualization of Protein Phosphorylation. Chem Biol 21, 186–197.

Ong, S.-E., Blagoev, B., Kratchmarova, I., Kristensen, D.B., Steen, H., Pandey, A., and Mann, M. (2002). Stable Isotope Labeling by Amino Acids in Cell Culture, SILAC, as a Simple and Accurate Approach to Expression Proteomics. Mol Cell Proteomics 1, 376–386.

Ori-McKenney, K.M., McKenney, R.J., Huang, H.H., Li, T., Meltzer, S., Jan, L.Y., Vale, R.D., Wiita, A.P., and Jan, Y.N. (2016). Phosphorylation of β-Tubulin by the Down Syndrome Kinase, Minibrain/DYRK1a, Regulates Microtubule Dynamics and Dendrite Morphogenesis. Neuron 90, 551–563.

Orso, G., Pendin, D., Liu, S., Tosetto, J., Moss, T.J., Faust, J.E., Micaroni, M., Egorova, A., Martinuzzi, A., McNew, J.A., et al. (2009). Homotypic fusion of ER membranes requires the dynamin-like GTPase Atlastin. Nature 460, 978–983.

Ostroff, L.E., Botsford, B., Gindina, S., Cowansage, K.K., LeDoux, J.E., Klann, E., and Hoeffer, C. (2017). Accumulation of Polyribosomes in Dendritic Spine Heads, But Not Bases and Necks, during Memory Consolidation Depends on Cap-Dependent Translation Initiation. J Neurosci 37, 1862–1872.

Owen, J.P., Bukshpun, P., Pojman, N., Thieu, T., Chen, Q., Lee, J., D'Angelo, D., Glenn, O.A., Hunter, J.V., Berman, J.I., et al. (2017). Brain MR Imaging Findings and Associated Outcomes in Carriers of the Reciprocal Copy Number Variation at 16p11.2. Radiology 286, 162934.

Park, P.J. (2009). ChIP–seq: advantages and challenges of a maturing technology. Nat Rev Genet 10, 669–680.

Park, S.H., Zhu, P.-P., Parker, R.L., and Blackstone, C. (2010). Hereditary spastic paraplegia proteins REEP1, spastin, and atlastin-1 coordinate microtubule interactions with the tubular ER network. J Clin Invest 120, 1097–1110.

Paşca, S.P., Panagiotakos, G., and Dolmetsch, R.E. (2014). Generating Human Neurons In Vitro and Using Them to Understand Neuropsychiatric Disease. Annu Rev Neurosci 37, 479–501.

Patricelli, M.P., Szardenings, A.K., Liyanage, M., Nomanbhoy, T.K., Wu, M., Weissig, H., Aban, A., Chun, D., Tanner, S., and Kozarich, J.W. (2007). Functional Interrogation of the Kinome Using Nucleotide Acyl Phosphates. Biochemistry-Us 46, 350–358.

Patricelli, M.P., Nomanbhoy, T.K., Wu, J., Brown, H., Zhou, D., Zhang, J., Jagannathan, S., Aban, A., Okerberg, E., Herring, C., et al. (2011). In Situ Kinase Profiling Reveals Functionally Relevant Properties of Native Kinases. Chem Biol 18, 699–710.

Pavez, M., Thompson, A.C., Arnott, H.J., Mitchell, C.B., D'Atri, I., Don, E.K., Chilton, J.K., Scott, E.K., Lin, J.Y., Young, K.M., et al. (2019). STIM1 Is Required for Remodeling of the Endoplasmic Reticulum and Microtubule Cytoskeleton in Steering Growth Cones. J Neurosci 39, 5095–5114.

Peebles, C.L., Yoo, J., Thwin, M.T., Palop, J.J., Noebels, J.L., and Finkbeiner, S. (2010). Arc regulates spine morphology and maintains network stability in vivo. Proc National Acad Sci 107, 18173–18178.

Pendin, D., McNew, J.A., and Daga, A. (2011). Balancing ER dynamics: shaping, bending, severing, and mending membranes. Curr Opin Cell Biol 23, 435–442.

Peng, A., and Maller, J.L. (2010). Serine/threonine phosphatases in the DNA damage response and cancer. Oncogene 29, 5977–5988.

Perez-Alvarez, A., Yin, S., Schulze, C., Hammer, J.A., Wagner, W., and Oertner, T.G. (2020). Endoplasmic reticulum visits highly active spines and prevents runaway potentiation of synapses. Nat Commun 11, 5083.

Pinto, D., Delaby, E., Merico, D., Barbosa, M., Merikangas, A., Klei, L., Thiruvahindrapuram, B., Xu, X., Ziman, R., Wang, Z., et al. (2014). Convergence of Genes and Cellular Pathways Dysregulated in Autism Spectrum Disorders. Am J Hum Genet 94, 677–694.

Plouffe, S.W., Meng, Z., Lin, K.C., Lin, B., Hong, A.W., Chun, J.V., and Guan, K.-L. (2016). Characterization of Hippo Pathway Components by Gene Inactivation. Mol Cell 64, 993–1008.

Poewe, W., Seppi, K., Tanner, C.M., Halliday, G.M., Brundin, P., Volkmann, J., Schrag, A.-E., and Lang, A.E. (2017). Parkinson disease. Nat Rev Dis Primers 3, 17013.

Polleux, F., and Snider, W. (2010). Initiating and Growing an Axon. Csh Perspect Biol 2, a001925.

Poon, C.L.C., Lin, J.I., Zhang, X., and Harvey, K.F. (2011). The Sterile 20-like Kinase Tao-1 Controls Tissue Growth by Regulating the Salvador-Warts-Hippo Pathway. Dev Cell 21, 896–906.

Portmann, T., Yang, M., Mao, R., Panagiotakos, G., Ellegood, J., Dolen, G., Bader, P.L., Grueter, B.A., Goold, C., Fisher, E., et al. (2014). Behavioral Abnormalities and Circuit Defects in the Basal Ganglia of a Mouse Model of 16p11.2 Deletion Syndrome. Cell Reports 7, 1077–1092.

Qin, W., Cho, K.F., Cavanagh, P.E., and Ting, A.Y. (2021). Deciphering molecular interactions by proximity labeling. Nat Methods 18, 133–143.

Qiu, S., Lu, Z., and Levitt, P. (2014). MET Receptor Tyrosine Kinase Controls Dendritic Complexity, Spine Morphogenesis, and Glutamatergic Synapse Maturation in the Hippocampus. J Neurosci 34, 16166–16179.

Quintero-Rivera, F., Sharifi-Hannauer, P., and Martinez-Agosto, J.A. (2010). Autistic and psychiatric findings associated with the 3q29 microdeletion syndrome: Case report and review. Am J Med Genet A 152A, 2459–2467.

Qureshi, A.Y., Mueller, S., Snyder, A.Z., Mukherjee, P., Berman, J.I., Roberts, T.P.L., Nagarajan, S.S., Spiro, J.E., Chung, W.K., Sherr, E.H., et al. (2014). Opposing Brain Differences in 16p11.2 Deletion and Duplication Carriers. J Neurosci 34, 11199–11211.

Rajan, I., and Cline, H.T. (1998). Glutamate Receptor Activity Is Required for Normal Development of Tectal Cell Dendrites In Vivo. J Neurosci 18, 7836–7846.

Raman, M., Earnest, S., Zhang, K., Zhao, Y., and Cobb, M.H. (2007). TAO kinases mediate activation of p38 in response to DNA damage. Embo J 26, 2005–2014.

Raymond, G.V., Bauman, M.L., and Kemper, T.L. (1995). Hippocampus in autism: a Golgi analysis. Acta Neuropathol 91, 117–119.

Redmond, L., and Ghosh, A. (2005). Regulation of dendritic development by calcium signaling. Cell Calcium 37, 411–416.

Redmond, L., Kashani, A.H., and Ghosh, A. (2002). Calcium Regulation of Dendritic Growth via CaM Kinase IV and CREB-Mediated Transcription. Neuron 34, 999–1010.

Rehberg, K., Kliche, S., Madencioglu, D.A., Thiere, M., Muller, B., Meineke, B.M., Freund, C., Budinger, E., and Stork, O. (2014). The Serine/Threonine Kinase Ndr2 Controls Integrin Trafficking and Integrin-Dependent Neurite Growth. J Neurosci 34, 5342–5354.

Renner, M., Lacor, P.N., Velasco, P.T., Xu, J., Contractor, A., Klein, W.L., and Triller, A. (2010). Deleterious Effects of Amyloid β Oligomers Acting as an Extracellular Scaffold for mGluR5. Neuron 66, 739–754.

Rhee, H.-W., Zou, P., Udeshi, N.D., Martell, J.D., Mootha, V.K., Carr, S.A., and Ting, A.Y. (2013). Proteomic Mapping of Mitochondria in Living Cells via Spatially Restricted Enzymatic Tagging. Science 339, 1328–1331.

Ricciardi, S., Ungaro, F., Hambrock, M., Rademacher, N., Stefanelli, G., Brambilla, D., Sessa, A., Magagnotti, C., Bachi, A., Giarda, E., et al. (2012). CDKL5 ensures excitatory synapse stability by reinforcing NGL-1–PSD95 interaction in the postsynaptic compartment and is impaired in patient iPSC-derived neurons. Nat Cell Biol 14, 911–923.

Richter, M., Murtaza, N., Scharrenberg, R., White, S.H., Johanns, O., Walker, S., Yuen, R.K.C., Schwanke, B., Bedürftig, B., Henis, M., et al. (2018). Altered TAOK2 activity causes autism-related neurodevelopmental and cognitive abnormalities through RhoA signaling. Mol Psychiatr 1–22.

Rodríguez-Fraticelli, A.E., Gálvez-Santisteban, M., and Martín-Belmonte, F. (2011). Divide and polarize: recent advances in the molecular mechanism regulating epithelial tubulogenesis. Curr Opin Cell Biol 23, 638–646.

Roll-Mecak, A., and Vale, R.D. (2008). Structural basis of microtubule severing by the hereditary spastic paraplegia protein spastin. Nature 451, 363–367.

Ron, D., and Walter, P. (2007). Signal integration in the endoplasmic reticulum unfolded protein response. Nat Rev Mol Cell Bio 8, 519–529.

Roux, K.J., Kim, D.I., Raida, M., and Burke, B. (2012). A promiscuous biotin ligase fusion protein identifies proximal and interacting proteins in mammalian cells. J Cell Biology 196, 801–810.

Rubeis, S.D., He, X., Goldberg, A.P., Poultney, C.S., Samocha, K., Cicek, A.E., Kou, Y., Liu, L., Fromer, M., Walker, S., et al. (2014). Synaptic, transcriptional, and chromatin genes disrupted in autism. Nature 515, 209–215.

Sala, C., Piëch, V., Wilson, N.R., Passafaro, M., Liu, G., and Sheng, M. (2001). Regulation of Dendritic Spine Morphology and Synaptic Function by Shank and Homer. Neuron 31, 115–130.

Sato, A. (2016). mTOR, a Potential Target to Treat Autism Spectrum Disorder. Cns Neurological Disord - Drug Targets 15, 533–543.

Sato, M., Ozawa, T., Inukai, K., Asano, T., and Umezawa, Y. (2002). Fluorescent indicators for imaging protein phosphorylation in single living cells. Nat Biotechnol 20, 287–294.

Schlaitz, A.-L., Thompson, J., Wong, C.C.L., Yates, J.R., and Heald, R. (2013). REEP3/4 Ensure Endoplasmic Reticulum Clearance from Metaphase Chromatin and Proper Nuclear Envelope Architecture. Dev Cell 26, 315–323.

Scorrano, L., Matteis, M.A.D., Emr, S., Giordano, F., Hajnóczky, G., Kornmann, B., Lackner, L.L., Levine, T.P., Pellegrini, L., Reinisch, K., et al. (2019). Coming together to define membrane contact sites. Nat Commun 10, 1287.

Selkoe, D.J. (2002). Alzheimer's Disease Is a Synaptic Failure. Science 298, 789–791.

Sharma, V., Wang, Q., and Lawrence, D.S. (2008). Peptide-based fluorescent sensors of protein kinase activity: Design and applications. Biochimica Et Biophysica Acta Bba - Proteins Proteom 1784, 94–99.

Shelton, D., Sutherland, J., Gripp, J., Camerato, T., Armanini, M., Phillips, H., Carroll, K., Spencer, S., and Levinson, A. (1995). Human trks: molecular cloning, tissue distribution, and expression of extracellular domain immunoadhesins. J Neurosci 15, 477–491.

Shen, K., Teruel, M.N., Subramanian, K., and Meyer, T. (1998). CaMKIIβ Functions As an F-Actin Targeting Module that Localizes CaMKIIα/β Heterooligomers to Dendritic Spines. Neuron 21, 593–606.

Sherman, S.P., and Bang, A.G. (2018). High-throughput screen for compounds that modulate neurite growth of human induced pluripotent stem cell-derived neurons. Dis Model Mech 11, dmm031906.

Sherwood, N.T., Sun, Q., Xue, M., Zhang, B., and Zinn, K. (2004). Drosophila Spastin Regulates Synaptic Microtubule Networks and Is Required for Normal Motor Function. Plos Biol 2, e429.

Shi, Y., Pontrello, C.G., DeFea, K.A., Reichardt, L.F., and Ethell, I.M. (2009). Focal Adhesion Kinase Acts Downstream of EphB Receptors to Maintain Mature Dendritic Spines by Regulating Cofilin Activity. J Neurosci 29, 8129–8142.

Shults, M.D., and Imperiali, B. (2003). Versatile Fluorescence Probes of Protein Kinase Activity. J Am Chem Soc 125, 14248–14249.

Smyth, J.T., DeHaven, W.I., Bird, G.S., and Putney, J.W. (2007). Role of the microtubule cytoskeleton in the function of the store-operated Ca2+ channel activator STIM1. J Cell Sci 120, 3762–3771.

Smyth, J.T., Beg, A.M., Wu, S., Putney, J.W., and Rusan, N.M. (2012). Phosphoregulation of STIM1 Leads to Exclusion of the Endoplasmic Reticulum from the Mitotic Spindle. Curr Biol 22, 1487–1493.

Smyth, J.T., Schoborg, T.A., Bergman, Z.J., Riggs, B., and Rusan, N.M. (2015). Proper symmetric and asymmetric endoplasmic reticulum partitioning requires astral microtubules. Open Biol 5, 150067.

Snapp, E.L., Sharma, A., Lippincott-Schwartz, J., and Hegde, R.S. (2006). Monitoring chaperone engagement of substrates in the endoplasmic reticulum of live cells. Proc National Acad Sci 103, 6536–6541.

Sottocornola, R., Royer, C., Vives, V., Tordella, L., Zhong, S., Wang, Y., Ratnayaka, I., Shipman, M., Cheung, A., Gaston-Massuet, C., et al. (2010). ASPP2 Binds Par-3 and Controls the Polarity and Proliferation of Neural Progenitors during CNS Development. Dev Cell 19, 126–137.

Spellman, D.S., Deinhardt, K., Darie, C.C., Chao, M.V., and Neubert, T.A. (2008). Stable Isotopic Labeling by Amino Acids in Cultured Primary Neurons Application to Brain-derived Neurotrophic Factor-dependent Phosphotyrosine-associated Signaling. Mol Cell Proteomics 7, 1067–1076.

Steger, M., Tonelli, F., Ito, G., Davies, P., Trost, M., Vetter, M., Wachter, S., Lorentzen, E., Duddy, G., Wilson, S., et al. (2016). Phosphoproteomics reveals that Parkinson's disease kinase LRRK2 regulates a subset of Rab GTPases. Elife 5, e12813.

Stephenson, J.R., Wang, X., Perfitt, T.L., Parrish, W.P., Shonesy, B.C., Marks, C.R., Mortlock, D.P., Nakagawa, T., Sutcliffe, J.S., and Colbran, R.J. (2017). A Novel Human CAMK2A Mutation Disrupts Dendritic Morphology and Synaptic Transmission, and Causes ASD-Related Behaviors. J Neurosci 37, 2216–2233.

Tada, T., Simonetta, A., Batterton, M., Kinoshita, M., Edbauer, D., and Sheng, M. (2007). Role of Septin Cytoskeleton in Spine Morphogenesis and Dendrite Development in Neurons. Curr Biol 17, 1752–1758.

Tang, S., and Yasuda, R. (2017). Imaging ERK and PKA Activation in Single Dendritic Spines during Structural Plasticity. Neuron 93, 1315-1324.e3.

Tang, S., Terzic, B., Wang, I.-T.J., Sarmiento, N., Sizov, K., Cui, Y., Takano, H., Marsh, E.D., Zhou, Z., and Coulter, D.A. (2019). Altered NMDAR signaling underlies autistic-like features in mouse models of CDKL5 deficiency disorder. Nat Commun 10, 2655.

Tassano, E., Uccella, S., Giacomini, T., Striano, P., Severino, M., Porta, S., Gimelli, G., and Ronchetto, P. (2018). Intragenic Microdeletion of ULK4 and Partial Microduplication of BRWD3 in Siblings with Neuropsychiatric Features and Obesity. Cytogenet Genome Res 156, 14–21.

Tassi, E., Biesova, Z., Fiore, P.P.D., Gutkind, J.S., and Wong, W.T. (1999). Human JIK, a Novel Member of the STE20 Kinase Family That Inhibits JNK and Is Negatively Regulated by Epidermal Growth Factor*. J Biol Chem 274, 33287–33295.

Tavares, I.A., Touma, D., Lynham, S., Troakes, C., Schober, M., Causevic, M., Garg, R., Noble, W., Killick, R., Bodi, I., et al. (2013). Prostate-derived Sterile 20-like Kinases (PSKs/TAOKs) Phosphorylate Tau Protein and Are Activated in Tangle-bearing Neurons in Alzheimer Disease. J Biol Chem 288, 15418–15429.

Tavazoie, S.F., Alvarez, V.A., Ridenour, D.A., Kwiatkowski, D.J., and Sabatini, B.L. (2005). Regulation of neuronal morphology and function by the tumor suppressors Tsc1 and Tsc2. Nat Neurosci 8, 1727–1734.

Taverna, E., Götz, M., and Huttner, W.B. (2014). The Cell Biology of Neurogenesis: Toward an Understanding of the Development and Evolution of the Neocortex. Annu Rev Cell Dev Bi 30, 1–38.

Tell, V., and Hilgeroth, A. (2013). Recent developments of protein kinase inhibitors as potential AD therapeutics. Front Cell Neurosci 7, 189.

Terasaki, M., and Reese, T.S. (1994). Interactions among endoplasmic reticulum, microtubules, and retrograde movements of the cell surface. Cell Motil Cytoskel 29, 291–300.

Terasaki, M., Chen, L.B., and Fujiwara, K. (1986). Microtubules and the endoplasmic reticulum are highly interdependent structures. J Cell Biology 103, 1557–1568.

Thanseem, I., Nakamura, K., Miyachi, T., Toyota, T., Yamada, S., Tsujii, M., Tsuchiya, K.J., Anitha, A., Iwayama, Y., Yamada, K., et al. (2010). Further evidence for the role of MET in autism susceptibility. Neurosci Res 68, 137–141.

Timm, T., Li, X., Biernat, J., Jiao, J., Mandelkow, E., Vandekerckhove, J., and Mandelkow, E. (2003). MARKK, a Ste20-like kinase, activates the polarity-inducing kinase MARK/PAR-1. Embo J 22, 5090–5101.

Timm, T., Matenia, D., Li, X.-Y., Griesshaber, B., and Mandelkow, E.-M. (2006). Signaling from MARK to Tau: Regulation, Cytoskeletal Crosstalk, and Pathological Phosphorylation. Neurodegener Dis 3, 207–217.

Timm, T., Marx, A., Panneerselvam, S., Mandelkow, E., and Mandelkow, E.-M. (2008). Structure and regulation of MARK, a kinase involved in abnormal phosphorylation of Tau protein. Bmc Neurosci 9, S9–S9.

Tolosa, E., Vila, M., Klein, C., and Rascol, O. (2020). LRRK2 in Parkinson disease: challenges of clinical trials. Nat Rev Neurol 16, 97–107.

Tonks, N.K. (2006). Protein tyrosine phosphatases: from genes, to function, to disease. Nat Rev Mol Cell Bio 7, 833–846.

Turk, B.E. (2005). Measuring kinase activity: finding needles in a haystack. Nat Methods 2, 251–252.

Ultanir, S.K., Hertz, N.T., Li, G., Ge, W.-P., Burlingame, A.L., Pleasure, S.J., Shokat, K.M., Jan, L.Y., and Jan, Y.-N. (2012). Chemical Genetic Identification of NDR1/2

Kinase Substrates AAK1 and Rabin8 Uncovers Their Roles in Dendrite Arborization and Spine Development. Neuron 73, 1127–1142.

Ultanir, S.K., Yadav, S., Hertz, N.T., Oses-Prieto, J.A., Claxton, S., Burlingame, A.L., Shokat, K.M., Jan, L.Y., and Jan, Y.-N. (2014). MST3 Kinase Phosphorylates TAO1/2 to Enable Myosin Va Function in Promoting Spine Synapse Development. Neuron 84, 968–982.

Urbanska, M., Gozdz, A., Swiech, L.J., and Jaworski, J. (2012). Mammalian Target of Rapamycin Complex 1 (mTORC1) and 2 (mTORC2) Control the Dendritic Arbor Morphology of Hippocampal Neurons. J Biol Chem 287, 30240–30256.

Vaillant, A.R., Zanassi, P., Walsh, G.S., Aumont, A., Alonso, A., and Miller, F.D. (2002). Signaling Mechanisms Underlying Reversible, Activity-Dependent Dendrite Formation. Neuron 34, 985–998.

Valente, E.M., Abou-Sleiman, P.M., Caputo, V., Muqit, M.M.K., Harvey, K., Gispert, S., Ali, Z., Turco, D.D., Bentivoglio, A.R., Healy, D.G., et al. (2004). Hereditary Early-Onset Parkinson's Disease Caused by Mutations in PINK1. Science 304, 1158–1160.

Vedrenne, C., Klopfenstein, D.R., and Hauri, H.-P. (2005). Phosphorylation Controls CLIMP-63–mediated Anchoring of the Endoplasmic Reticulum to Microtubules. Mol Biol Cell 16, 1928–1937.

Vermilyea, S.C., Babinski, A., Tran, N., To, S., Guthrie, S., Kluss, J.H., Schmidt, J.K., Wiepz, G.J., Meyer, M.G., Murphy, M.E., et al. (2020). In Vitro CRISPR/Cas9-Directed Gene Editing to Model LRRK2 G2019S Parkinson's Disease in Common Marmosets. Sci Rep-Uk 10, 3447.

Voeltz, G.K., Rolls, M.M., and Rapoport, T.A. (2002). Structural organization of the endoplasmic reticulum. Embo Rep 3, 944–950.

Voeltz, G.K., Prinz, W.A., Shibata, Y., Rist, J.M., and Rapoport, T.A. (2007). A Class of Membrane Proteins Shaping the Tubular Endoplasmic Reticulum. Cell 130, 754.

Volkmar, F.R., and Greenough, W.T. (1972). Rearing Complexity Affects Branching of Dendrites in the Visual Cortex of the Rat. Science 176, 1445–1447.

Wagner, W., Brenowitz, S.D., and Hammer, J.A. (2011). Myosin-Va Transports the Endoplasmic Reticulum into the Dendritic Spines of Purkinje Neurons. Nat Cell Biol 13, 40–48.

Wang, S., Tukachinsky, H., Romano, F.B., and Rapoport, T.A. (2016). Cooperation of the ER-shaping proteins atlastin, lunapark, and reticulons to generate a tubular membrane network. Elife 5, e18605.

Wang, X., He, Y., Ye, Y., Zhao, X., Deng, S., He, G., Zhu, H., Xu, N., and Liang, S. (2018a). SILAC–based quantitative MS approach for real-time recording protein-mediated cell-cell interactions. Sci Rep-Uk 8, 8441.

Wang, Y., Zeng, C., Li, J., Zhou, Z., Ju, X., Xia, S., Li, Y., Liu, A., Teng, H., Zhang, K., et al. (2018b). PAK2 Haploinsufficiency Results in Synaptic Cytoskeleton Impairment and Autism-Related Behavior. Cell Reports 24, 2029–2041.

Waterman-Storer, C.M., and Salmon, E.D. (1997). Actomyosin-based Retrograde Flow of Microtubules in the Lamella of Migrating Epithelial Cells Influences Microtubule Dynamic Instability and Turnover and Is Associated with Microtubule Breakage and Treadmilling. J Cell Biology 139, 417–434.

Weaving, L.S., Christodoulou, J., Williamson, S.L., Friend, K.L., McKenzie, O.L.D., Archer, H., Evans, J., Clarke, A., Pelka, G.J., Tam, P.P.L., et al. (2004). Mutations of CDKL5 Cause a Severe Neurodevelopmental Disorder with Infantile Spasms and Mental Retardation. Am J Hum Genetics 75, 1079–1093.

Wegner, A.M., Nebhan, C.A., Hu, L., Majumdar, D., Meier, K.M., Weaver, A.M., and Webb, D.J. (2008). N-WASP and the Arp2/3 Complex Are Critical Regulators of Actin in the Development of Dendritic Spines and Synapses*. J Biol Chem 283, 15912–15920.

Weiss, L.A., Shen, Y., Korn, J.M., Arking, D.E., Miller, D.T., Fossdal, R., Saemundsen, E., Stefansson, H., Ferreira, M.A.R., Green, T., et al. (2008). Association Between Microdeletion and Microduplication at 16p11.2 and Autism. Obstet Gynecol Surv 63, 361–363.

Wiesel, T.N., and Hubel, D.H. (1963). SINGLE-CELL RESPONSES IN STRIATE CORTEX OF KITTENS DEPRIVED OF VISION IN ONE EYE. J Neurophysiol 26, 1003–1017.

Winden, K.D., Ebrahimi-Fakhari, D., and Sahin, M. (2018). Abnormal mTOR Activation in Autism. Annu Rev Neurosci 41, 1–23.

Witte, H., and Bradke, F. (2008). The role of the cytoskeleton during neuronal polarization. Curr Opin Neurobiol 18, 479–487.

Woerden, G.M., Bos, M., Konink, C., Distel, B., Trezza, R.A., Shur, N.E., Barañano, K., Mahida, S., Chassevent, A., Schreiber, A., et al. (2021). TAOK1 is associated with neurodevelopmental disorder and essential for neuronal maturation and cortical development. Hum Mutat 42, 445–459.

Wong, R.O.L., and Ghosh, A. (2002). Activity-dependent regulation of dendritic growth and patterning. Nat Rev Neurosci 3, 803–812.

Wu, H., and Voeltz, G.K. (2021). Reticulon-3 Promotes Endosome Maturation at ER Membrane Contact Sites. Dev Cell 56, 52-66.e7.

Wu, G.Y., Zou, D.J., Rajan, I., and Cline, H. (1999). Dendritic Dynamics In Vivo Change during Neuronal Maturation. J Neurosci 19, 4472–4483.

Wu, G.-Y., Deisseroth, K., and Tsien, R.W. (2001). Spaced stimuli stabilize MAPK pathway activation and its effects on dendritic morphology. Nat Neurosci 4, 151–158.

Wu, H., Carvalho, P., and Voeltz, G.K. (2018). Here, there, and everywhere: The importance of ER membrane contact sites. Science 361, eaan5835.

Xie, B., Fan, X., Lei, Y., Chen, R., Wang, J., Fu, C., Yi, S., Luo, J., Zhang, S., Yang, Q., et al. (2016). A novel de novo microdeletion at 17q11.2 adjacent to NF1 gene associated with developmental delay, short stature, microcephaly and dysmorphic features. Mol Cytogenet 9, 41.

Xie, Y., Vessey, J.P., Konecna, A., Dahm, R., Macchi, P., and Kiebler, M.A. (2007). The GTP-Binding Protein Septin 7 Is Critical for Dendrite Branching and Dendritic-Spine Morphology. Curr Biol 17, 1746–1751.

Yabut, O., Domogauer, J., and D'Arcangelo, G. (2010). Dyrk1A Overexpression Inhibits Proliferation and Induces Premature Neuronal Differentiation of Neural Progenitor Cells. J Neurosci 30, 4004–4014.

Yadav, S., Oses-Prieto, J.A., Peters, C.J., Zhou, J., Pleasure, S.J., Burlingame, A.L., Jan, L.Y., and Jan, Y.-N. (2017). TAOK2 Kinase Mediates PSD95 Stability and Dendritic Spine Maturation through Septin7 Phosphorylation. Neuron 93, 379–393.

Yamagata, Y., Kobayashi, S., Umeda, T., Inoue, A., Sakagami, H., Fukaya, M., Watanabe, M., Hatanaka, N., Totsuka, M., Yagi, T., et al. (2009). Kinase-Dead Knock-In Mouse Reveals an Essential Role of Kinase Activity of Ca2+/Calmodulin-Dependent Protein Kinase II in Dendritic Spine Enlargement, Long-Term Potentiation, and Learning. J Neurosci 29, 7607–7618.

Yang, N., Higuchi, O., Ohashi, K., Nagata, K., Wada, A., Kangawa, K., Nishida, E., and Mizuno, K. (1998). Cofilin phosphorylation by LIM-kinase 1 and its role in Rac-mediated actin reorganization. Nature 393, 809–812.

Yasuda, R., Harvey, C.D., Zhong, H., Sobczyk, A., Aelst, L. van, and Svoboda, K. (2006). Supersensitive Ras activation in dendrites and spines revealed by two-photon fluorescence lifetime imaging. Nat Neurosci 9, 283–291.

Yasuda, S., Tanaka, H., Sugiura, H., Okamura, K., Sakaguchi, T., Tran, U., Takemiya, T., Mizoguchi, A., Yagita, Y., Sakurai, T., et al. (2007). Activity-Induced Protocadherin Arcadlin Regulates Dendritic Spine Number by Triggering N-Cadherin Endocytosis via TAO2β and p38 MAP Kinases. Neuron 56, 456–471.

Yazdani, U., and Terman, J.R. (2006). The semaphorins. Genome Biol 7, 211–211.

Yeh, R.-H., Yan, X., Cammer, M., Bresnick, A.R., and Lawrence, D.S. (2002). Real Time Visualization of Protein Kinase Activity in Living Cells*. J Biol Chem 277, 11527–11532.

Yuste, R., and Bonhoeffer, T. (2004). Genesis of dendritic spines: insights from ultrastructural and imaging studies. Nat Rev Neurosci 5, 24–34.

Yustein, J.T., Xia, L., Kahlenburg, J.M., Robinson, D., Templeton, D., and Kung, H.-J. (2003). Comparative studies of a new subfamily of human Ste20-like kinases: homodimerization, subcellular localization, and selective activation of MKK3 and p38. Oncogene 22, 6129–6141.

Zach, S., Felk, S., and Gillardon, F. (2010). Signal Transduction Protein Array Analysis Links LRRK2 to Ste20 Kinases and PKC Zeta That Modulate Neuronal Plasticity. Plos One 5, e13191.

Zempel, H., Thies, E., Mandelkow, E., and Mandelkow, E.-M. (2010). A Oligomers Cause Localized Ca2+ Elevation, Missorting of Endogenous Tau into Dendrites, Tau Phosphorylation, and Destruction of Microtubules and Spines. J Neurosci 30, 11938–11950.

Zempel, H., Luedtke, J., Kumar, Y., Biernat, J., Dawson, H., Mandelkow, E., and Mandelkow, E. (2013). Amyloid-β oligomers induce synaptic damage via Tau-dependent microtubule severing by TTLL6 and spastin. Embo J 32, 2920–2937.

Zhou, Q., Homma, K.J., and Poo, M. (2004). Shrinkage of Dendritic Spines Associated with Long-Term Depression of Hippocampal Synapses. Neuron 44, 749–757.

Zhou, X.X., Fan, L.Z., Li, P., Shen, K., and Lin, M.Z. (2017). Optical control of cell signaling by single-chain photoswitchable kinases. Science 355, 836–842.

Zihni, C., Mitsopoulos, C., Tavares, I.A., Ridley, A.J., and Morris, J.D.H. (2006). Prostate-derived Sterile 20-like Kinase 2 (PSK2) Regulates Apoptotic Morphology via C-Jun N-terminal Kinase and Rho Kinase-1*. J Biol Chem 281, 7317–7323.

Zihni, C., Mitsopoulos, C., Tavares, I.A., Baum, B., Ridley, A.J., and Morris, J.D.H. (2007). Prostate-derived Sterile 20-like Kinase 1-α Induces Apoptosis JNK- AND CASPASE-DEPENDENT NUCLEAR LOCALIZATION IS A REQUIREMENT FOR MEMBRANE BLEBBING. J Biol Chem 282, 6484–6493.

Zou, D.-J., and Cline, H.T. (1999). Postsynaptic Calcium/Calmodulin-Dependent Protein Kinase II Is Required to Limit Elaboration of Presynaptic and Postsynaptic Neuronal Arbors. J Neurosci 19, 8909–8918.